

JAERI - M
85-158

COMPARISONS OF ROSA-III AND FIST
BWR LOSS OF COOLANT ACCIDENT
SIMULATION TESTS

October 1985

Kanji TASAKA, Mitsuhiro SUZUKI, Yasuo KOIZUMI
Yoshinari ANODA, Hiroshige KUMAMARU
Hideo NAKAMURA, Taisuke YONOMOTO, J. A. FINDLAY*
W. A. SUTHERLAND*, W. S. HWANG*, S. A. del BANCO*
and L. S. LEE*

JAERI-M レポートは、日本原子力研究所が不定期に公開している研究報告書です。
入手の問合わせは、日本原子力研究所技術情報部情報資料課（〒319-11 茨城県那珂郡東海村）
あて、お申しこしてください。なお、このほかに財団法人原子力弘済会資料センター（〒319-11 茨城
県那珂郡東海村日本原子力研究所内）で複写による実費頒布をおこなっております。

JAERI-M reports are issued irregularly.
Inquiries about availability of the reports should be addressed to Information Division, Department
of Technical Information, Japan Atomic Energy Research Institute, Tokai-mura, Naka-gun,
Ibaraki-ken 319-11, Japan.

© Japan Atomic Energy Research Institute, 1985

編集兼発行 日本原子力研究所
印刷 山田軽印刷所

COMPARISONS OF ROSA-III AND FIST
BWR LOSS OF COOLANT ACCIDENT SIMULATION TESTS

Kanji TASAKA, Mitsuhiro SUZUKI, Yasuo KOIZUMI,
Yoshinari ANODA, Hiroshige KUMAMARU, Hideo NAKAMURA,
Taisuke YONOMOTO, J.A. FINDLAY*, W.A. SUTHERLAND*,
W.S. HWANG*, S.A. del BANCO* and L.S. LEE*

Department of Reactor Safety Research
Tokai Research Establishment, JAERI

(Received September 25, 1985)

A common understanding and interpretation of BWR system response and the controlling phenomena in LOCA transients has been achieved through the evaluation and comparison of counterpart tests performed in the ROSA-III and FIST test facilities. These facilities, which are designed to simulate the thermal-hydraulic response of BWR systems, are operated respectively by the Japan Atomic Energy Research Institute (JAERI) and the General Electric Company. Comparison is made between three types of counterpart tests, each performed under similar test conditions in the two facilities. They are large break, small break, and steamline break LOCA's. The system responses to these tests in each facility are quite similar. The sequence of events are similar, and the timing of these events are similar. Differences that do occur are due to minor differences in modeling objectives, facility scaling, and test conditions. Parallel channel flow interactions effects in the ROSA-III four channel (half length) core, although noticeable in the large break test, do not result in major differences with the single channel response in FIST. In the small break tests the timing of events is offset by the earlier ADS actuation in FIST. The steamline test responses are similar except there is no heatup in FIST, resulting from a different ECCS trip modeling. Overall comparisons between ROSA-III and FIST system responses in LOCA tests is very good.

Keywords: BWR, LOCA, Counterpart Test, ROSA-III, FIST, Thermal-hydraulic Response, Large Break, Small Break, Steam Line Break, Similarity, Scaling, Comparative Evaluations

* General Electric Co.

ROSA-ⅢとFISTにおけるBWRの冷却材
喪失事故の相互比較実験

日本原子力研究所東海研究所原子炉安全工学部

田坂 完二・鈴木 光弘・小泉 安郎

安濃田良成・熊丸 博滋・中村 秀夫

与能本泰介^{*}・J. A. Findlay^{*}

W. A. Sutherland^{*}・W. S. Hwang^{*}

S. A. del Banco^{*}・L. S. Lee^{*}

(1985年9月25日受理)

原研のROSA-ⅢとGE社のFIST両実験装置において行われた相互比較実験の結果を比較検討し、BWR LOCAの主要現象を明らかにした。BWRの熱水力挙動を模擬するために設計されている両実験装置で同等の実験条件で実験した大破断、小破断、主蒸気系配管破断の3種類のタイプの実験の結果を比較した。両装置における系の挙動は非常によく似かよっている。各事象の順序が類似しているばかりでなくそのタイミングも類似している。差異はあるとしてもそれらは装置の目的、スケーリングの考え方および実験条件のわずかなちがいによるものである。ROSA-Ⅲ装置は実寸の半分の長さの4バンドルをもち、チャンネル間の相互作用が大破断実験においては検知される。しかし大筋においてはFISTの単チャンネルの結果と差異はない。小破断における各事象のタイミングの差はFISTでADSが早く作動することにより相殺されている。蒸気系配管破断においてはECCS作動ロジックのちがいによりFISTで温度上昇が無い以外は両装置の結果によい相似性がある。全体としてROSA-ⅢとFIST両装置におけるLOCA挙動の相似性は大変満足すべきものである。

* ゼネラルエレクトリック社

Contents

1.	INTRODUCTION	1
1.1	Background	1
1.2	Tests	1
1.3	Approach	2
2.	TEST FACILITIES	5
3.	TEST CONDITIONS	17
3.1	Large Break	17
3.2	Small Break	22
3.3	Main Steamline Break	27
4.	TEST RESULTS	31
4.1	Large Break	31
4.2	Small Break	42
4.3	Main Steamline Break	52
5.	SUMMARY	63
6.	CONCLUSIONS	64
7.	REFERENCES	65

APPENDICES

A.1	ROSA-III Test Facility and Test Procedure	66
A.2	Fist Test Facility	71

目 次

1. 序	1
1.1 背 景	1
1.2 実 験	1
1.3 方 法 論	2
2. 実験装置	5
3. 実験条件	17
3.1 大 破 断	17
3.2 小 破 断	22
3.3 主蒸気系配管破断	27
4. 実験結果	31
4.1 大 破 断	31
4.2 小 破 断	42
4.3 主蒸気系配管破断	52
5. 要 約	63
6. 結 論	64
7. 参考文献	65
付 録	
A. 1 ROSA-Ⅲ装置と実験手順	66
A. 2 FIST装置	71

Illustrations

<u>Figure</u>	<u>Title</u>
1-1	ROSA-III Test Facility
1-2	FIST Test Facility
2-1	Facility Regions
2-2A	Axial Power Distribution
2-2B	FIST Axial Power Distribution
2-2C	ROSA Axial Power Distribution
2-3	Facility Elevations, and Level Instruments
2-4	Volumes from Bottom of Downcomer
3.1-1A	Power, Large Break LOCA
3.1-1B	Power, Large Break LOCA
3.1-1C	Power, Large Break LOCA
3.1-2A	HPCS Flow vs. Pressure, Large Break LOCA
3.1-2B	LPCS Flow vs. Pressure, Large Break LOCA
3.1-2C	LPCI Flow vs. Pressure, Large Break LOCA
3.2-1A	Power, Small Break LOCA
3.2-1B	Power, Small Break LOCA
3.2-1C	Power, Small Break LOCA
3.2-2A	LPCS Flow vs. Pressure, Small Break LOCA
3.2-2B	LPCI Flow vs. Pressure, Small Break LOCA
3.3-1A	Power, Main Steamline Break LOCA
3.3-1B	Power, Main Steamline Break LOCA
3.3-1C	Power, Main Steamline Break LOCA
3.3-2	HPCS Flow vs. Pressure, Main Steamline Break LOCA
4.1-1A	Break Flow, Large Break LOCA
4.1-1B	Break Flow, Large Break LOCA
4.1-2	Break Temperature, Large Break LOCA
4.1-3A	System Pressure, Large Break LOCA
4.1-3B	System Pressure, Large Break LOCA
4.1-4A	Steamline Flow, Large Break LOCA
4.1-4B	Steamline Flow, Large Break LOCA

Illustrations

<u>Figure</u>	<u>Title</u>
4.1-5	Core Flow, Large Break LOCA
4.1-6	Feedwater Flow, Large Break LOCA
4.1-7	Downcomer Liquid Volume, Large Break LOCA
4.1-8	Downcomer Liquid Level, Large Break LOCA
4.1-9	Mixture Level Inside Shroud, Large Break LOCA
4.1-10	Bundle Inlet Flows, Large Break LOCA
4.1-11	Rod Temperatures, Large Break LOCA
4.1-12	ROSA 983 Rod Temperatures, Large Break LOCA
4.1-13A	HPCS Flow, Large Break LOCA
4.1-13B	LPCS Flow, Large Break LOCA
4.1-13C	LPCI Flow, Large Break LOCA
4.1-13D	Total ECCS Flow, Large Break LOCA
4.1-14	Total Vessel Liquid Mass, Large Break LOCA
4.2-1	Break Flow, Small Break LOCA
4.2-2	Break Temperature, Small Break LOCA
4.2-3A	System Pressure, Small Break LOCA
4.2-3B	System Pressure, Small Break LOCA
4.2-4A	Steamline Flow, Small Break LOCA
4.2-4B	Steamline Flow, Small Break LOCA
4.2-5	Core Flow, Small Break LOCA
4.2-6	Feedwater Flow, Small Break LOCA
4.2-7	Downcomer Liquid Volume, Small Break LOCA
4.2-8A	ROSA 984 Downcomer Level, Small Break LOCA
4.2-8B	FIST 6SB2C Downcomer Level, Small Break LOCA
4.2-9	Mixture Level in Downcomer, Small Break LOCA
4.2-10	Mixture Level in Core Shroud, Small Break LOCA
4.2-11	Bundle Inlet Flows, Small Break LOCA
4.2-12A	Rod Temperatures, Small Break LOCA
4.2-12B	Rod Temperatures, Small Break LOCA
4.2-13A	LPCS and LPCI Flows, Small Break LOCA
4.2-13B	Total ECCS Flow, Small Break LOCA

Illustrations

<u>Figure</u>	<u>Title</u>
4.2-14	Total Vessel Liquid Mass, Small Break LOCA
4.3-1A	Break Flow, Main Steamline Break LOCA
4.3-1B	Break Flow, Main Steamline Break LOCA
4.3-2A	System Pressure, Main Steamline Break LOCA
4.3-2B	System Pressure, Main Steamline Break LOCA
4.3-3	Core Flow, Main Steamline Break LOCA
4.3-4	Feedwater Flow, Main Steamline Break LOCA
4.3-5A	ROSA 952 Downcomer Level, Main Steamline Break LOCA
4.3-5B	FIST 6MSB1 Downcomer Level, Main Steamline Break LOCA
4.3-6	Mixture Level in Downcomer, Main Steamline Break LOCA
4.3-7	Mixture Level in Core Shroud, Main Steamline Break LOCA
4.3-8A	Rod Temperatures, Main Steamline Break LOCA
4.3-8B	Rod Temperatures, Main Steamline Break LOCA
4.3-9A	HPCS Flow, Main Steamline Break LOCA
4.3-9B	LPCS an LPCI Flow, Main Steamline Break LOCA
4.3-9C	Total ECCS Flow, Main Steamline Break LOCA
4.3-10	Total Vessel Liquid Mass, Main Steamline Break LOCA
A.1-1	Core Cross-Section of ROSA-III Test Facility
A.1-2	Details of Simulated Fuel Rod

Tables

<u>Tables</u>	<u>Title</u>
2-1	Comparison of ROSA-III and FIST Facilities
2-2	Scaling of Fluid Volumes
2-3	Downcomer Region
2-4	Metal Heat Sources in Each Vessel Region
3.1-1	Large Break Counterpart Tests, Initial Conditions and Boundary Conditions.
3.2-1	Small Break Counterpart Tests, Initial Conditions and Boundary Conditions
3.3-1	Steamline Break Counterpart Tests, Initial Conditions and Boundary Conditions
4.1-1	Large Break Counterpart Tests, Timing of Key Events
4.2-1	Small Break Counterpart Tests, Timing of Key Events
4.3-1	Steamline Break Counterpart Tests, Timing of Key Events
A.1-1	Primary Characteristics of ROSA-III and BWR/6-251
A.2-1	Primary Characteristics of FIST and BWR/6-218
A.2-2	FIST Heater Pattern

1. INTRODUCTION

1.1 BACKGROUND

Experimental programs, using test facilities designed to simulate BWR systems, have evaluated and quantified controlling phenomena in loss-of-coolant accident situations. Namely, the water level response and ADS actuation time affect significantly the core cooling conditions in a small break LOCA. On the other hand, the CCFL at the core inlet region affects the core cooling conditions in a large recirculation loop break LOCA. The evaluation of applicability of the experiment results to BWR LOCA's is the current interest of the programs. The Japan Atomic Energy Research Institute (JAERI) performed a wide variety of experiments in the Rig of Safety Assessment-III (ROSA-III) facility⁽¹⁾ shown in Figure 1-1. Scaled to a 848 bundle BWR/6-251, ROSA-III has four half length electrically heated bundles to study multi-channel effects on the core cooling phenomena. The General Electric Company also performed various safety related transient experiments in the Full Integral Simulation Test (FIST) facility* shown in Figure 1-2⁽²⁾. As full height simulation scaled to a 624 bundle BWR/6-218, FIST has one full length electrically heated bundle. The objective of this study is to develop a common understanding and interpretation of the controlling phenomena observed in loss-of-coolant accident (LOCA) experiments performed in these two test facilities. Further study to generalize the experimental results is on a way in each program using a computer code.

1.2 TESTS

Three types of tests performed in the ROSA-III and FIST facilities are chosen for comparison. Each test type was performed under similar test conditions. The three test types are: 1) a large break in a recirculation pump suction line with HPCS, LPCS, and one LPCI, ROSA Test 983⁽³⁾ and FIST Test 6DBA1B⁽⁴⁾, 2) a small break in a recirculation pump suction line with LPCS and three LPCI, ROSA Test 984⁽⁵⁾, and FIST Test 6SB2C⁽⁴⁾, and 3) a break in a steamline, ROSA Test 952⁽⁶⁾, and FIST Test 6MSB1⁽⁴⁾. FIST simulated availability of HPCS, LPCS and one LPCI in the steamline break test, whereas availability of all ECC System was simulated in ROSA-III. However, only the HPCS system was activated in the ROSA-III test.

* This program is jointly sponsored by the U.S. Nuclear Regulatory Commission, the Electric Power Research Institute, and the General Electric Company.

The three ROSA-III tests were performed after the three FIST tests. The ROSA Tests 983 and 984 were performed as counterpart tests of FIST Tests 6DBA1B and 6SB2C respectively. To achieve this, the standard ROSA-III test conditions were modified to match the FIST initial conditions and boundary conditions. ROSA Test 952 was not performed as a counterpart test, but most of the important test conditions were similar to those of FIST Test 6MSB1.

1.3 APPROACH

Evaluation of the ROSA-III and FIST system response comparisons consists of three parts. First is the similarity of the test conditions, i.e., the initial conditions and boundary conditions, such as the power, ECCS pump capacity, and break area. Second is the similarity of each system response to the test conditions, such as timing of key events, depressurization rate, regional mass and level transients, bundle hydraulic performance and cooling mechanism, and cladding temperatures. Third is the effect of facility differences and different scaling compromises in each facility.

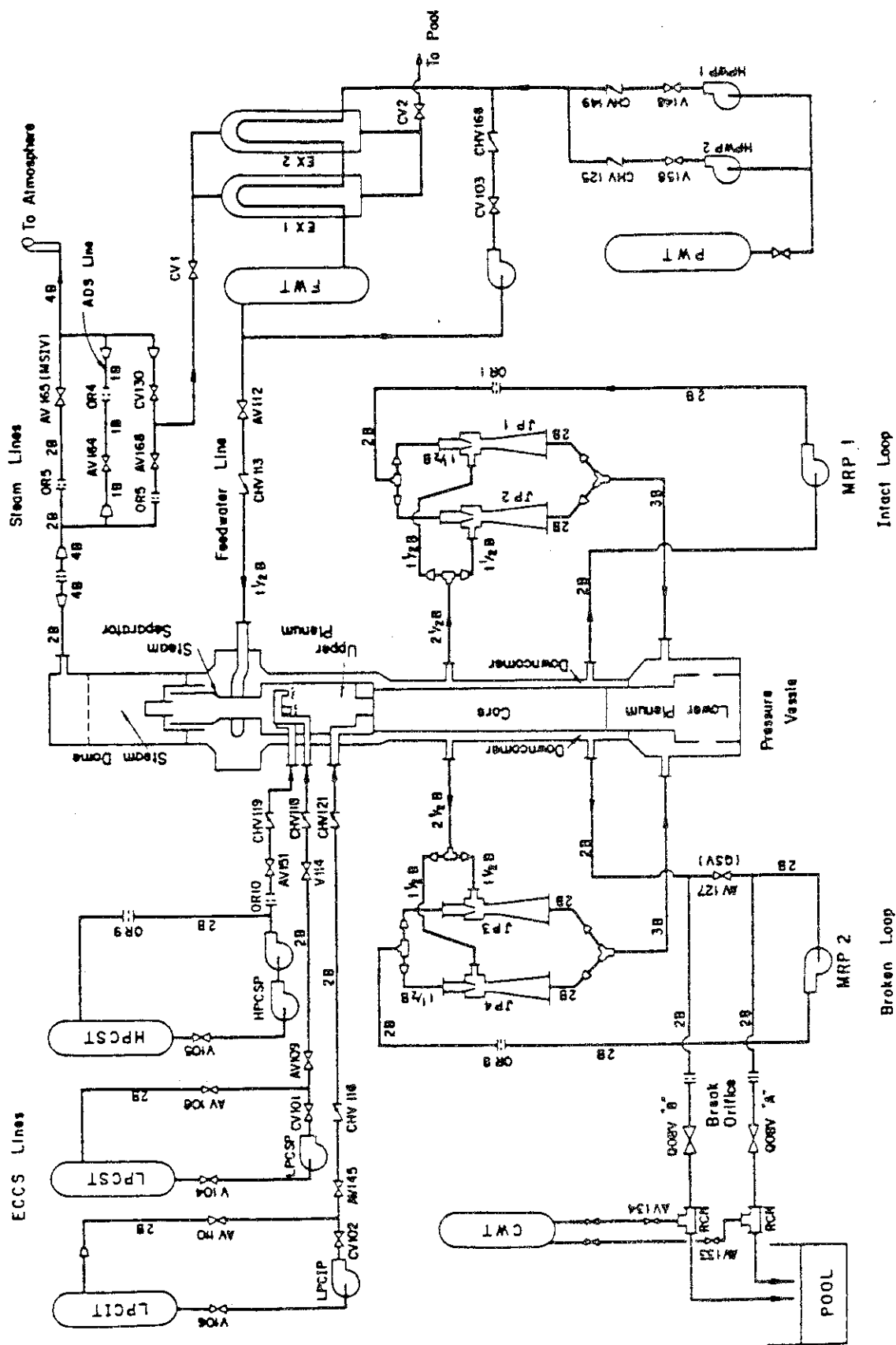


Figure 1-1 ROSA-III Test Facility

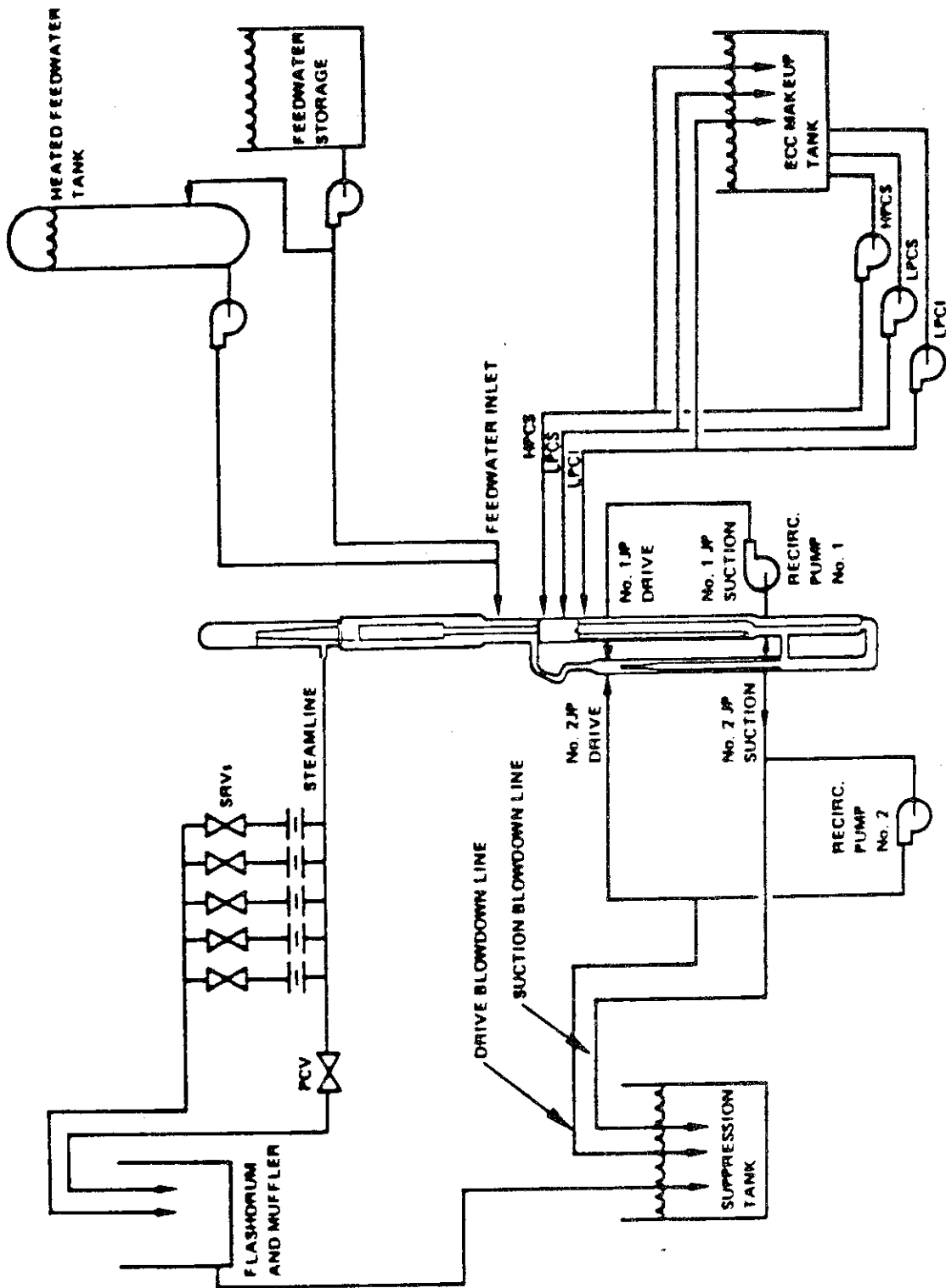


Figure 1-2 FIST Test Facility

2. TEST FACILITIES

The objective for both ROSA-III and FIST is for the scaled test apparatus to simulate, on a real time basis, BWR system thermal-hydraulic response following a postulated LOCA. Both facilities have the capability to establish initial thermal-hydraulic conditions typical of a BWR, as well as the important BWR system features that govern the mass and energy transfer rates. These system features include power, vessel internals, channeled bundles, internal flows, recirculation pump loops, feedwater supply, steam system pressure control and automatic depressurization system (ADS), and emergency core cooling systems (ECCS). The vessel regions, shown in Figure 2-1, simulate the lower plenum, guide tubes, bundles and bypass, upper plenum, steam separator, downcomer, and steam dome. The simulated break, size and location, gives the correct break flow rate and flow quality.

The ROSA-III facility is volumetrically scaled (1/424) to a BWR/6-251 with 848 fuel bundles. The four half length bundle concept was adopted to study thermal-hydraulic interaction among the bundles. The FIST facility⁽⁷⁾ is volumetrically scaled (1/624) to a BWR/6-218 with 624 fuel bundles. The full height vessel and single electrically heated bundle provide full scale values for fluid conditions, velocities, and static heads.

An overall comparison of the ROSA-III and FIST facilities is given in Table 2-1. This table summarizes the pertinent information on the bundles, region volumes and heights, and the break areas. Each of these is discussed in more detail in the following paragraphs. The overall comparison is quite good, particularly the volumetric scaling. The notable difference is the height scaling.

The bundles in each facility consists of 62 heated rods and two water rods in an 8x8 square array. The rod diameter and spacing are the same. The rods are electrically heated with a chopped cosine axial power distribution and an axial peaking factor of 1.4, as shown in Figures 2-2A, B and C. The 1.88 m (6.17 ft.) ROSA-III bundles and the

FIST 3.81 m (12.5 ft.) bundle have equivalent axial power shapes when compared on a normalized length basis as seen in Figure 2-2A. Also shown in this figure are the relative locations of the rod thermocouples in each bundle. Figure 2-2B shows the actual rod TC elevations in FIST, and Figure 2-2C shows ROSA-III. The ROSA-III bundles have a local peaking factor of 1.1 and FIST 1.042, but this difference has a negligible effect. ROSA-III simulation of two full size bundles with four half length bundles doubles the core flow area. The flow areas of the four inlet orifices and upper tieplates are reduced to preserve the core region CCFL performance characteristics, as seen in Table 2-1. The relative heights and elevations of the bundles are shown in Figure 2-3.

The volume of each test vessel region is scaled to the corresponding volume in the reference BWR*. This approach preserves the relative water and steam mass distribution within the vessel, which directly affects system depressurization, internal flows, and core cooling. The regional volumes are compared in Table 2-1 on a per-full-size-bundle basis, since ROSA-III has four half length bundles and FIST is scaled to one. The scaled system volumes are within six percent. The ROSA-III upper plenum and recirculation loop regions are larger than FIST, and the other regions are correspondingly smaller.

The total water volumes, however, which are given in Table 2-2, compare within ten percent. The combined separator, upper plenum, bundles, and bypass saturated fluid volumes compare closely between the two facilities. The larger ROSA-III subcooled fluid volume in the downcomer, jet pumps, and recirculation loop region is almost balance by the larger lower-plenum-plus-guide-tube subcooled fluid volume in FIST. The distribution of the downcomer fluid volumes with respect to the Level 1 and Level 2 trip elevations is important because ECCS flow, MSIV closure, and ADS activation are initiated by these settings. These elevations and volumes are shown in Table 2-3 and Figure 2-4. The level instruments are also shown. The impact of this scaling will be covered in the discussion of each test.

* The scaling basis and comparisons to the reference systems are discussed further in Appendices A.1 and A.2.

Height scaling is also compared in Table 2-1 and Figure 2-3. The FIST facility, with full scale elevations, preserves region cross-sectional areas, region void fractions, and elevation heads. The shorter scaling in ROSA III does not have a large effect on overall system response. The half length bundles are balanced with short jet pumps to simulate static head effects. The top of the jet pumps is at the 66% core elevation in ROSA-III and FIST, as well as in the BWR. The ROSA-III vessel and interval regions are shorter than FIST. The shorter vessel regions lead to less level swell during flashing. The height scaling has a small effect on the test response. The simulated breaks are placed in the same relative locations so that the mass and energy fluxes are simulated, and are sized to give mass and energy flow rates in proportion to the volume scaling. The large break areas are only six percent different between the two facilities. Because they have different reference systems, the FIST recirculation suction line large break area is 4% larger than ROSA-III, and the drive line break is 22% larger. The small break areas are within 2%. The FIST steamline break area is 25% larger than ROSA-III for the first 5.5 seconds of the transient, and equal thereafter. The steamline break tests were modeled differently.

The FIST ADS area is 6% larger than the corresponding ROSA-III ADS area. The effect of this difference is a slightly higher ADS flow rate in FIST. Since heat stored in the metal structure, when released to the water, will slow the depressurization rate, ADS area in FIST was increased to compensate for this effect. Table 2-4 shows the regional metal volumes and surface areas for the two facilities. The stored heat in the regions containing water has the greatest impact on the depressurization rate. In these regions, which include the lower plenum, guide tube, bypass, bundles, and upper plenum, ROSA-III has 36% more metal per full size bundle than FIST. Localized stored heat effects are also significant. For example, in FIST the large bypass metal mass caused refilling oscillations for some tests. The large lower plenum metal mass in ROSA-III increases the flashing in this region.

Overall the match between ROSA-III and FIST is quite good. The major differences are the number of core flow paths (parallel channel flow) and the region heights. The effect of these differences is evaluated in discussion of the test comparisons in Section 4.

Table 2-1
COMPARISON OF ROSA-III AND FIST FACILITIES

Item	ROSA-III		FIST	
	Total	Per Full Size Bundle	Total	ROSA-III/FIST Per Full Size Bundle
Bundles				
Array	8x8	-	8x8	-
No. of Bundles	4 ⁽¹⁾	-	1	-
Heated Length (m)	1.88	-	3.81	0.5
Local Peaking Factor	1.10	-	1.04	-
Axial Peaking Factor	1.40	-	1.40	-
No. of Heated Rods/Bundle	62	-	62	-
No. of Water Rods/Bundle	2	-	2	-
O.D. of Heated Rods (mm)	12.27	-	12.27	-
Flow Area (cm ²)	387.1	96.8 ⁽¹⁾	96.8	1.00
UTP Flow Area (cm ²)	119.1	59.5 ⁽¹⁾	79.1	0.75
SEO Flow Area (cm ²)	60.8	30.4 ⁽¹⁾	29.9	1.02
Maximum Power (MW)	4.46 ⁽²⁾	2.23	7.00	-
Volumes (m³)				
Total System	1.418	0.709	0.712	1.00
Steam Dome	0.371 ⁽⁵⁾	0.186	0.218	0.85
Downcomer	0.340 ⁽⁵⁾	0.170	0.170 ⁽³⁾	1.00
Jet Pumps; Recirc. Loops	0.172	0.086	0.024	3.58
Steam Separator	0.031	0.016	0.047	0.34
Upper Plenum	0.124	0.062	0.044	1.41
Bundles	0.096	0.048	0.043	1.12
Bypass	0.060	0.030	0.037	0.81
Lower Plenum	0.167	0.083	0.088	0.94
Guide Tubes	0.057	0.028	0.042	0.67
Heights (m)				
Total Vessel	6.00	-	19.42	0.31
Steam Dome	1.00 ⁽⁵⁾	-	6.09	0.16
Downcomer	4.51	-	10.80	0.42
Jet Pumps	2.41	-	4.50	0.54
Steam Separator	1.12	-	2.10	0.53
Upper Plenum	0.69	-	1.83	0.38
Bypass	2.21	-	4.39	0.50
Lower Plenum	1.28	-	4.11	0.31
Break Flow Areas (mm²)				
ADS	349.6 ⁽⁶⁾	174.8	186.7	0.94
Large Recirc. Break	619.2	309.6	331.4	0.94
Recirc. Suction	539.1	269.5	279.6	0.96
Drive Line	80.1	40.0	51.8	0.78
Small Recirc. Break	14.52	7.26	7.44	0.98
Steamline Break	754.8	377.4	501/377 ⁽⁴⁾	0.75/1.00

(1) Four, half-length bundles were used in ROSA-III.

(2) Power decay delayed 9 seconds to compensate for low initial power.

(3) After loop isolation.

(4) FIST steamline break area changes from 501 to 377mm² at 5.5 seconds.

(5) Based on a water level of 5.0m which is used in normal ROSA-III tests.

(6) Normal ADS area for ROSA-III tests is 188.6mm².

Table 2-2

SCALING OF FLUID VOLUMES

Volumes	$\frac{1}{2} \times \text{ROSA-III (m}^3\text{)}$		FIST (m ³)		$\frac{1}{2} \text{ ROSA-III/FIST}$	
	Free Vol.	Water Vol.	Free Vol.	Water Vol.	Free Vol.	Water Vol.
Total Vessel	0.709	0.438	0.712	0.396	1.00	1.11
Steam Dome	0.186	0.	0.218	0.	0.85	-
Downcomer	0.170 ⁽⁶⁾	0.170 ⁽⁶⁾	0.170	1.70	1.00	1.00
Jet Pumps/ Loops	0.086	0.086	0.024 ⁽¹⁾	0.024 ⁽¹⁾	3.58	3.58
Steam	0.016	0.004 ⁽²⁾	0.047	0.010 ⁽³⁾	0.34	0.40
Separators						
Upper Plenum	0.062	0.017 ⁽²⁾	0.044	0.010 ⁽³⁾	1.41	1.70
Bundles	0.048	0.020 ⁽⁴⁾	0.043	0.015 ⁽⁵⁾	1.12	1.33
Bypass	0.030	0.030	0.037	0.037	0.81	0.81
Lower Plenum	0.083	0.083	0.088	0.088	0.94	0.94
Guide Tubes	0.028	0.028	0.042	0.042	0.67	0.67

(1) After loops isolated.

(2) $\alpha = 0.73$, $x = 0.125$, homogeneous equilibrium, Run 952 initial Conditions.(3) $\alpha = 0.78$, $x = 0.16$, homogeneous equilibrium, Run 952 initial Conditions.(4) $\alpha = 0.59$, $x = 0.07$, homogeneous equilibrium, Run 952 initial Conditions.(5) $\alpha = 0.65$, $x = 0.09$, homogeneous equilibrium, Run 952 initial Conditions.

(6) Based on water level of 5.0m.

SUMMARY OF WATER VOLUMES

Volumes	$\frac{1}{2} \text{ ROSA-III (m}^3\text{)}$	FIST (m ³)	Difference (m ³)
Downcomer + Jet Pump/Loops	0.256	0.194	0.062
Separator + Upper Plenum + Bundles + Bypass	0.071	0.072	-0.001
Lower Plenum + Guide Tubes	0.111	0.130	-0.019
Total	0.438	0.396	0.042

Table 2-3

DOWNCOMER REGION

<u>Level</u>	<u>A. Elevations (m)</u>			
	<u>Large Break</u>	<u>Small Break</u>	<u>Steamline</u>	<u>FIST⁽¹⁾</u>
	<u>ROSA 983</u>	<u>ROSA 984</u>	<u>ROSA 952</u>	
Water Level	5.06	5.21	5.14	14.15
Level 3	4.77	4.96	5.00	13.48
Level 2	4.60	4.46	4.76	12.19
Level 1	3.62	4.00	4.25	9.55
D.C. Bottom	0.49	0.49	0.49	3.35

<u>Level</u>	<u>B. Volumes from Downcomer Bottom (m³)⁽²⁾</u>			
	<u>Large Break</u>	<u>Small Break</u>	<u>Steamline</u>	<u>FIST</u>
	<u>½ ROSA 983</u>	<u>½ ROSA 984</u>	<u>½ ROSA 952</u>	
Top of Vessel	0.3556	0.3556	0.3556	0.3925
Steamline	0.3556	0.3556	0.3556	0.2358
Top DP Tap	0.3556	0.3556	0.3556	0.1911
Water Level	0.1802	0.2064	0.1938	0.1698
Level 2	0.1154	0.0973	0.1348	0.1072
Level 1	0.0460	0.0612	0.0712	0.0551
Bottom DP Tap	0.0572	0.0572	0.0572	0.0504
Jet Pump Top	0.0293	0.0293	0.0293	0.0369
Recirc. Suction	0.0050	0.0050	0.0050	0.0073
D.C. Bottom	0.0000	0.0000	0.0000	0.0000

(1) BWR elevations. Bottom of facility is 0.74 m BWR elevation.

(2) Includes volume between the separator cans and inner pipe.

See Figure 2-4.

Table 2-4

METAL HEAT SOURCES IN EACH VESSEL REGION

Region	Metal Volume (m ³)			Surface Area (m ²)		
	<u>½ ROSA</u>	<u>FIST</u>	<u>½ ROSA/FIST</u>	<u>½ ROSA</u>	<u>FIST</u>	<u>½ ROSA/FIST</u>
Steam Dome	0.140	0.091	1.5	2.9	5.1	0.6
Downcomer	0.240	0.129	1.9	5.5	8.8	0.6
Jet Pump; Loops	0.095	0.002 ⁽²⁾	48.	5.6	1.2	4.7
Separator	0.002	0.003	0.7	1.0	2.4	0.4
Upper Plenum	0.005	0.019	0.3	0.7	1.0	0.7
Bundles	0.043	0.031	1.4	15.0	12.6	1.2
Bypass	0.015	0.069	0.2	5.2	5.1	1.0
Lower Plenum	0.195 ⁽¹⁾	0.076	2.6	6.9	5.7	1.2
Guide Tubes	<u>0.010</u>	<u>0.002</u>	<u>5.0</u>	<u>1.6</u>	<u>1.5</u>	<u>1.1</u>
Total	0.750	0.422	1.78	44.5	43.4	1.03
Average Thickness 16.9mm			9.7mm	1.74		

(1) Heater connectors included

(2) Jet pumps only

Water Regions	Metal Volume (m ³)		
	<u>½ ROSA</u>	<u>FIST</u>	<u>½ ROSA/FIST</u>
Upper Plenum	0.005	0.019	0.26
Bundles	0.043	0.031	1.39
Bypass	0.015	0.069	0.22
Lower Plenum	0.195	0.076	2.57
Guide Tubes	<u>0.010</u>	<u>0.002</u>	<u>5.00</u>
Total	0.268	0.197	1.36

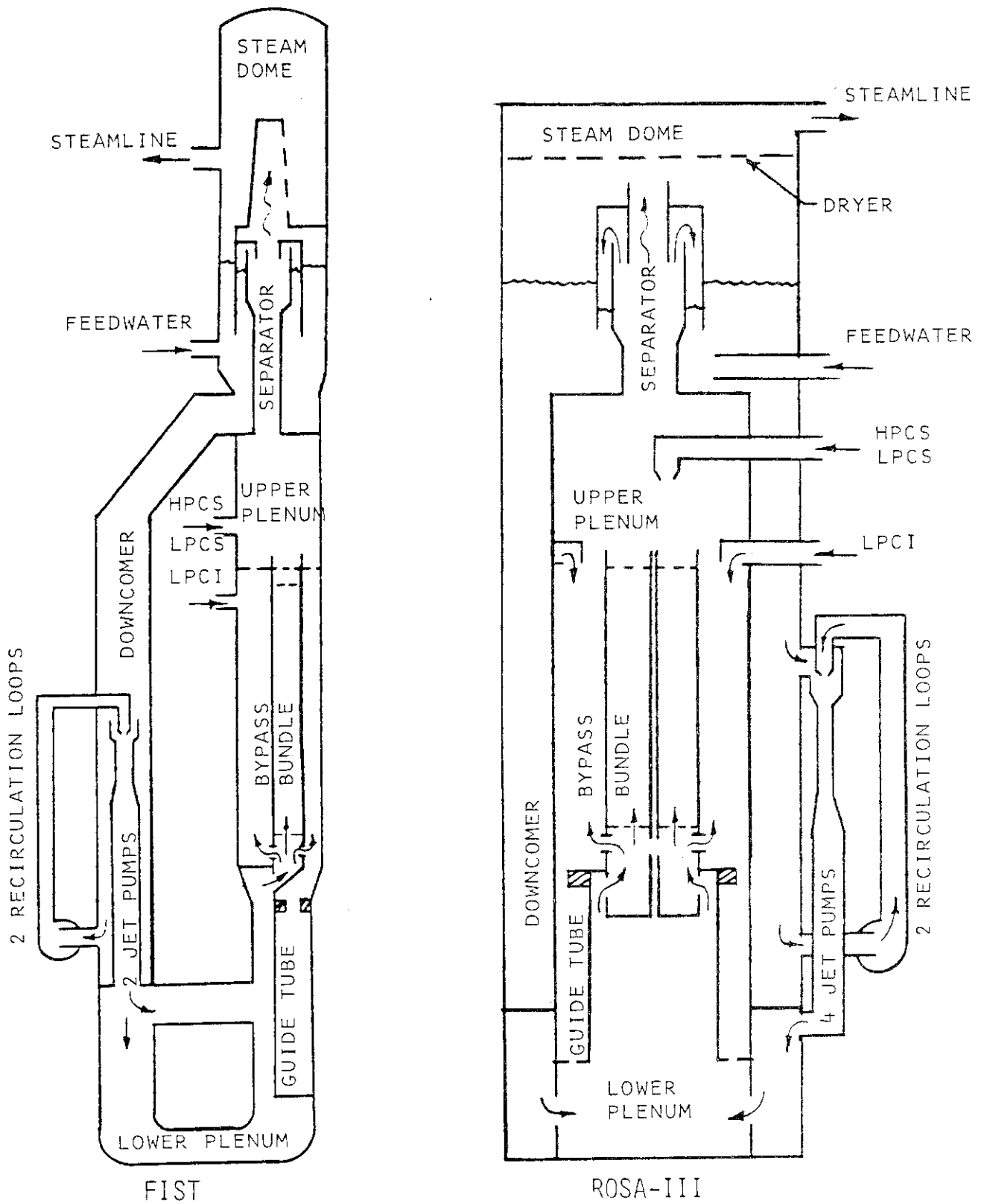


Figure 2-1 Facility Regions

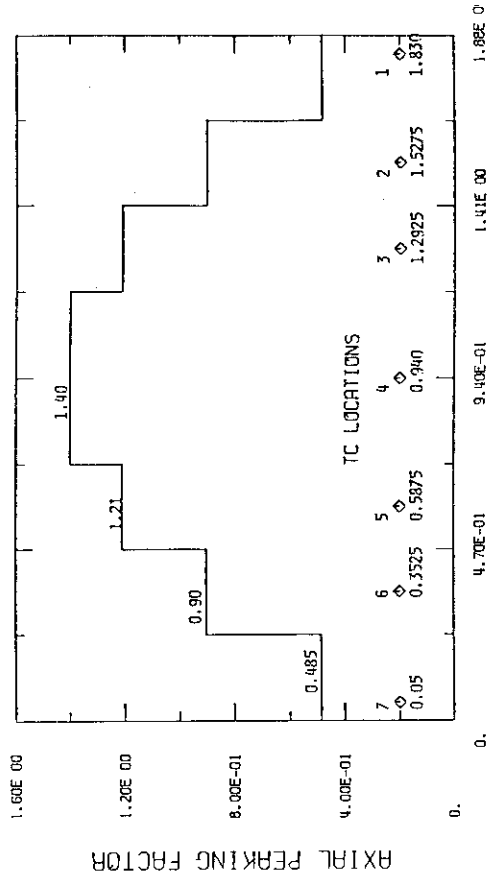


FIG. 2-2C ROSA AXIAL POWER DISTRIBUTION

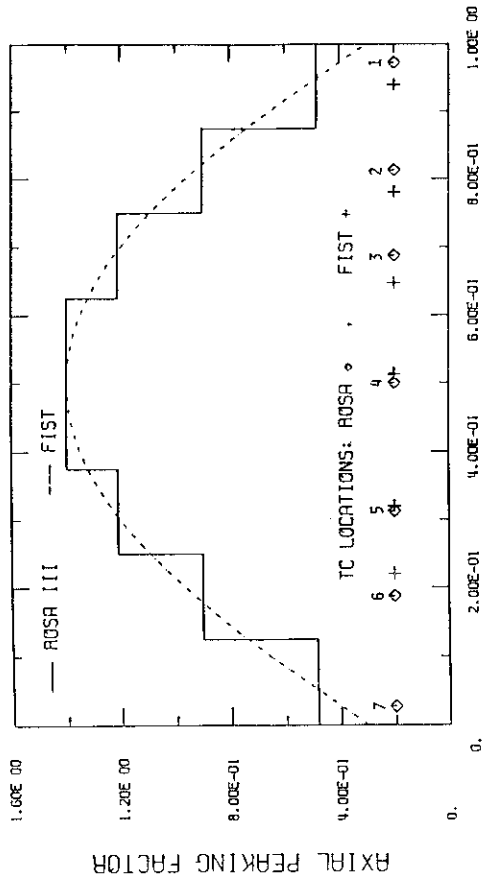


FIG. 2-2A AXIAL POWER DISTRIBUTION

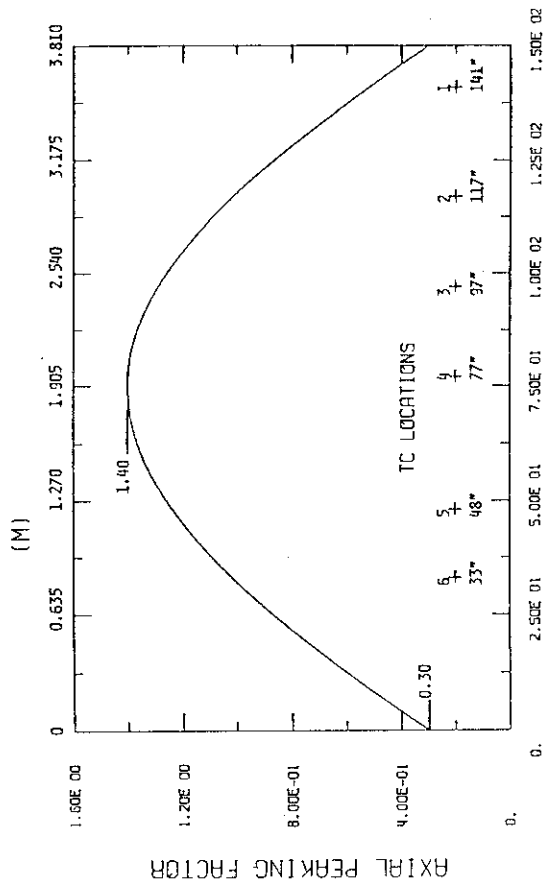


FIG. 2-2B FIST AXIAL POWER DISTRIBUTION

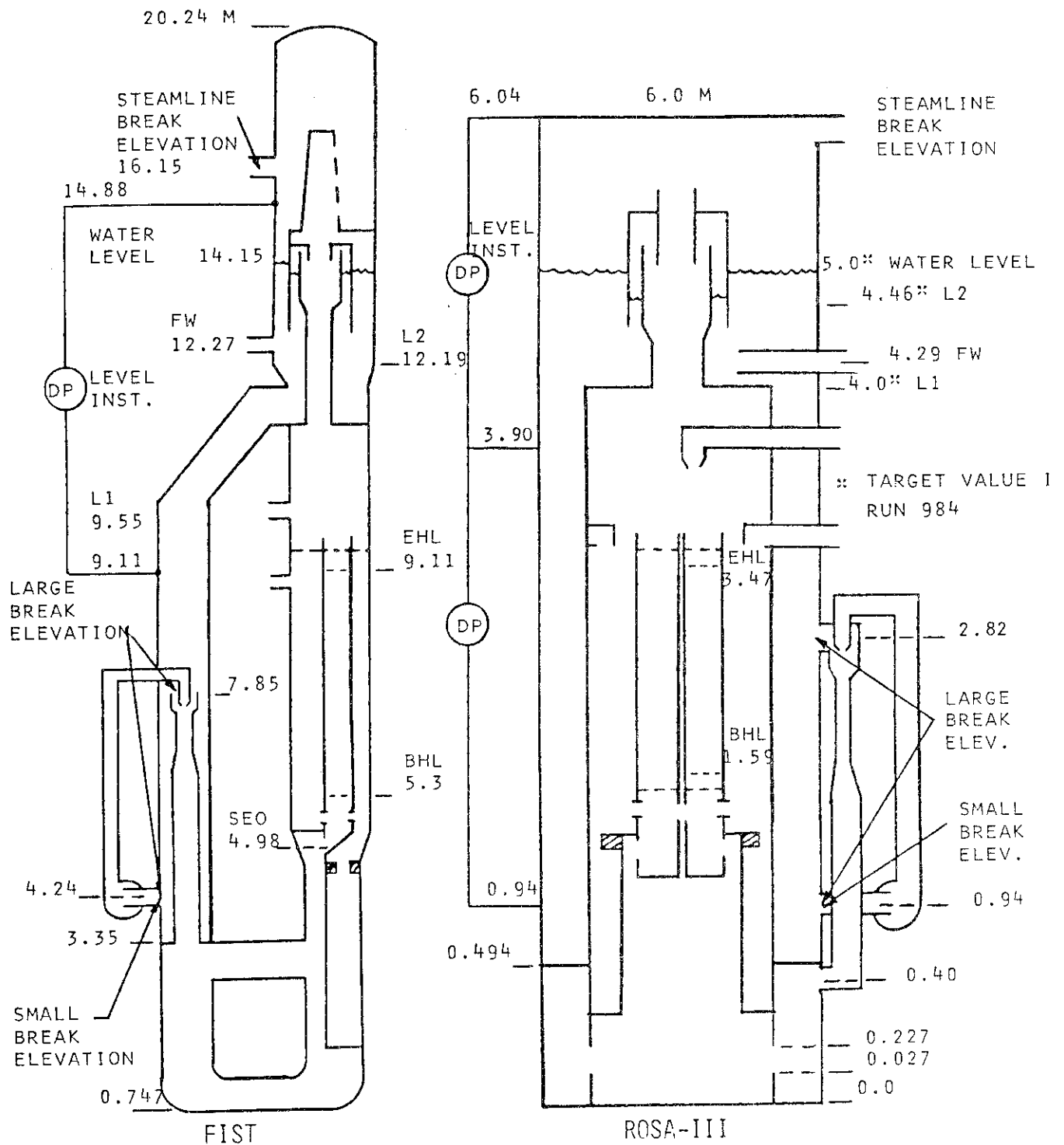


Figure 2-3 Facility Elevations (m), and Level Instruments

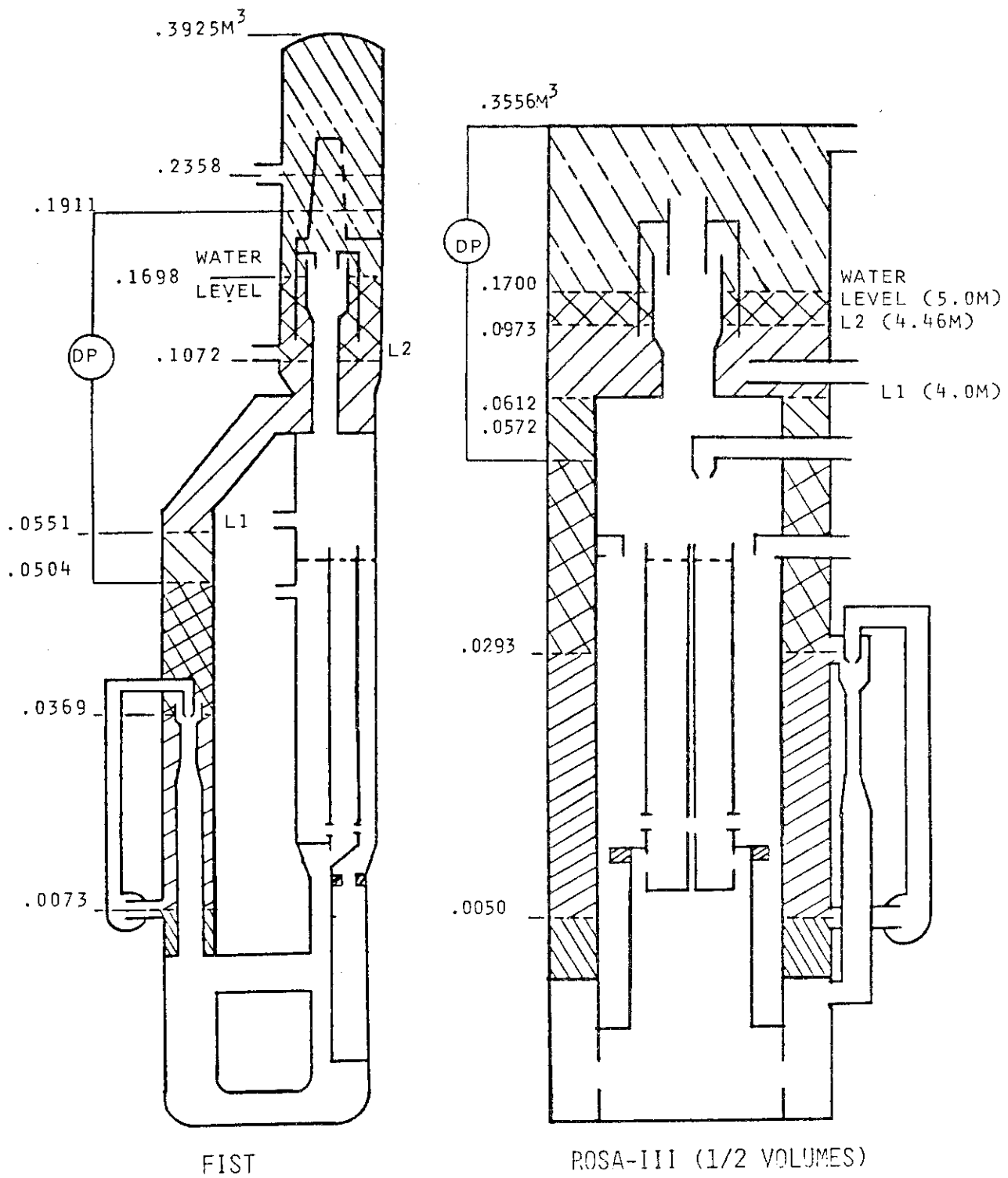


Figure 2-4 Volumes From Bottom of Downcomer (m³)

3. TEST CONDITIONS

3.1 LARGE BREAK

Comparison of initial conditions and boundary conditions are made in Table 3.1-1 for large break tests ROSA 983 and FIST 6DBA1B. The initial system pressures are the same. On a per full size bundle basis, the initial powers and flows should be equal. However, because of power supply limitations, the ROSA-III initial power per full size bundle is 36% of the initial power in FIST. Steamline flow and feedwater flow in ROSA-III are also reduced due to the lower initial core power. The lower initial power and larger total core flow area tend to reduce the bundle void fraction and increase the initial mass in this region.* Although core flow is adjusted to give the specified inlet subcooling, it is very close to the core flow in FIST. The water levels are set with the objective of achieving the same scaled water volume in the downcomer. However, the water level for this test is slightly different, 0.1802m^3 in ROSA-III compared with 0.1698m^3 in FIST.

The transient power curves for the two facilities are compared in Figures 3.1-1A,B, and C. The ROSA-III initial bundle power is held constant until the per bundle power is equal to the decreasing bundle power in FIST (about eight seconds after break initiation) after which the power in ROSA-III is also decayed. As shown in Figure 3.1-1A, this limitation does not appreciably affect the integrated power input to the system as the area under the two curves are not significantly different. ROSA-III power is slightly higher than FIST from 9 seconds until 27 seconds, as shown with an expanded time scale in Figure 3.1-1B, and thereafter the powers are equal. The comparison over the entire test range is plotted with an expanded power scale in Figure 3.1-1C. The test boundary conditions are also compared in Table 3.1-1. In both facilities break initiation is defined as the test start. The combined recirculation line break area in FIST is six percent larger than in

* The core inlet flow rate in this counterpart test is twice that normally used in ROSA-III tests. Thus, in most ROSA-III tests the quality and void fraction in the core are close to BWR values.

ROSA-III. The ROSA-III recirculation suction nozzle area, which determines the dominant break flow in this test, is only four percent smaller. In FIST the drive line break area was scaled to the reference BWR jet pump drive nozzles. In ROSA-III the objective was to adjust this area to match the FIST drive line break. Miscommunication resulted in 22% smaller area in ROSA-III. This drive line break area was 28% smaller than the total flow area of the jet pump drive nozzles in ROSA-III. The FISTS ADS is activated 105 seconds after the Level 1 trips signal (110 seconds after test start), and the ROSA-III ADS is activated 115 seconds after test start by a timer. This difference does not have a significant effect because system pressure is very low by this time. The recirculation pumps are tripped off at time zero in both tests. The FIST recirculation loops are isolated, the broken loop at time zero and the intact loop at 13 seconds, to prevent flashing in these overscaled volumes affecting system response. The loop isolation timing is chosen to minimize flashing without compromising the pump coastdown simulation. It is not necessary to isolate the ROSA-III recirculation loops since these volumes are included in the volume scaling. The feedwater valve is closed at time zero in FIST and at 2 to 4 seconds in ROSA-III. In FIST, the pressure control system simulates the BWR system which keeps the turbine inlet pressure at 6.7 MPa by regulating the turbine valve. In ROSA-III, the pressure control system maintains the vessel pressure at 6.7 MPa. ROSA-III MSIV is closed at 13 seconds, whereas MSIV closure is activated by the Level 1 trip in FIST. The ECC Systems are activated by a timed trip, the HPCS at 27 seconds in both tests and the LPCS and one LPCI at 50 seconds and 35 seconds in ROSA-III and FIST respectively. Injection of LPCS and LPCI are further specified to be activated at system pressures below 1.77 MPa and 1.47 MPa, respectively, in ROSA-III. These pressures in FIST are 1.97 MPa and 1.68 MPa. This simulates the pump shut-off head of a reference BWR. The ECCS pump characteristics, shown as flow as a function of system pressure, are compared in Figure 3.1-2A, 2B, and 2C. The maximum HPCS pressure, Figure 3.1-2A, is determined by the time at which this system is tripped on, since HPCS can deliver flow up to initial system pressure. The ECC Systems in each facility are designed to simulate those in a BWR. This simulation is described further in Appendix A.1 and A.2.

Table 3.1-1

LARGE BREAK COUNTERPART TESTS
INITIAL CONDITIONS AND BOUNDARY CONDITIONS

<u>Initial Conditions</u>		<u>ROSA 983</u>		<u>FIST 6DBA1B</u>	<u>ROSA/FIST Per Full Size Bundle</u>
		<u>Total</u>	<u>Per Full Size Bundle</u>		
Pressure	(MPa)	7.19	-	7.19	-
Power	(MW)	3.62	1.81	5.05	0.36
Core Inlet Subcooling	(K)	11.6	-	9.85	-
Core Inlet Flow	(kg/s)	35.90	17.95	18.55	0.97
Feedwater Flow	(kg/s)	1.26	0.63	2.45	0.26
Feedwater Temperature	(K)	296	-	486	-
Steam Flow	(kg/s)	1.30	0.65	2.63	0.25
Water level	(m)	5.06 ⁽¹⁾	-	14.15	-
Total Liquid Mass	(kg)	706 ⁽²⁾	353	277 ⁽³⁾	1.27
<u>Boundary Conditions</u>					
Power Trip (Fig. 3.1-1)	(s)	9	-	0	-
Break Initiation	(s)	0	-	0	-
Recirc. Line Break ⁽⁸⁾	(mm ²)	619.2	309.6	331.4	0.94
Steamline Break	(mm ²)	-	-	-	-
ADS Flow Area	(mm ²)	349.6	174.8	186.7	0.94
ADS Trip	(s)	115	-	L1+105	-
Pump Trip	(s)	0	-	0	-
Feedwater Line Trip	(s)	2-4	-	0	-
MSIV Trip	(s)	13	-	L1	-
HPCS Trip	(s)	27 ⁽⁴⁾	-	27 ⁽⁶⁾	-
LPCS Trip	(s)	50 ⁽⁵⁾	-	35 ⁽⁷⁾	-
LPCI Trip	(s)	50	-	35	-
HPCS Temperature	(K)	322	-	322	-
LPCS Temperature	(K)	322	-	322	-
LPCI Temperature	(K)	322	-	322	-
HPCS Flow (Fig. 3.2-1A)	(kg/s)	0.80	0.40	0.59	0.68
LPCS Flow (Fig. 3.2-1B)	(kg/s)	1.38	0.69	0.72	0.95
LPCI Flow (Fig. 3.2-1C)	(kg/s)	1.38	0.69	0.52	1.32
Total ECCS Flow	(kg/s)	3.54	1.77	1.83	0.97
Broken Loop Isolation	(s)	N/A	-	0	-
Intact Loop Isolation	(s)	N/A	-	13	-

- (1) Some uncertainty due to flow effects on the downcomer differential pressure measurement.
- (2) The slip ratio was 1.0. The loop mass is included, the feedwater line is not included.
- (3) Estimated mass
- (4) Shutoff pressure is 1.77 MPa.
- (5) Shutoff pressure is 1.47 MPa.
- (6) Shutoff pressure is 1.97 MPa.
- (7) Shutoff pressure is 1.68 MPa.
- (8) See Table 2-1 for suction and drive break areas.

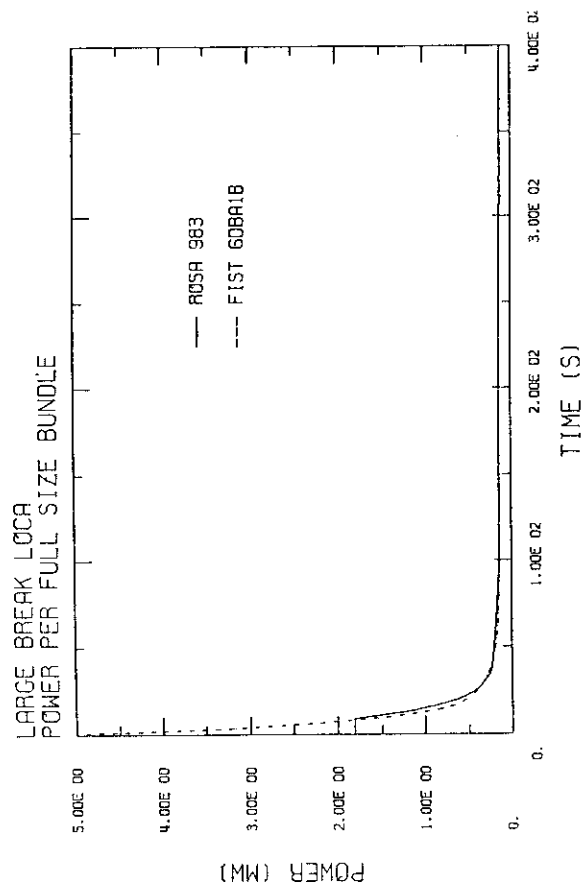


FIG. 3.1-1A POWER

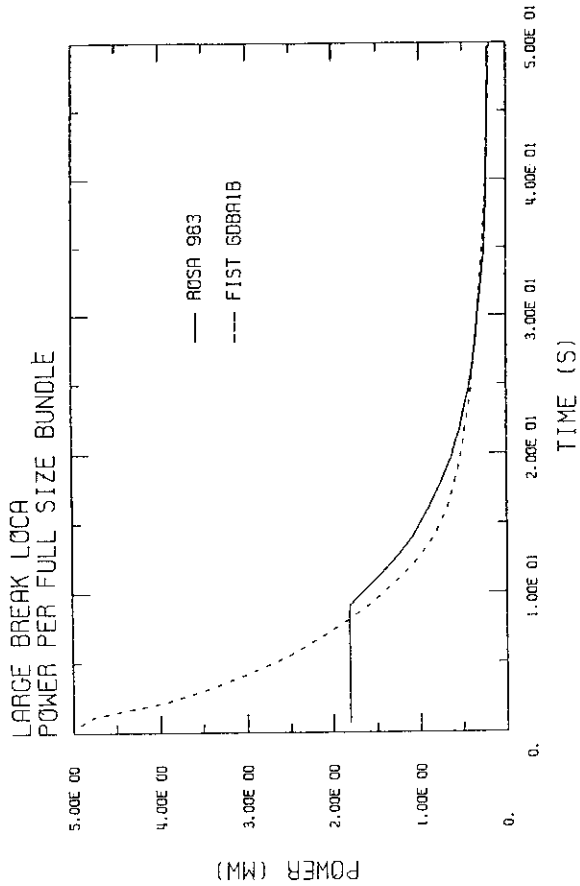


FIG. 3.1-1B POWER

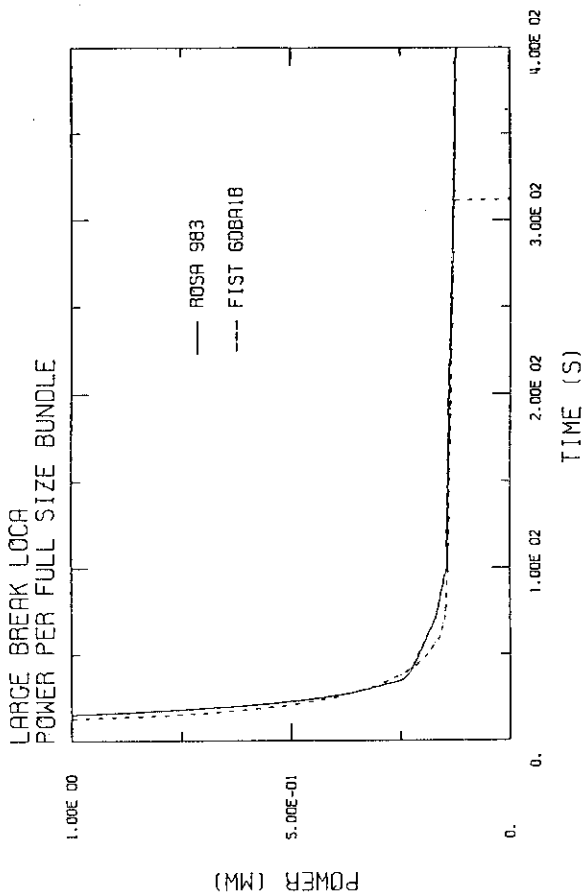


FIG. 3.1-1C POWER

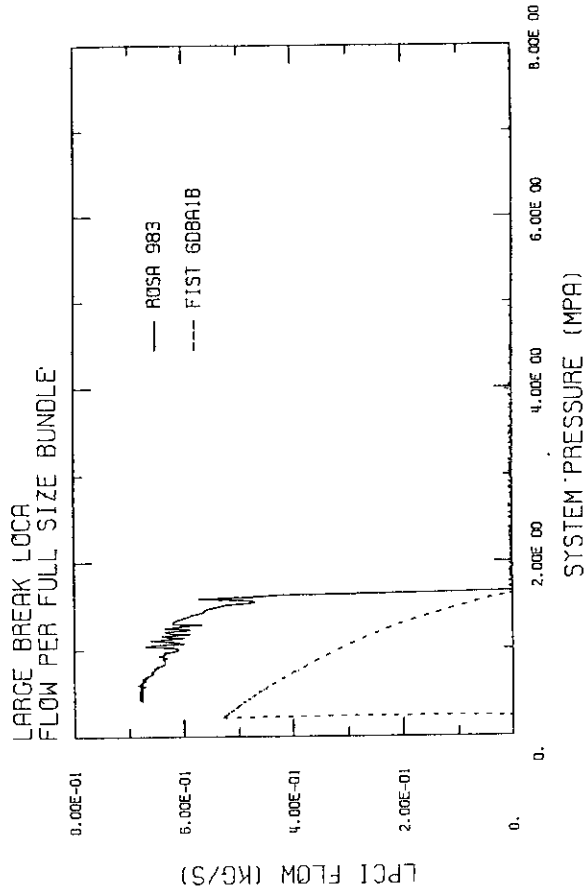


FIG. 3.1-2C LPCI FLOW VS. PRESSURE

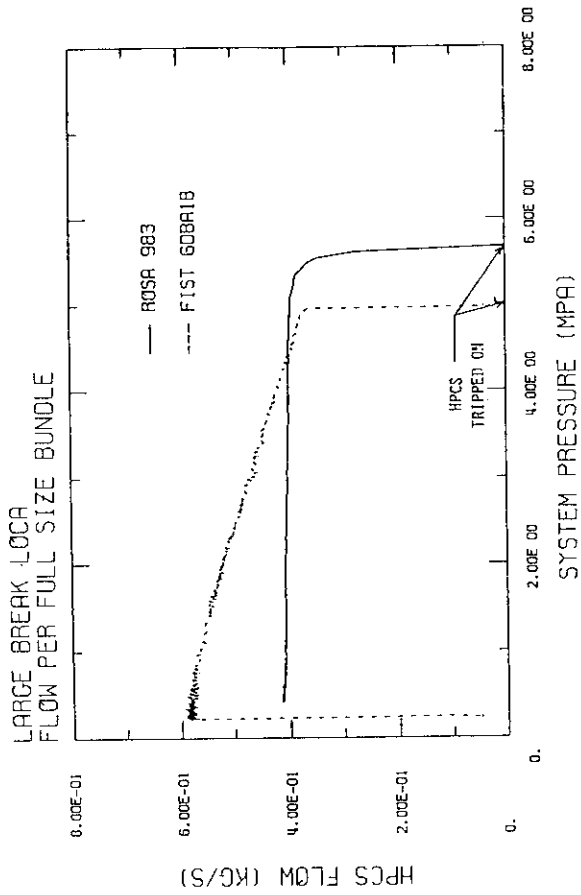


FIG. 3.1-2A HPCS FLOW VS. PRESSURE

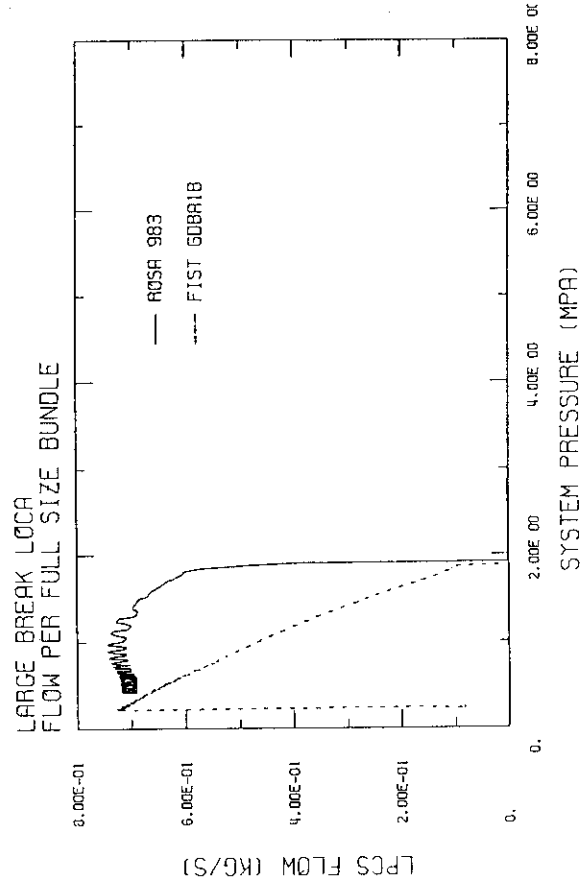


FIG. 3.1-2B LPCS FLOW VS. PRESSURE

3.2 SMALL BREAK

The initial conditions and boundary conditions for small break tests ROSA 984 and FIST 6SB2C are compared in Table 3.2-1. These conditions are essentially the same as for large break tests, and the Section 3.1 discussion also applies here.

The power curves are compared in Figure 3.2-1A, B, and C. Figure 3.2-1A shows the good overall agreement between the two facilities. Again the ROSA-III core power is held constant until it is equal to the decay power curve. The ROSA-III power per one full size bundle is slightly higher than FIST power until about 25 seconds, as seen in Figure 3.2-1B, and slightly lower thereafter, as seen in Figure 3.2-1C. The power is the same to each of the four ROSA-III half length bundles. The small break test boundary conditions are also compared in Table 3.2-1. The break areas are opened at time zero in both tests. The ROSA-III break size^(a) is 7.26mm^2 per full size bundle. The break was simulated by one of two break simulation devices. The FIST break area^(b) is slightly larger, at 7.44mm^2 , and is simulated by a single orifice in the recirculation suction line (Figure 1-2). The pumps are tripped off at test start in both tests. To prevent flashing from these volumes and draining of loop water into the downcomer the FIST broken loop is isolated at the start of the test and the intact loop at 20 seconds. The loops do not need to be isolated in ROSA-III. The feedwater valve is closed at 2 to 4 seconds in ROSA-III and at the start of the test in FIST. This difference has little effect on the responses. The MSIV's are tripped to close by the Level 1 indication in both tests, with a three second delay in ROSA-III and no delay in FIST. The FIST ADS flow area, which is made oversize to partially compensate for the facility excess stored heat, is 6% larger than the ROSA-III ADS area. In both tests, the ADS is tripped by the Level 1 signal and is activated after a 120 second time delay. This is an important trip in the small break tests because it establishes how long the system depressurization, and corresponding low pressure ECCS injection, is delayed. The downcomer

(a) split break

(b) single-ended break

liquid-level instruments that initiate the trip are shown in Figure 2-3. This figure shows the elevations of the level instrument pressure taps, water level, and level trips. Figure 2-4 and Table 2-3 give the downcomer liquid volumes at these elevations. It can be seen that the liquid volume lost from the downcomer before the Level 1 trip is similar, 0.1452m^3 in ROSA-III and 0.1147m^3 ($0.1698-0.0551$) for FIST. In both tests, the ECCS make-up is provided by one LPCS and three LPCI's. In FIST, these systems are tripped by a simulated high containment pressure, which occurs at test start, with a 35-second delay. In ROSA-III, the systems are tripped by Level 1 with a 40-second delay. The difference in the trip signals has little effect on the system responses since the low pressure systems do not inject coolant until the system pressure drops below 2.0 MPa following ADS. This is shown by the ECCS flow versus pressure curves, Figure 3.2-2A and B. The LPCS and LPCI pressure versus flow curves are similar to those in the large-break tests. ROSA-III has a 30% higher maximum ECCS flow rate than FIST (Table 3.2-1), primarily due to the contribution from the three LPCI's which have a combined maximum flow rate 45 percent greater. The LPCS flows are very nearly the same in both tests. In FIST the broken loop is isolated at test start and the intact loop at 20 seconds to minimize the effects of flashing from these oversize volumes. The loops are not isolated in ROSA-III.

Table 3.2-1

SMALL BREAK COUNTERPART TESTS
INITIAL CONDITIONS AND BOUNDARY CONDITIONS

		ROSA 984		FIST 6SB2C	ROSA/FIST Per Full Size Bundle
		Total	Per Full Size Bundle		
<u>Initial Conditions</u>					
Pressure	(MPa)	7.22	-	7.23	-
Power	(MW)	3.62	1.81	5.05	0.36
Core Inlet Subcooling	(K)	12.9	-	10.0	-
Core Inlet Flow	(kg/s)	30.2	15.1	19.1	0.79
Feedwater Flow	(kg/s)	1.1	0.55	2.3	0.24
Feedwater Temperature	(K)	296	-	478	-
Steam Flow	(kg/s)	1.3	0.65	2.6	0.25
Water Level	(m)	5.21 ⁽⁵⁾	-	14.0	-
Total Liquid Mass	(kg)	710 ⁽⁶⁾	355	277	1.28
<u>Boundary Conditions</u>					
Power Trip (Fig. 3.2-1)	(s)	7	-	0	-
Break Initiation	(s)	0	-	0	-
Recirc. Line Break	(mm ²)	14.52	7.26	7.44	0.98
Steamline Break	(mm ²)	-	-	-	-
ADS Flow Area	(mm ²)	349.6	174.8	186.7	0.94
ADS Trip	(s)	L1+120	-	L1+120	1.00
Pump Trip	(s)	0	-	0	1.00
Feedwater Line Trip	(s)	2-4	-	0	1.00
MSIV Trip	(s)	L1+3	-	L1	1.00
HPCS Trip	(s)	-	-	-	-
LPCS Trip	(s)	L1+40 ⁽¹⁾	-	35 ⁽³⁾	-
LPCI Trip	(s)	L1+40 ⁽²⁾	-	35 ⁽⁴⁾	-
HPCS Temperature	(K)	-	-	-	-
LPCS Temperature	(K)	305	-	305	-
LPCI Temperature	(K)	305	-	305	-
HPCS Flow	(kg/s)	0	0	0	-
LPCS Flow (Fig. 3.2-2A)	(kg/s)	1.40	0.70	0.68	1.03
LPCI Flow (Fig. 3.2-2B) -	(kg/s)	3.48	1.74	1.20	1.45
Total ECCS Flow	(kg/s)	4.88	2.44	1.88	1.30
Broken Loop Isolation	(s)	N/A	-	0	-
Intact Loop Isolation	(s)	N/A	-	20	-

(1) Shutoff pressure is 1.86 MPa.

(2) Shutoff pressure is 1.57 MPa.

(3) Shutoff pressure is 1.97 MPa.

(4) Shutoff pressure is 1.68 MPa.

(5) Some uncertainty due to flow effects on the downcomer differential pressure.

(6) A slip ratio of one is assumed. The loop mass is included. The feedwater line is not included.

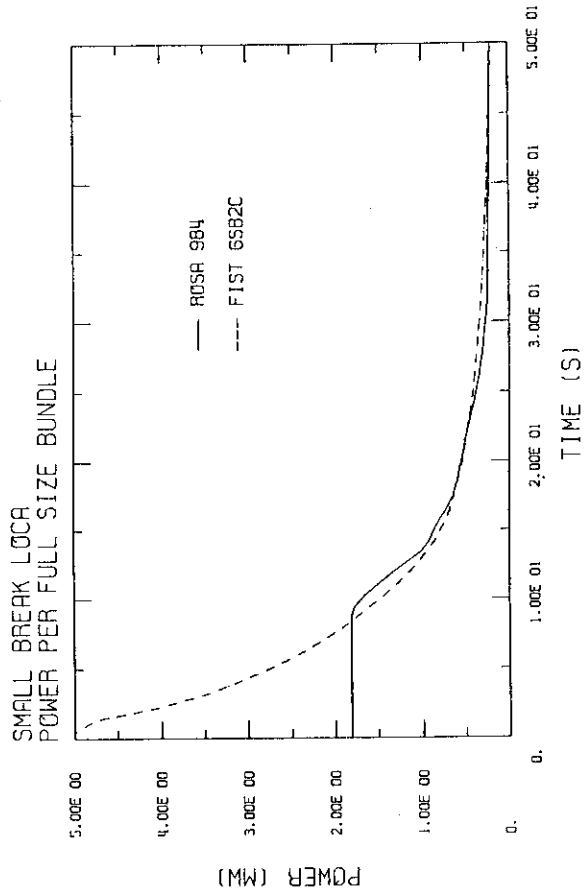


FIG. 3.2-1B POWER

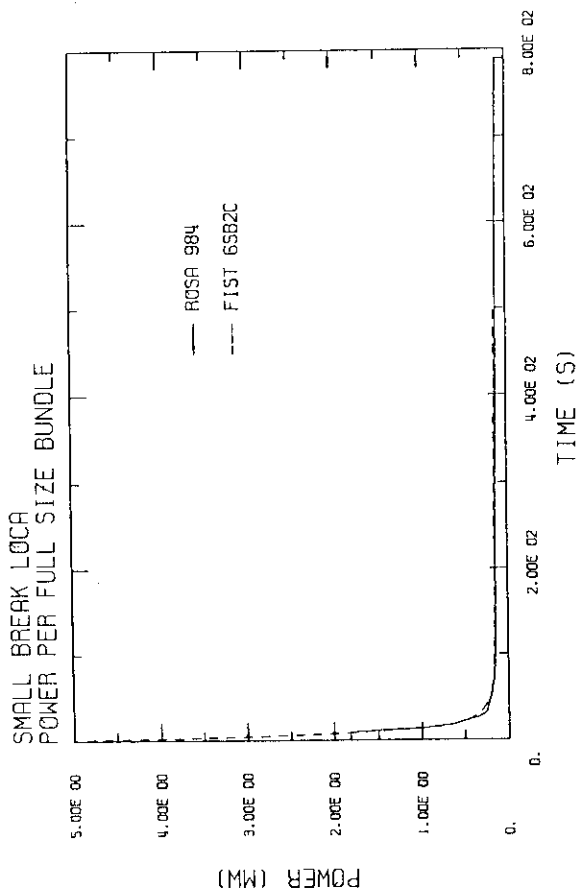


FIG. 3.2-1A POWER

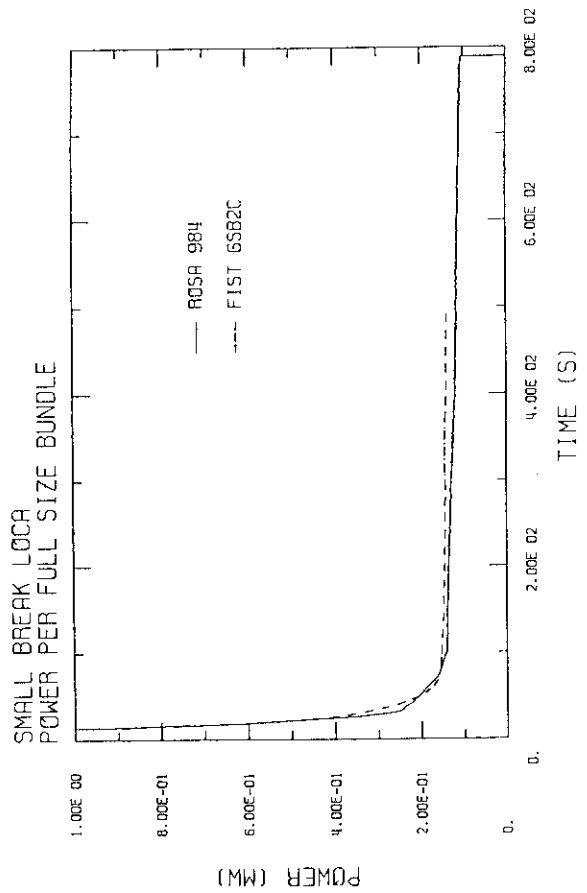


FIG. 3.2-1C POWER

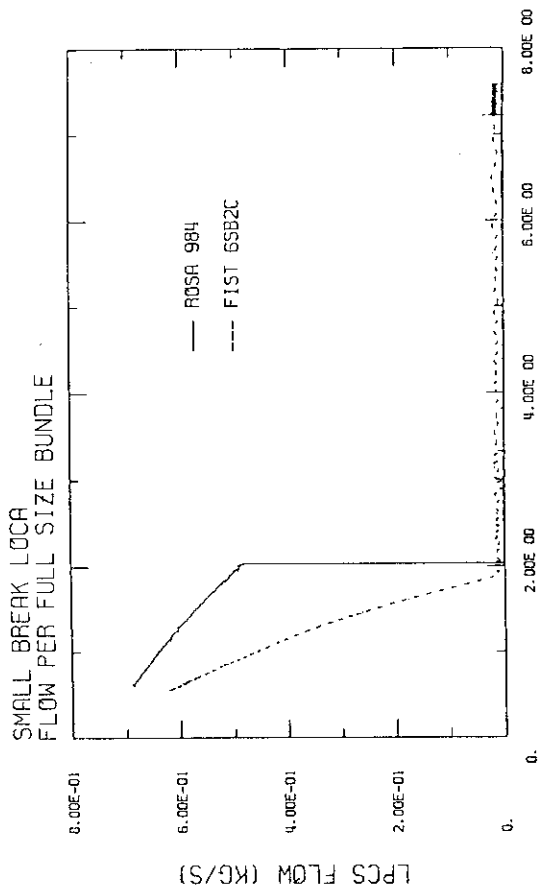


FIG. 3.2-2A LPCS FLOW VS. PRESSURE

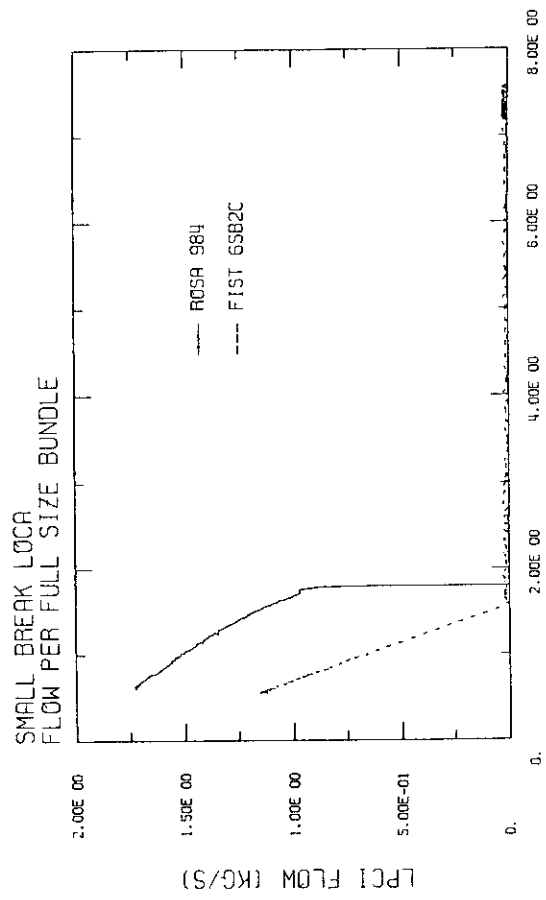


FIG. 3.2-2B LPCI FLOW VS. PRESSURE

3.3 STEAMLINE BREAK

The initial conditions and boundary conditions are summarized in Table 3.3-1 for ROSA 952 and FIST 6MSB1. The system pressure, core inlet temperature, and core outlet quality compare very closely between the two tests. The comparison of the power curves in Figure 3.3-1A shows the initial ROSA-III power held constant for the first eight seconds before it is decayed. After six seconds, the ROSA-III power is higher than FIST. For the first 50 seconds this difference is shown in Figure 3.3-1B. The longer term difference is shown in Figure 3.3-1C. ROSA-III Tests 983 and 984 were performed as counterpart tests of FIST Tests 6DBA1B and 6SB2C respectively. The power curves for these tests compare closely between the two facilities. ROSA Test 952 was not performed as a counterpart test of FIST Test 6MSB1, so no effort was made to precisely match the two power curves. This difference in the power curves reflects the different heater designs and approaches used in each facility to take rod stored heat into account in simulating the bundle heat transfer. The relatively higher power for the ROSA-III steamline break test was determined analytically to give conservative fuel rod responses.

From zero to 5.5 seconds the relative FIST break area is larger than ROSA-III. FIST simulates flow through one broken main steamline plus flow back through the three intact main steamlines before MSIV closure. A 31.0mm orifice is used to simulate the one broken steamline after 5.5 seconds when the MSIV's are closed. The 31.0mm orifice used throughout in ROSA-III corresponds to 100% of one steamline. There is no ADS activation in either test. The recirculation pumps are tripped at test start. In FIST, both recirculation loops are isolated at 7 seconds to minimize the effects of loop flashing, while still allowing the pump coastdown. The FIST feedwater valve is closed at test start and the ROSA-III valve at 1.3 seconds. Steamline break system depressurization is much more rapid in the early blowdown phase than in either the large recirculation line break or the small recirculation line break.

The ROSA-III HPCS is tripped at Level 2, with a 27-second delay assuming failure of high containment pressure signal, whereas FIST HPCS is tripped on a simulated high containment pressure that occurs as soon as the break is initiated, plus a 27 second delay. In ROSA-III, the LPCS and LPCI trip settings are Level 1 with a 40-second delay, and in FIST the trips are high containment pressure (test start), with a 35-second delay. However, since the LPCS and LPCI systems in ROSA-III did not tripped on, only the HPCS flow characteristics are compared, Figure 3.3-2. The curves reflect the pressure at which the systems are activated, whereas they are capable of injecting coolant up to the initial system pressure.

Table 3.3-1

STEAMLINE BREAK COUNTERPART TESTS
INITIAL CONDITIONS AND BOUNDARY CONDITIONS

<u>Initial Conditions</u>		ROSA 952		FIST 6MSB1	ROSA/FIST Per Full Size Bundle
		Total	Per Full Size Bundle		
Pressure	(MPa)	7.35	-	7.17	-
Power	(MW)	3.96	1.98	4.62	0.43
Core Inlet Subcooling	(K)	10.7	-	9.0	-
Core Inlet Flow	(kg/s)	16.6	8.3	17.0	0.49
Feedwater Flow	(kg/s)	2.04	1.02	2.34	0.44
Feedwater Temperature	(K)	491	-	489	-
Steam Flow	(kg/s)	2.06	1.03	2.49	0.41
Water Level	(m)	5.14 ⁽⁵⁾	-	14.0	-
Total Liquid Mass	(kg)	661 ⁽¹⁾	331 ⁽¹⁾	277	1.19
<u>Boundary Conditions</u>					
Power Trip (Fig. 3.3-1)	(s)	8	-	0	-
Break Initiation	(s)	0	-	0	-
Recirc. Line Break	(mm ²)	-	-	-	-
Steamline Break	(mm ²)	754.8	377.4	501/377 ⁽²⁾	0.75/1.00
ADS Flow Area	(mm ²)	-	-	-	-
ADS Trip	(s)	-	-	-	-
Pump Trip	(s)	0	-	0	-
Feedwater Line Trip	(s)	1.3	-	0	-
MSIV Trip	(s)	0	-	5.5	-
HPCS Trip	(s)	L2+27	-	27	-
LPCS Trip	(s)	L1+40	-	35 ⁽³⁾	-
LPCI Trip	(s)	L1+40	-	35 ⁽⁴⁾	-
HPCS Temperature	(K)	313	-	324	-
LPCS Temperature	(K)	313	-	319	-
LPCI Temperature	(K)	313	-	319	-
HPCS Flow (Fig. 3.3-2)	(kg/s)	0.84	0.42	0.57	0.73
LPCS Flow	(kg/s)	0	0	0.68	-
LPCI Flow	(kg/s)	0	0	0.51	-
Total ECCS Flow	(kg/s)	0.84	0.42	1.76	0.24
Broken Loop Isolation	(s)	N/A	-	7	-
Intact Loop Isolation	(s)	N/A	-	7	-

(1) Total liquid mass of the ROSA-III includes mass in jet pumps and recirculation loops. The feedwater line is not included

(2) The FIST steamline break area is changed from 501 mm² to 377 mm² at 5.5 seconds.

(3) Shutoff pressure is 1.97 MPa.

(4) Shutoff pressure is 1.68 MPa.

(5) Some uncertainty due to flow effect on the downcomer differential pressure.

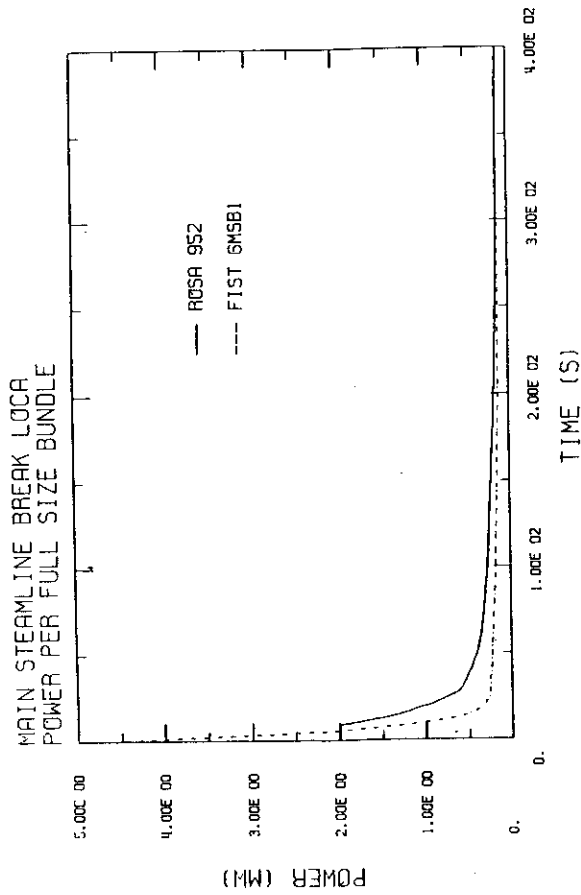


FIG. 3.3-1A POWER

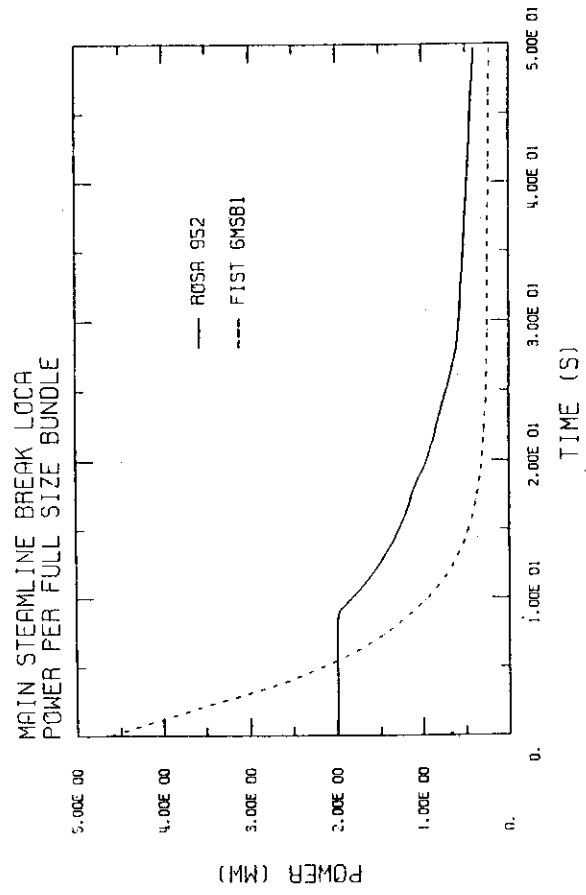


FIG. 3.3-1B POWER

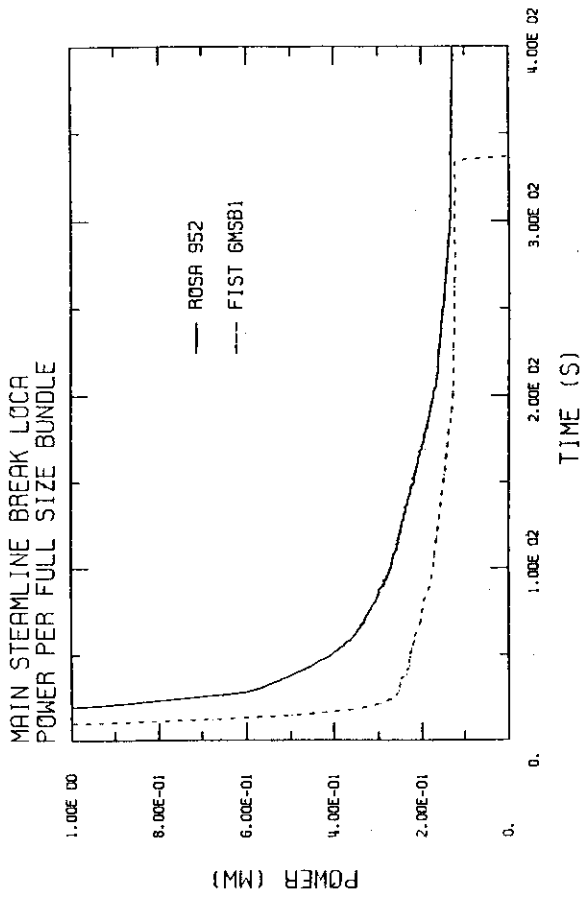


FIG. 3.3-1C POWER

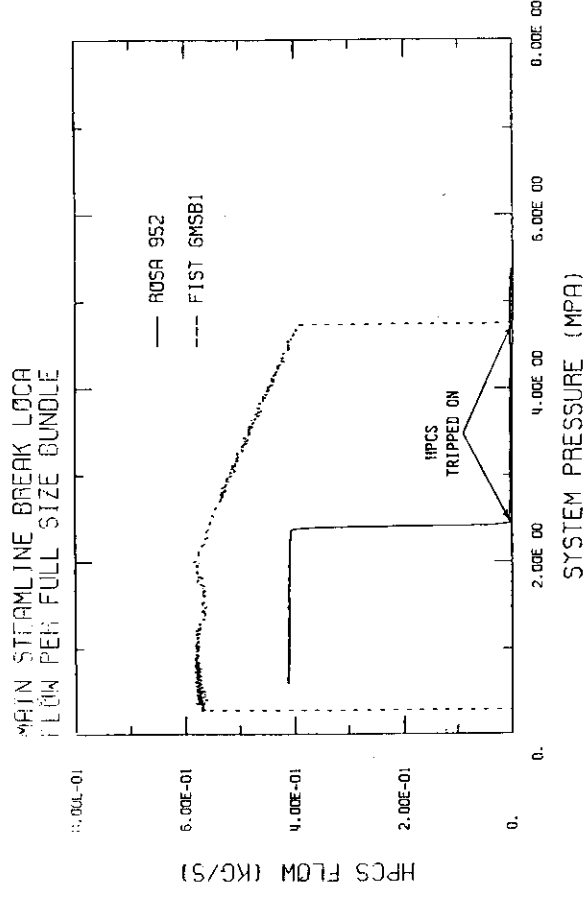


FIG. 3.3-2 HP/CS FLOW VS. PRESSURE

4. TEST RESULTS

4.1 LARGE BREAK

The large break LOCA transient tests begin with the opening of the break valves. At the same time the recirculation pumps are tripped off, the feedwater valves start closing, and the bundle power starts decaying (as discussed in Section 3, the power decay is delayed by 8 seconds in ROSA-III). The timing of these and other key events that follow are compared in Table 4.1-1.

Following break initiation, there is an inter-relationship of the short term system responses. The initial break flow rate, shown in two time frames in Figure 4.1-1A and B, is influenced by the subcooling at the break, Figure 4.1-2. This subcooling is a function of the downcomer temperature, which is lower in FIST, and the system pressure, Figure 4.1-3A. The pressure at the beginning of the transient is fixed by the pressure controller, which regulates the steam flow, shown in Figures 4.1-4A and B. Initially, FIST is controlled at a slightly higher pressure than ROSA-III, as seen in Figure 4.1-3A. The result is greater subcooling upstream of the FIST break, and therefore a higher flow rate during the subcooled phase of the break as seen in Figure 4.1-1A. Also there is some friction loss between the downcomer and the break location in ROSA-III. [In ROSA-III the break flow is measured by drag disks and gamma densitometers. In FIST, drag disks and turbine meters are used.]

The sudden break initiation reverses the drive line flow in the broken loop. This rapidly reduces the core flow, as seen in Figure 4.1-5. The FIST core flow decreases from 18.55 kg/sec to 6 kg/sec in about one second. As the recirculation pump in the intact loop coasts down the core flow continues to decrease gradually. The ROSA-III core flow experiences a similar initial decrease from 18 kg/sec to 4 kg/sec and a subsequent gradual decay.

The downcomer water is lost out of the break very rapidly. Makeup from the feedwater line is quickly shut off, as seen in Figure 4.1-6, and has no significant contribution to the downcomer level transient.

The downcomer liquid volume is shown in Figure 4.1-7 as a function of time. FIST, having a greater subcooled break flow and recirculation flow, and smaller initial downcomer mass, depletes downcomer water more rapidly than ROSA-III. The FIST Level 1 MSIV trip is reached at 4.5 seconds. The MSIV starts closing and is almost completely closed at 7 seconds, as shown by the steam flow in Figure 4.1-4A. The ROSA-III MSIV closure, which is timed, occurs at 13 seconds. This causes FIST pressure, Figure 4.1-3A, to rise slightly faster than ROSA-III during this period. At 5 seconds in FIST and 12 seconds in ROSA-III, the top of the jet pumps are uncovered, Figure 4.1-7, reducing the core flow to almost zero, Figure 4.1-5. Finally, the downcomer level reaches the recirculation line suction nozzle level, at 8 seconds in FIST and 17 seconds in ROSA-III. When the suction line is uncovered the break flow is no longer subcooled liquid but saturated steam. Figures 4.1-1A and B show the break mass flow suddenly drop at uncovering, and Figure 4.1-2 shows that the temperature becomes saturated. Venting of steam out of the break causes the system pressure to decrease rapidly, Figures 4.1-3A and B, which is also reflected in the saturation temperature, Figure 4.1-2. The downcomer level transient response during the early phase of the LOCA is shown in Figure 4.1-8. The normalized water levels are compared, where 100% is the initial water level and 0% is the level of the recirculation line suction nozzle.

The different recirculation line break uncovering timing causes an earlier system depressurization in FIST. As a consequence, the FIST system pressure, Figure 4.1-3B, remains slightly lower than ROSA-III throughout the remainder of the transient. The small steam flow when the ADS is activated, Figure 4.1-4B, does not have a significant effect on the system pressure. The FIST ADS flow is lower than ROSA-III because the system pressure is lower.

The earlier break uncover and depressurization in FIST also leads to earlier lower plenum flashing and associated level swell (11.5 seconds versus 18 seconds). Following lower plenum flashing, a two-phase level forms in the lower plenum, at 18 seconds in FIST and at 27 seconds in ROSA-III, as seen in Figure 4.1-9. While there is a level in the lower plenum the liquid draining from the bundles is controlled by CCFL at the inlet orifices. The lower plenum level in FIST reaches the bottom of the jet pumps at 39 seconds and some lower plenum steam vents out the jet pumps. This leads to increased bundle drainage and level drop, and causes rod heat up in FIST. Parallel channel flow (cf. Reference 8) in ROSA-III redistributes lower plenum steam among the bundles when the lower plenum level forms. This is indicated by the bundle inlet flow rates in Figure 4.1-10. Bundle A shows upflow while bundles B and D are in countercurrent flow. Bundle C shows some countercurrent flow, then upflow. This parallel channel flow effect on temperatures in the different bundles is discussed below.

Core uncover and heatup beings at very nearly the same time in both facilities, 39 seconds in ROSA-III and 41 seconds in FIST. In FIST, Figure 4.1-11, the HPCS and LPCS liquid supplied to the upper plenum flows down through the upper tieplates and starts quenching the bundle from the top. This, together with the contribution from the LPCI, start bundle reflood at 100 seconds, and limits the PCT to 656K (721°F) at location 4 (core midplane). ROSA-III bundle D, which shows countercurrent flow at the inlet orifice, heats up at the very top due to core uncover and with only the HPCS, less liquid downflow through the upper tieplate. Bundle B, which also shows countercurrent flow at the inlet orifice, has slightly lower temperatures (Figure 4.1-12). The activation of the LPCS and LPCI quench the rods and reflood the bundles. Upflow into bundles A and C, keeps them full of a two-phase mixture and well cooled.

Even though the bundles, as well as the complete systems, are of different lengths, the thermal-hydraulic response is consistent between the two facilities. The hot bundles are in counter-current flow. The

PCT is slightly higher in FIST, mainly because the absence of parallel channel flow effects causes the jet pumps to vent some lower plenum steam which drains liquid from the bundle.

The FIST ECC Systems come on at 27, 64, and 75 seconds, as shown in Figures 4.1-13A, B, and C. These curves are consistent with the flow vs. pressure curves, Figures 3.1-2A, B, and C, and the system pressure, Figure 4.1-3B. The core spray injection into the upper plenum provides liquid for downflow through the upper tieplate, and leads to a CCFL breakdown at 125 seconds. In ROSA-III, the HPCS also comes on at 27 seconds, and the LPCS and LPCI at 85 and 95 seconds respectively. The HPCS flow is less and the LPCI greater than in FIST. The total ECCS injection is the same in both tests, as shown in Figure 4.1-13D.

The total vessel liquid mass in each facility, Figure 4.1-14, compare very closely. This demonstrates that the net boundary flows are equal. These flows are the break flow, steamline flow, feedwater flow, and ECCS flows.

Summary

Overall, the ROSA-III and FIST system responses for the large break tests compare very well. In particular the system pressure responses and the system masses compare very well between the two tests. This demonstrates that the mass flow and energy flow rates are very similar. The ROSA-III hot bundle hydraulic response during heatup and rewet is similar to that of the FIST bundle. The inlet flow to the hot bundle is counter current, controlled by CCFL at the inlet orifice. And finally, the height scaling in ROSA-III does not have a significant effect on the system response.

Differences in responses attributed to facility differences are the slightly delayed system depressurization in ROSA-III caused by the later recirculation break uncovering. This is due to large initial downcomer liquid mass and lower subcooled break flow in ROSA-III. The delayed system depressurization in ROSA-III also delays the LPCS and LPCI

injection about twenty seconds. The FIST bundle has more bundle uncover than ROSA-III because it does not have parallel channels. Lower plenum steam flows out the FIST jet pumps when they uncover allowing more liquid to drain from the bundle.

Table 4.1-1

LARGE BREAK COUNTERPART TESTS
TIMING OF KEY EVENTS

Key Events	Time (sec.)	
	ROSA 983	FIST 6DBA1B
Break Valves Open	0.0	0.0
Pump Coast-Down Begins	0.0	0.0
Feedwater Line Closes	2.0-4.0	1.0
Power Decay Initiated	8.0	0.1
Level 1 Trip	NA	4.5
Jet Pump Suction Uncovers	12.0	5.0
MSIV Closes	13.0-15.0	7.0
Recirc. Suction Break Uncovers	17.0	8.0
Lower Plenum Flashing Begins	18.0	11.5
Guide Tube Flashing Begins	20.0	12.0
Lower Plenum Level Forms	27.1	18.0
Jet Pump Exit Uncovers	-	39.0
Jet Pump Loop Isolated (Intact)	0	13.0
HPCS Flow Begins	27.0	27.0
Bundle Heat-Up Begins	39.6	41.0
PCT Occurs	81.2	110.0
PCT Temperature	575K	656K
PCT Location	Position 2 ⁽¹⁾	Position 4
LPCS Flow Begins	85.0	54.0
LPCI Flow Begins	95.0	75.0
ADS Actuation	115.0	110.0
Bypass/GT Refill Begins	-	115.0
Bypass CCFL Breakdown	-	115.0
Bypass Refilled	-	125.0
Bundle Reflooding Begins	92.3	125.0
Bundle Reflooded	114.6	125.0
UTP CCFL Breakdown	-	125.0
Bundle Quenched	120.8	125.0
Jet Pump Exit Recovers	-	145.0
End of test	450.0	315.0

(1) Bundle D.

LARGE BREAK LOCA

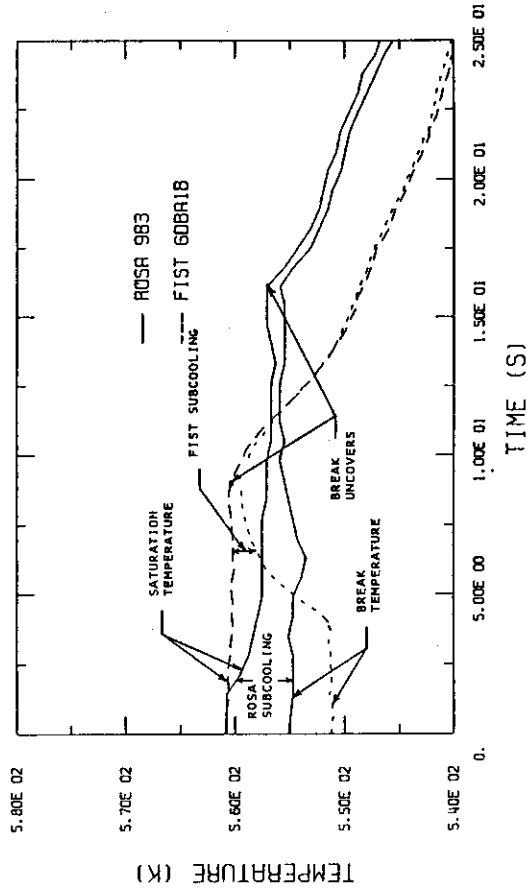


FIG. 4.1-2 BREAK TEMPERATURE

LARGE BREAK LOCA

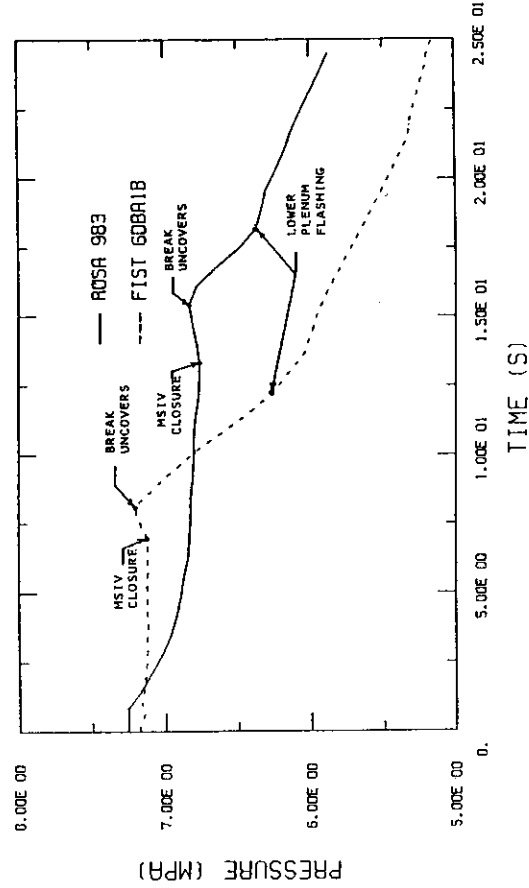


FIG. 4.1-3A SYSTEM PRESSURE

LARGE BREAK LOCA
FLOW PER FULL SIZE BUNDLE

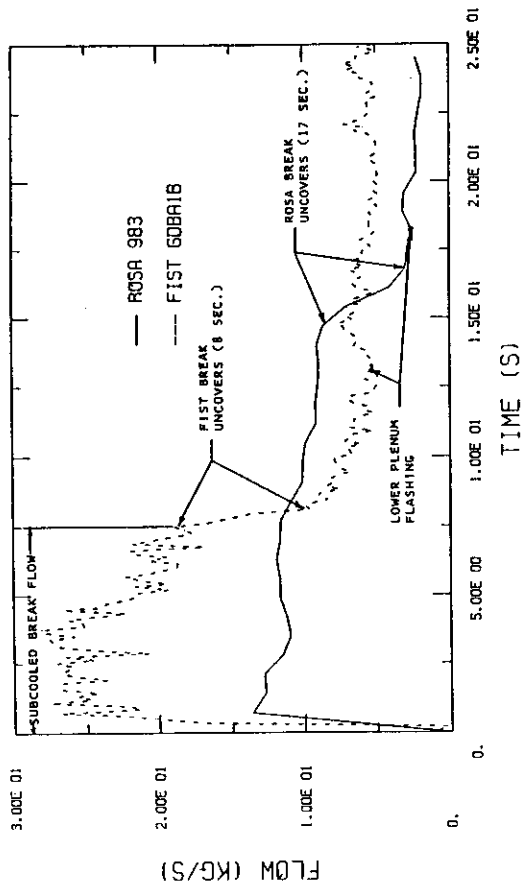


FIG. 4.1-1A BREAK FLOW

LARGE BREAK LOCA
FLOW PER FULL SIZE BUNDLE

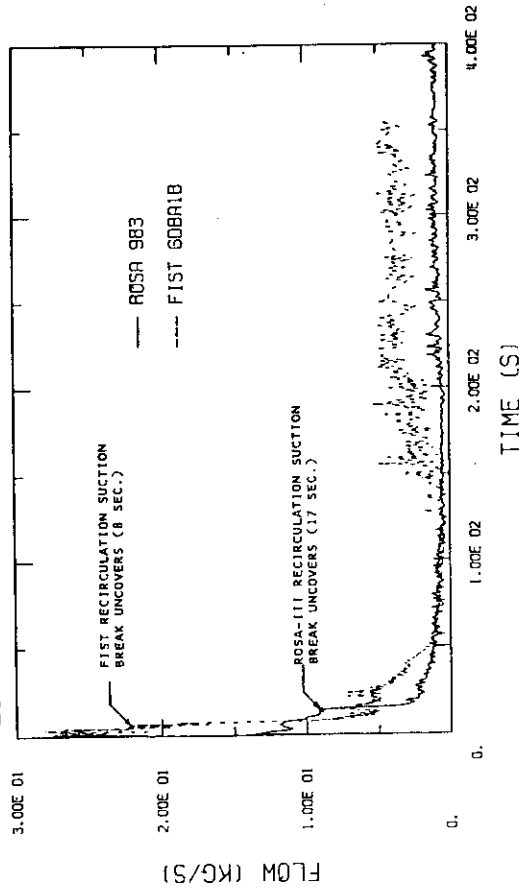


FIG. 4.1-1B BREAK FLOW

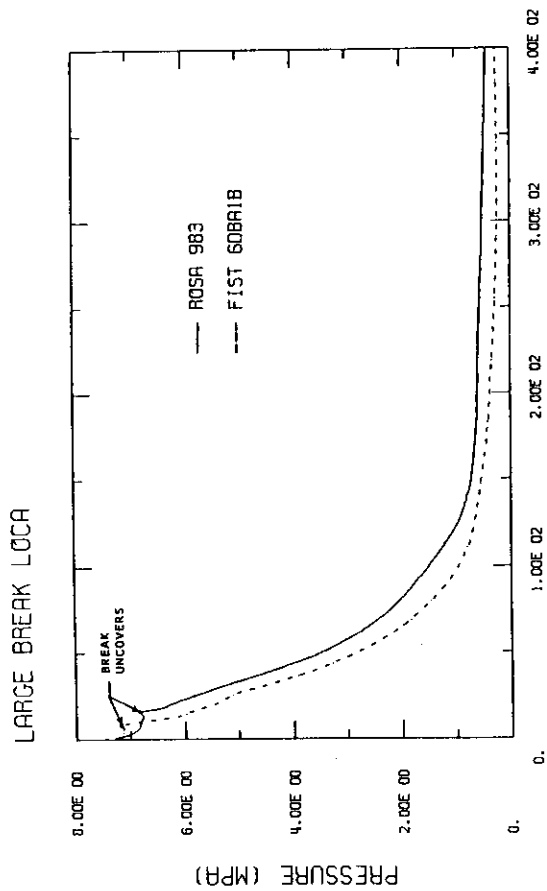


FIG. 4.1-3B SYSTEM PRESSURE

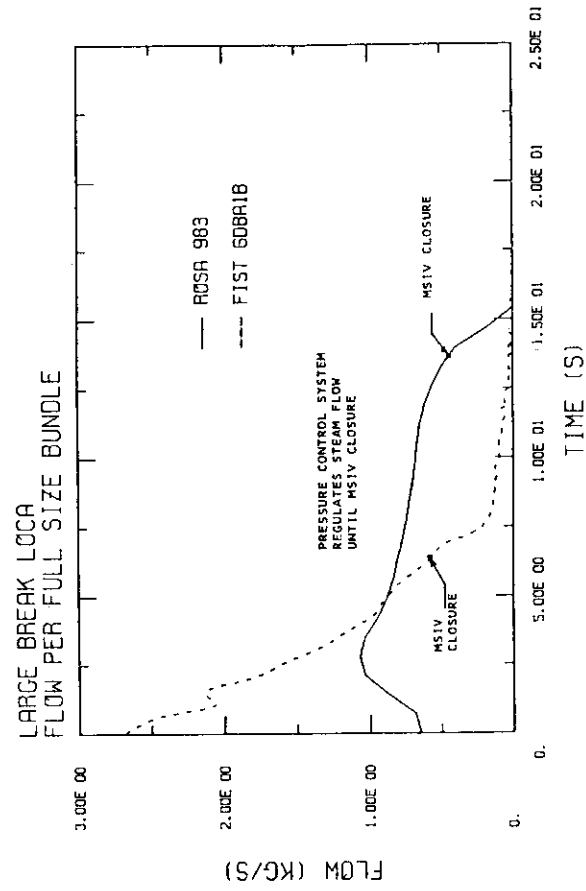


FIG. 4.1-4A STEAMLINE FLOW

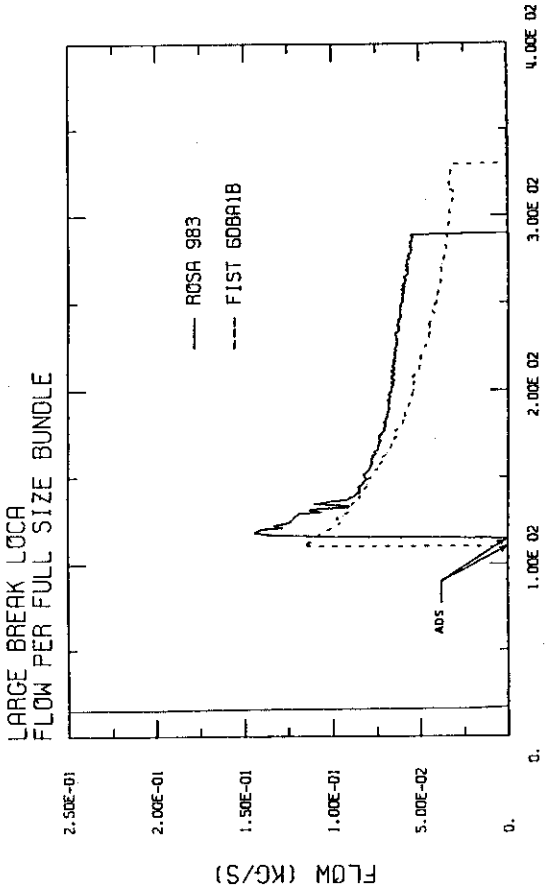


FIG. 4.1-4B STEAMLINE FLOW

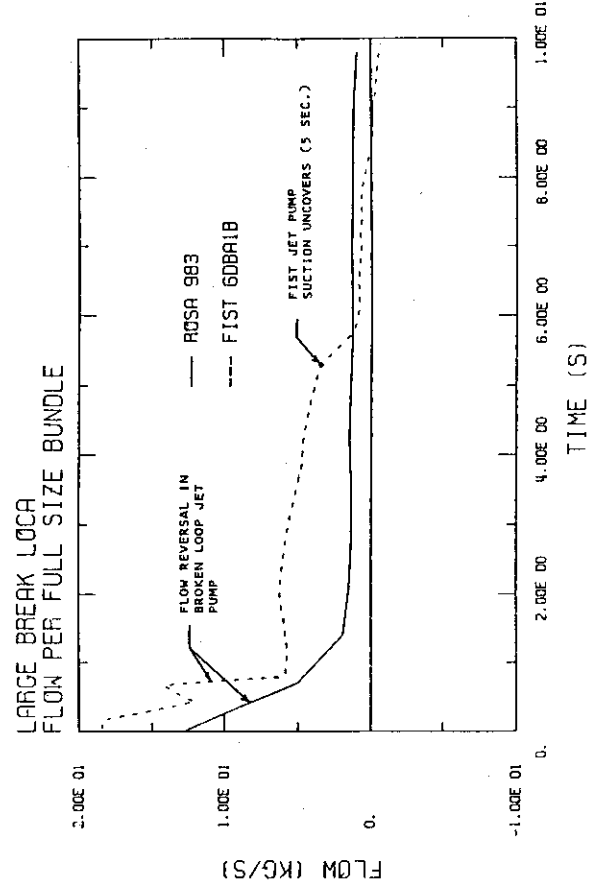
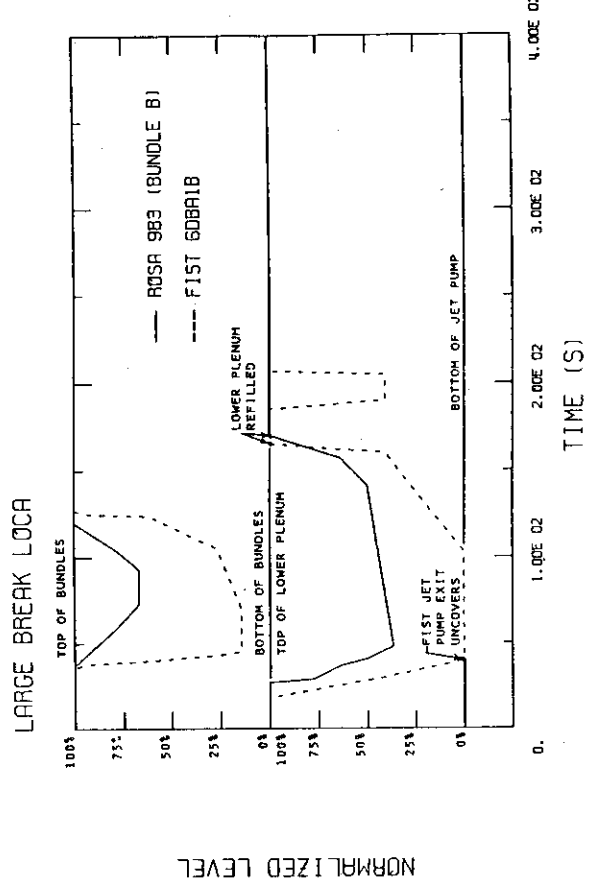
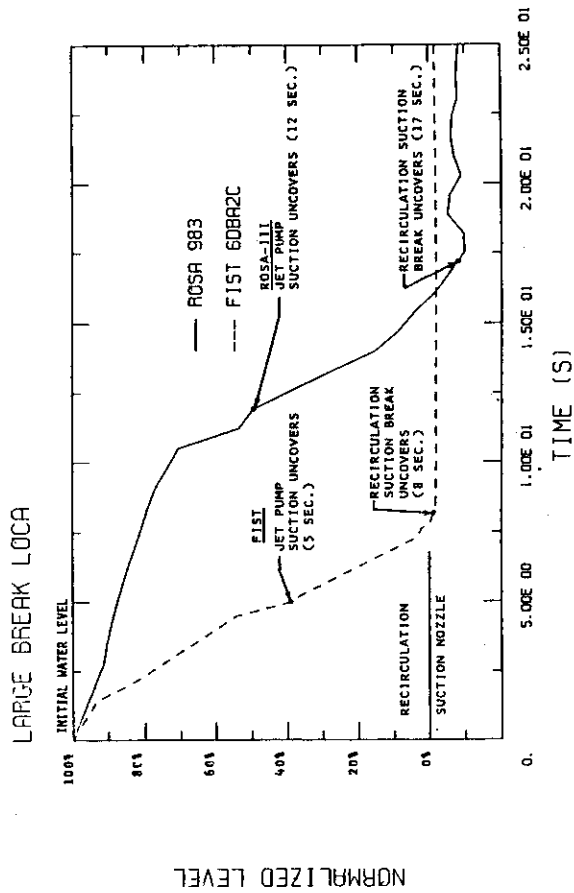
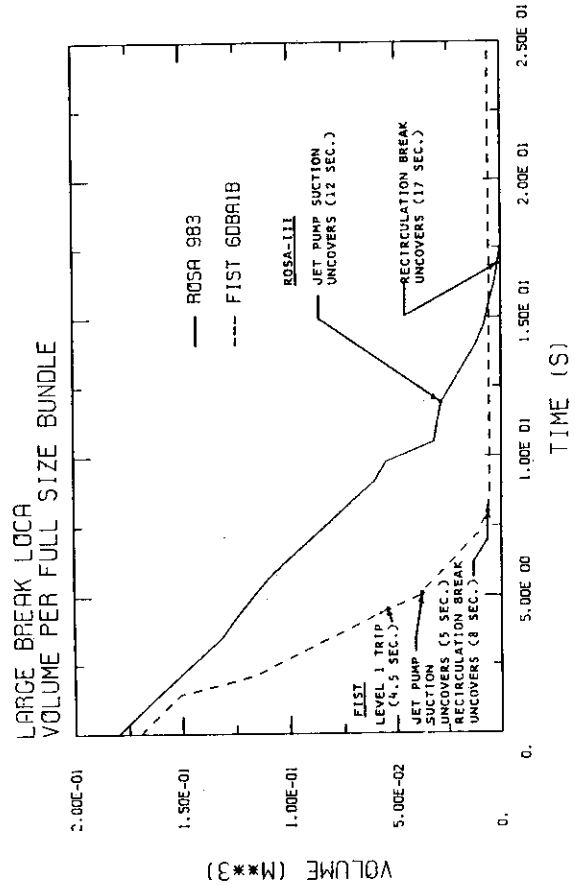
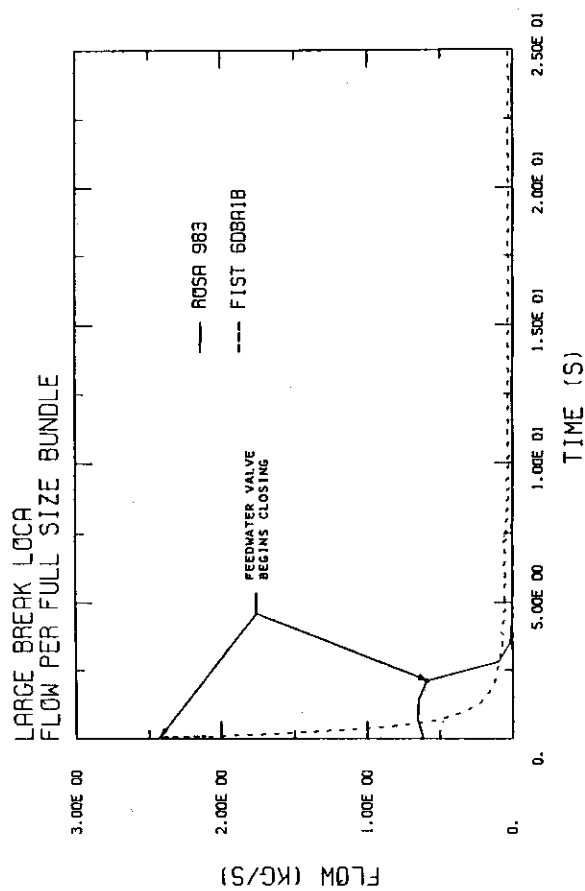


FIG. 4.1-5 CORE FLOW



LARGE BREAK LOCA

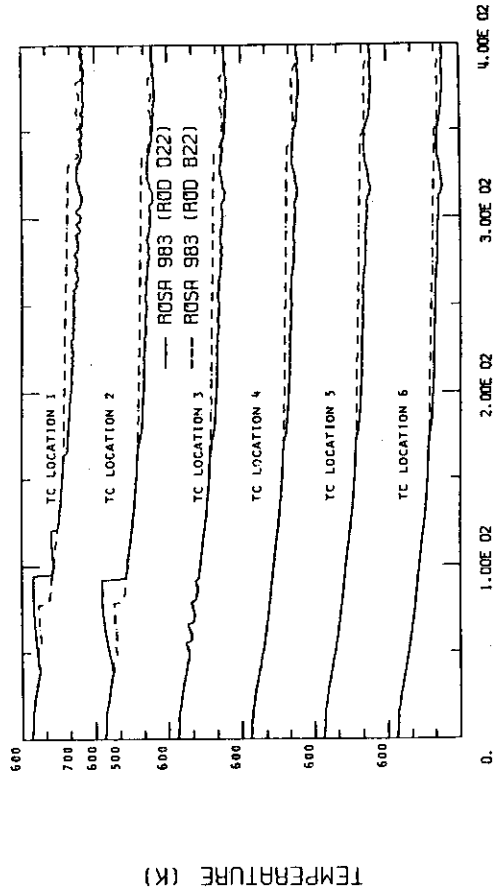


FIG. 4.1-12 ROSA 983 ROD TEMPERATURES

LARGE BREAK LOCA
FLOW PER FULL SIZE BUNDLE

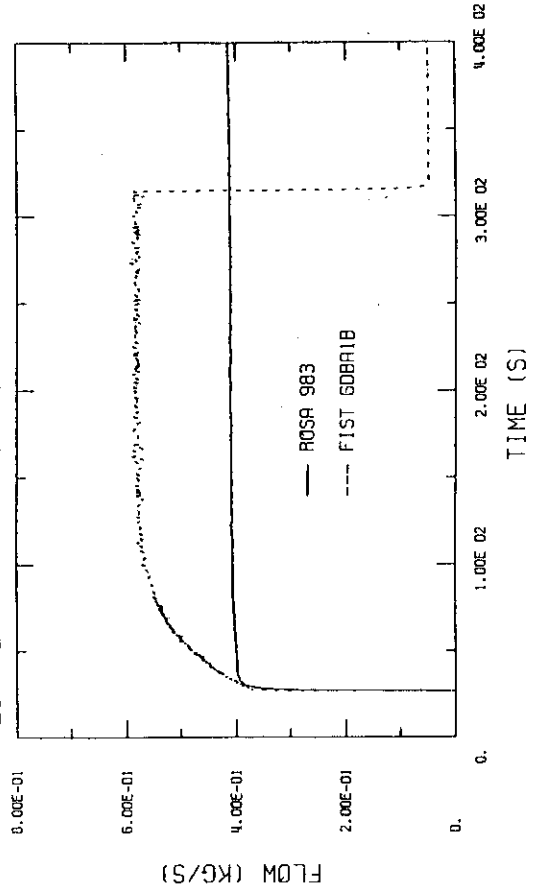


FIG. 4.1-13A HPCS FLOW

LARGE BREAK LOCA

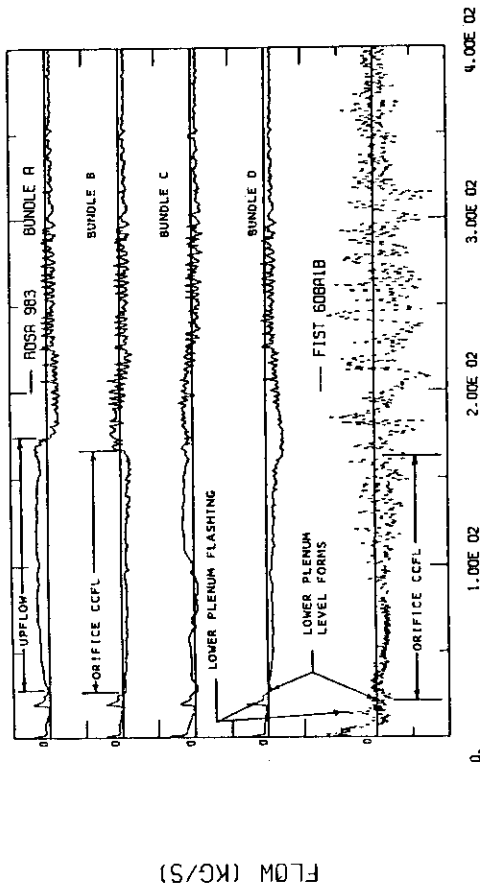


FIG. 4.1-10 BUNDLE INLET FLOWS

LARGE BREAK LOCA

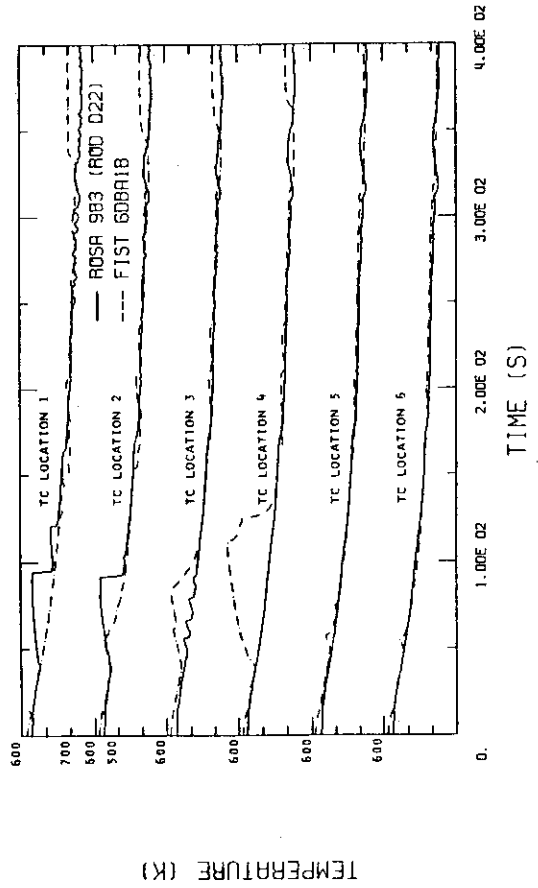


FIG. 4.1-11 ROD TEMPERATURES

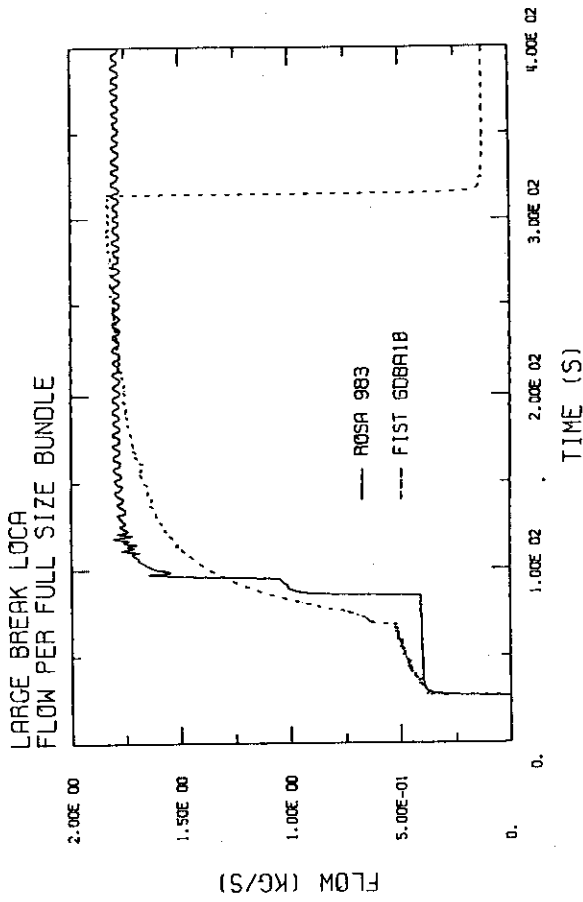


FIG. 4.1-13B LPCS FLOW

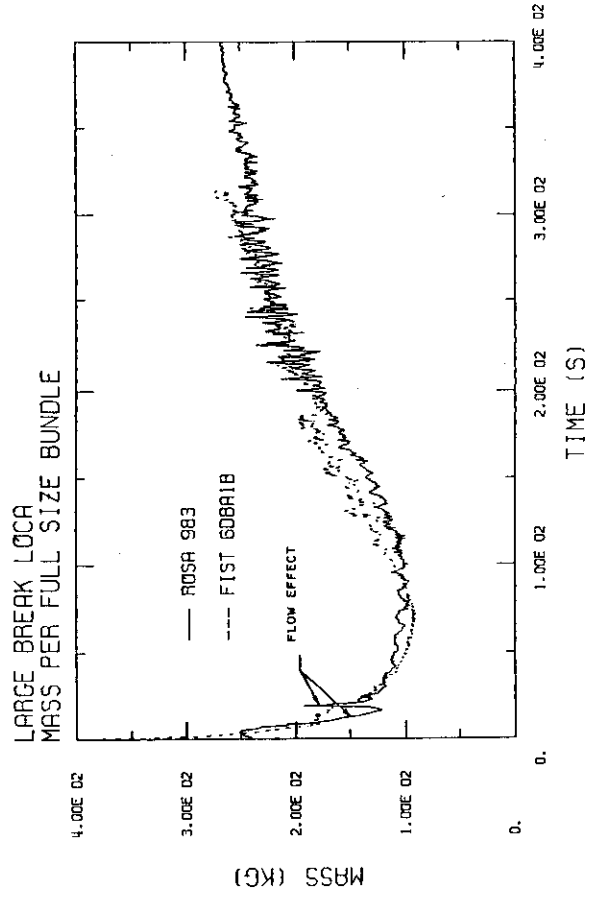


FIG. 4.1-13C LPCI FLOW

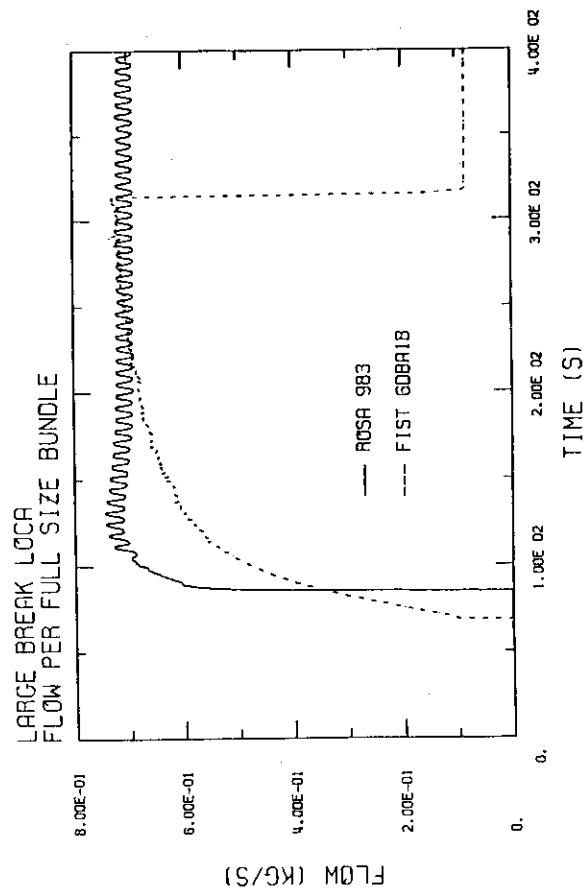


FIG. 4.1-13D LPCI FLOW

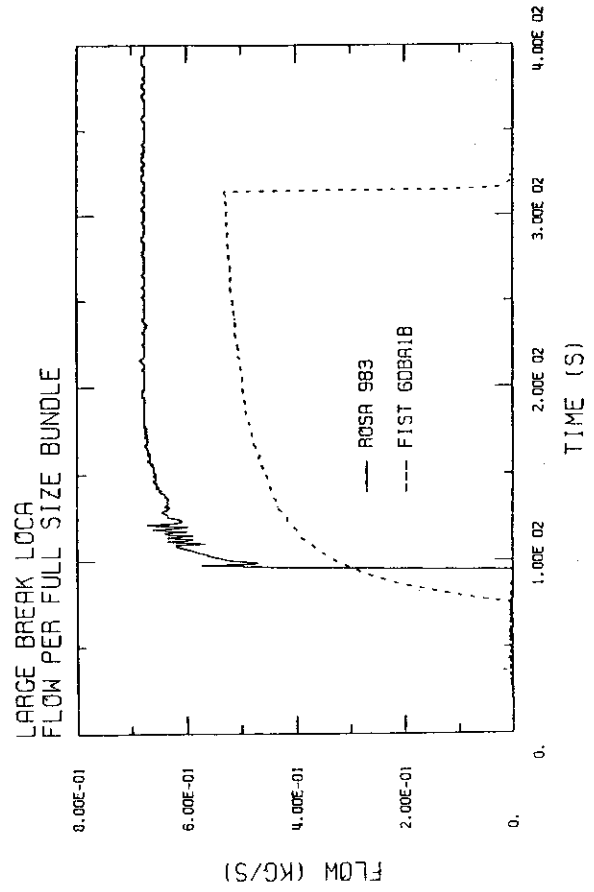


FIG. 4.1-14 TOTAL VESSEL LIQUID MASS

4.2 SMALL BREAK

The timing of the key test response events are compared in Table 4.2-1 for the small break tests. This table shows the sequence of events, and gives an overview picture of the two tests. It also focuses on key events and controlling phenomena. Comparing the two tests shows the sequence of events is similar but the timings are somewhat different. The system responses of the two small break tests show that the sequence of events is characterized by three phases. During the first phase the steamline flow is regulated to keep the system pressure constant. The downcomer water level reaches Level 1, activating the trips for MSIV closure, ADS, and ECCS. The MSIV closure causes the pressure to rise. After a specified time delay, activation of the ADS starts the second phase with rapid system depressurization and increased rate of coolant loss. Core uncover and rod heatup occur during this phase. Phase three begins with ECCS injection which refloods the core.

The break flow shown in Figure 4.2-1 is measured by the low range drag disk in ROSA-III and the blowdown tank level rise in FIST. The FIST flow measurement has a time lag due to the length of piping to the tank. It does not give instantaneous flow rates. The mass flow rates before ADS are influenced by the subcooling at the break. The subcooling is the difference between saturation temperature and the fluid temperature at the break. Figure 4.2-2 shows the break subcooling for FIST and the subcooling at the pressure vessel side of the break in ROSA-III. After flashing occurs in the downcomer, the break flows become two-phase mixtures of steam and water, and the uncertainty in the break flow measurement, is higher.

The system pressures, Figures 4.2-3A and B, show the short term and long term system response. Before MSIV closure, the pressure control systems regulate the steam flows, Figures 4.2-4A and B, to maintain system pressure. In ROSA-III, the system pressure set point is 6.7 MPa (970 psia). In FIST the pressure control system is set slightly higher.

The recirculation pumps are tripped off at the test start, and as the pumps coast down the core flows decrease, as shown in Figure 4.2-5. Also, near the beginning of each test the feedwater valves are closed, Figure 4.2-6.

Level 1 is reached at 75 seconds in FIST (Figure 4.2-7), 53 seconds earlier than in ROSA-III. In both facilities the downcomer level is sensed by the wide range instruments shown in Figure 2-3. These measurements are shown in Figures 4.2-8A and B for ROSA-III and FIST respectively. The normalized downcomer liquid level in both tests are shown in Figure 4.2-9. The figure shows the downcomer liquid level in FIST decreasing faster than in ROSA-III. The downcomer liquid volumes are compared in Table 2-3 and Figure 2-4. Per full size bundle, the liquid volume in the ROSA-III downcomer is 0.1452m^3 between the normal water level at 5.21m and L1 at 4.0m. Thus the time to reach Level 1 is shorter in FIST.

The MSIVs were tripped closed by the downcomer liquid level signal (L1) in both tests. The valves close at 77 seconds in FIST and at 131 seconds in ROSA-III, consistent with the difference in their Level 1 trips. After the main steam isolation valves (MSIV) close, the system pressures begin to increase gradually in both tests as seen in Figure 4.2-3A.

ADS, actuated by the downcomer L1 level signals in both tests, started at 195 seconds in FIST and 249 seconds in ROSA-III. The depressurization rate after ADS is greater in FIST, as shown in Figure 4.2-3B. FIST depressurizes slightly faster because of the 6% larger ADS orifice, used in FIST to compensate for excess stored energy, and a slightly higher ROSA-III ADS flow resistance piping due to a pipe diameter of 25mm, an orifice diameter of 21.1mm, and a control valve upstream of the orifice. The resulting difference in the integrated ADS flow, i.e. area under the respective curves in Figure 4.2-4B, is small, with a corresponding small effect on system inventory.

The ADS depressurization leads to flashing in the downcomer, lower plenum, guide tubes, and bypass, and swelling of the downcomer and upper plenum levels. The level swell is greater in FIST than in ROSA-III because flashing in a tall, narrow volume produces more swell than in a shorter, wider volume. On a normalized basis, the downcomer mixture level transients are similar in both tests, even if the time to reach Level 1 is 53 seconds later in ROSA-III due to the larger initial downcomer mass (Figure 4.2-3).

Once the level swell transient has subsided, the downcomer, upper plenum and lower plenum levels fall. CCFL at the FIST side entry orifice (SEO) limits the downflow of liquid from the bundle to the lower plenum, and a mixture level forms in the lower plenum. Although conductivity elements in ROSA-III do not indicate a level formation in the lower plenum after flashing, Figure 4.2-11 shows that the orifice flow reverses in Bundles B, C, and D while it remains in the upward direction in Bundle A for about 40 seconds. This indication of parallel channel flow (cf. Reference 8) shows that a small level has formed near the orifices. However, this brief period of parallel channel flow has little effect on the core unconverged heatup.

The mixture level in the FIST lower plenum (Figure 4.2-10), drops to the bottom of the jet pumps, which allows some steam to vent out the jet pumps. The mixture level in the FIST upper plenum drops to the top of the core and then into the bundle, as seen in Figure 4.2-10. In ROSA-III the mixture level also drops into those bundles which are in countercurrent flow at the inlet orifice, Figure 4.2-11. Bundle A, remains full as long as it is in upflow at the side entry orifice (about 330 seconds), but its level drops quickly to that of the other bundles, Figure 4.2-10.

As the mixture level drops in the bundles, the rods begin to heat up, as seen in Figure 4.2-12A. FIST heat up occurs earlier, consistent with the difference in ADS timing, level swell timing, and mixture level drop timing in the bundle. The heat up duration is also about the same, which results in the ROSA-III bundles having approximately the same PCT as in the FIST bundle. The PCT's are 710K and 769K respectively

(Table 4.2-1), both occurring at the same relative position (i.e., #4). Figure 4.2-9 and 4.2-10 show the system refill and bundle reflood shortly after the LPCS and LPCI systems begin injecting coolant. The LPCS initiates FIST bundle cooling from the top, Figure 4.2-12A, while reflooding quenches the rods from the bottom in both facilities.

The earlier system depressurization (i.e., ADS) in FIST also leads to earlier injection of LPCS and LPCI water. The LPCS and LPCI trips themselves, Table 3.2-1, are not important as they occur before the system pressures reach the shutoff head of these low pressure pumps. The LPCS and LPCI injection begins at 310 and 335 seconds in FIST, and at 469 and 502 seconds in ROSA-III, as seen in Table 4.2-1 and Figure 4.2-13A. The ECCS flow responses for the two facilities, shown in Figures 4.2-13A and B, are similar but with the same offset in time due to the difference in ADS timing.

Figure 4.2-14 shows the total vessel liquid mass inventory transient for the two facilities. Shortly after ECCS injection begins, the liquid inventories start to recover. Except for this offset in time, again due to ADS timing differences, the mass response is similar in both facilities. The comparison is very good, and demonstrates a good simulation of BWR mass and energy rates in both facilities.

Summary

The basic sequence of events and the system responses in the two small break tests are very similar. The timing of downcomer water level reaching Level 1, initiating the MSIV closure and ADS actuation, has a noticeable effect on the timing of flashing, level response, bundle heat up, and PCT. However, this timing difference does not have a significant effect on overall system responses, and the depressurization and liquid mass histories are quite similar. The bundle heatup and quenching is very similar, with the Peak Clad Temperature (PCT) occurring near the same location and having very nearly the same value.

Table 4.2-1

SMALL BREAK COUNTERPART TESTS
TIMING OF KEY EVENTS

Key Events	Time (sec.)	
	ROSA 984	FIST 6SB2C
Break Valves Open	0.0	0.0
Pump Coast-Down Begins	0.0	0.0
Feedwater Line Closes	2-4	0.0
Power Decay Initiated	9	0.0
Pressure Control System Activated	16	0.0
Intact Jet Pump Loop Isolated	NA	20
Level 1 Trip	128	75
MSIV Closes	131	77
Jet Pump Suction Uncovers	NA	165
ADS Actuation	249	195
Lower Plenum Flashing	255	195
Jet Pump Suction Recovers	NA	200
Lower Plenum Level Forms	NA	200
Top of Bundles Uncover	329	237
Bundle Heat-Up Begins	330	250
Jet Pump Exit Uncovers	NA	290
LPCS Flow Begins	469	310
Bottom of Core Uncovers	458	325
LPCI Flow Begins	502	335
Bundle Reflood Begins	490	370
PCT Occurs	504	400
PCT Temperature	710K	769K
PCT Location	Position 4 ⁽¹⁾	Position 4
Bundle Reflood Completed	528	420
Bundle Quenched	527	420
Jet Pump Exit Recovered	NA	420
Lower Plenum Refilled	NA	465
End of Test	788	508

(1) Bundle A.

SMALL BREAK LOCA
FLOW PER FULL SIZE BUNDLE

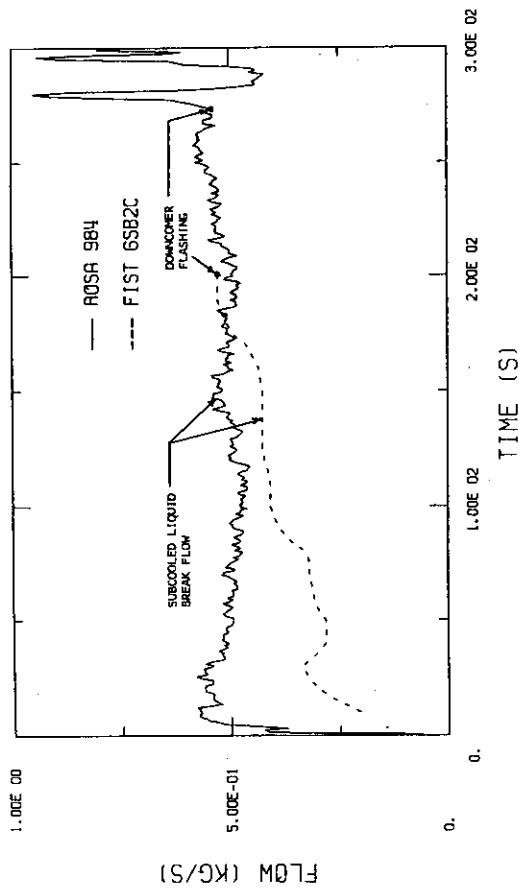


FIG. 4.2-1 BREAK FLOW

SMALL BREAK LOCA

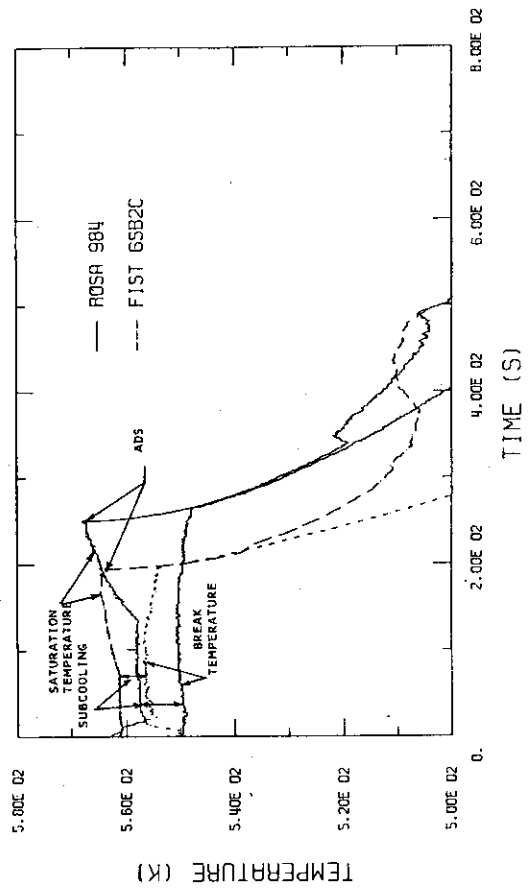


FIG. 4.2-2 BREAK TEMPERATURE

SMALL BREAK LOCA

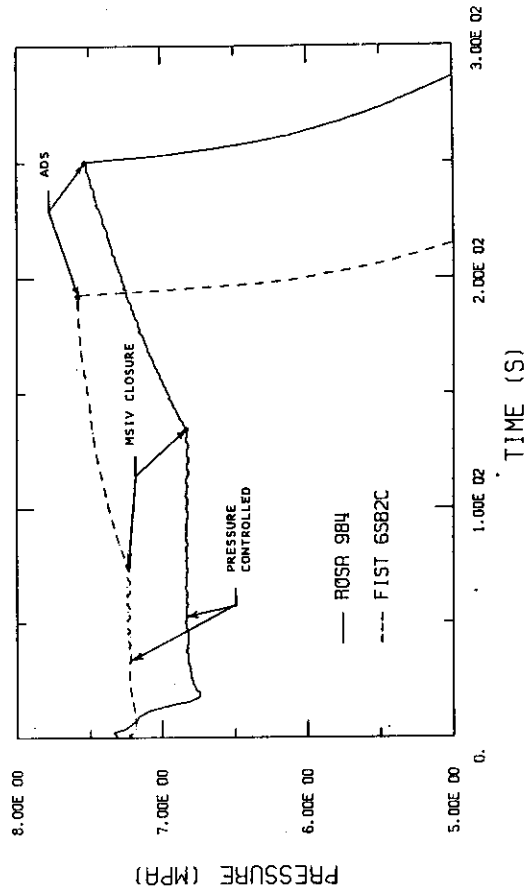


FIG. 4.2-3A SYSTEM PRESSURE

SMALL BREAK LOCA

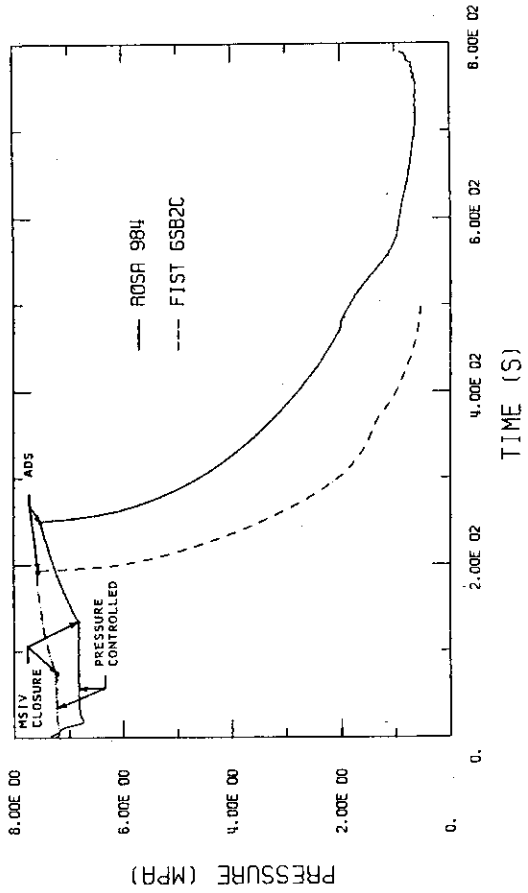


FIG. 4.2-3B SYSTEM PRESSURE

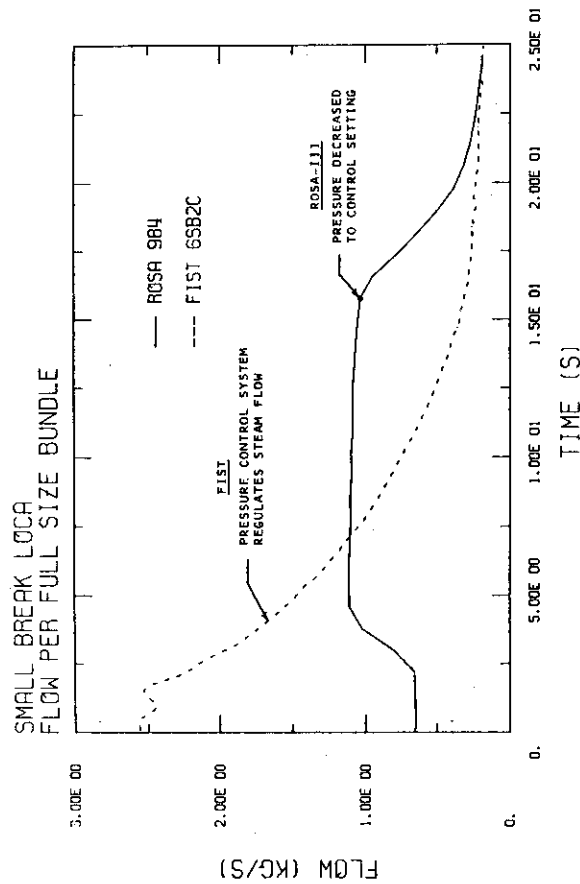


FIG. 4.2-4A STEAMLINE FLOW

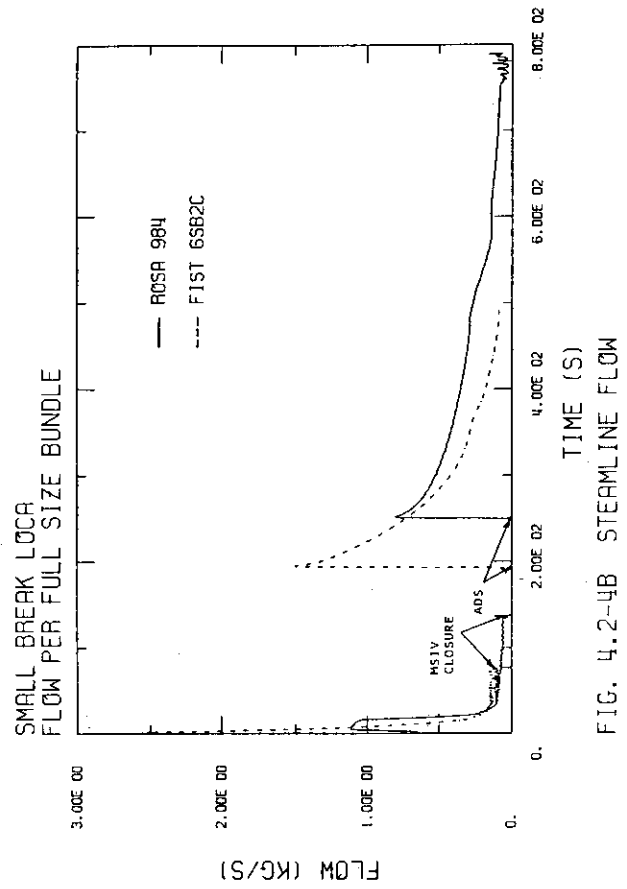


FIG. 4.2-4B STEAMLINE FLOW

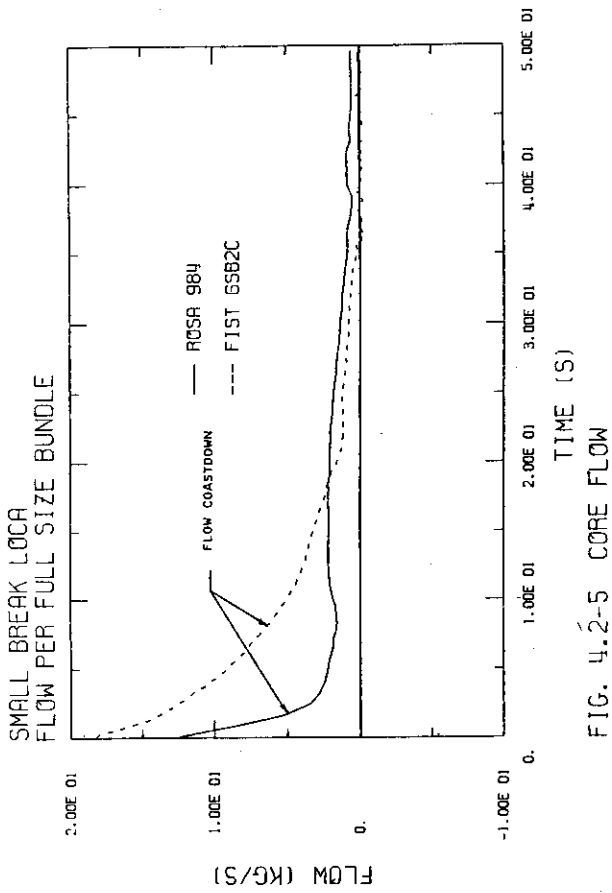


FIG. 4.2-5 CORE FLOW

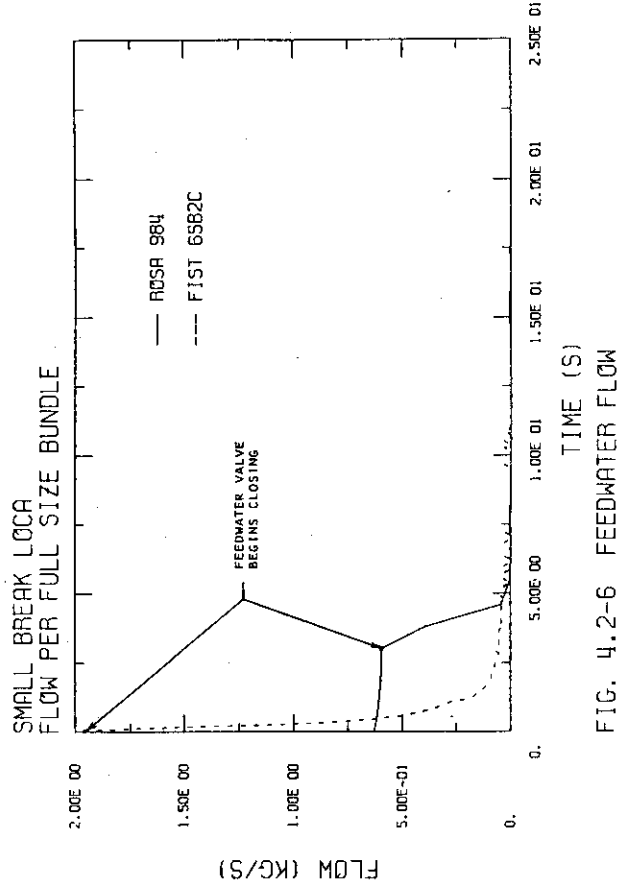
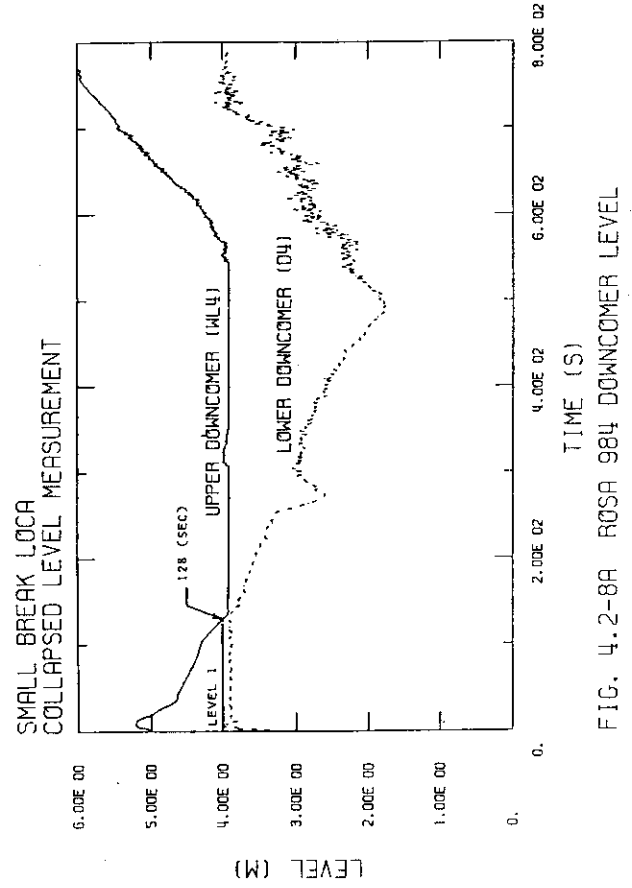
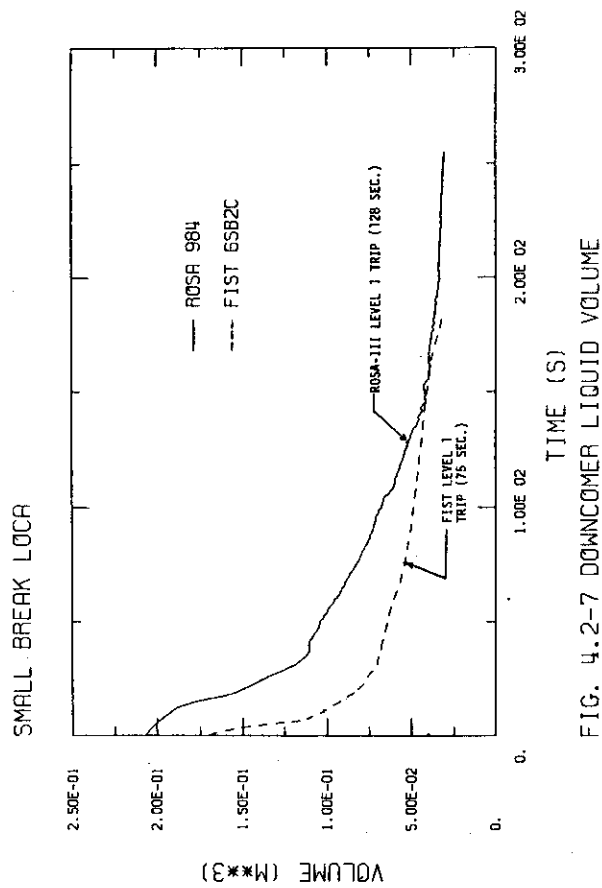
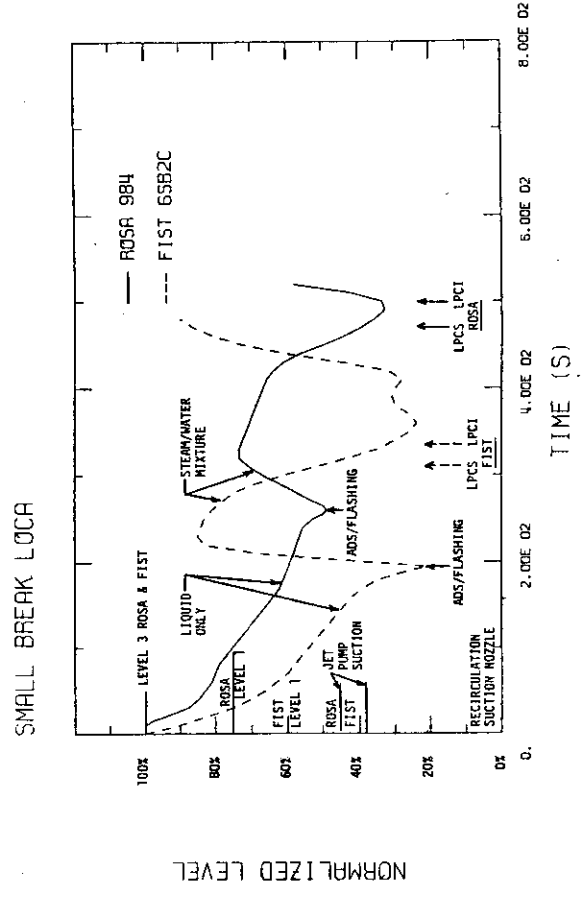
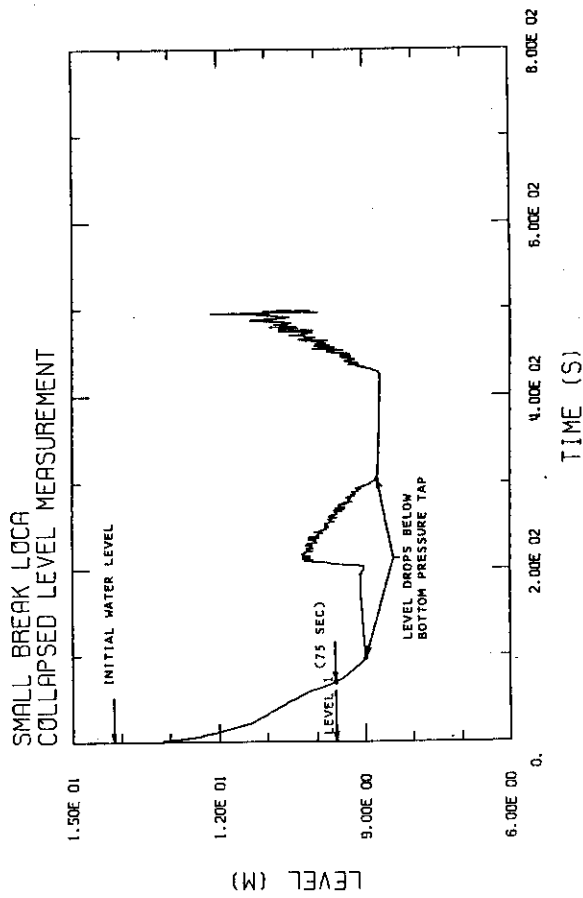


FIG. 4.2-6 FEEDWATER FLOW



SMALL BREAK LOCA

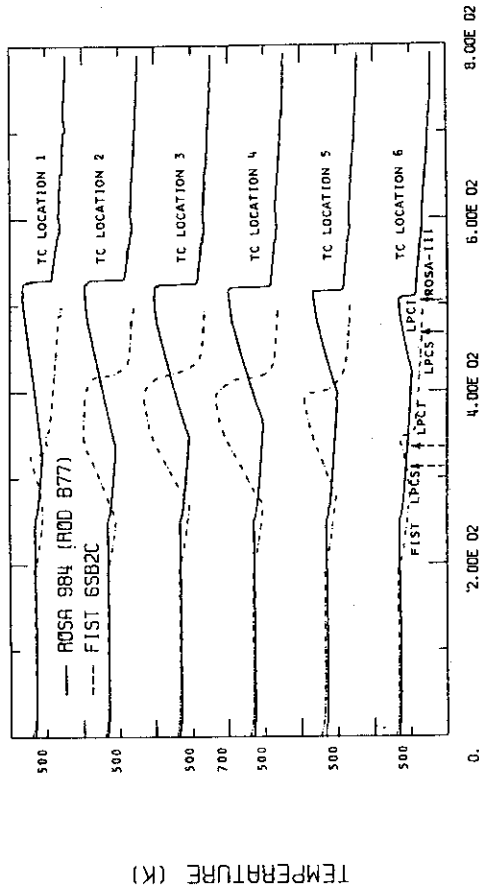


FIG. 4.2-12A ROD TEMPERATURES

SMALL BREAK LOCA

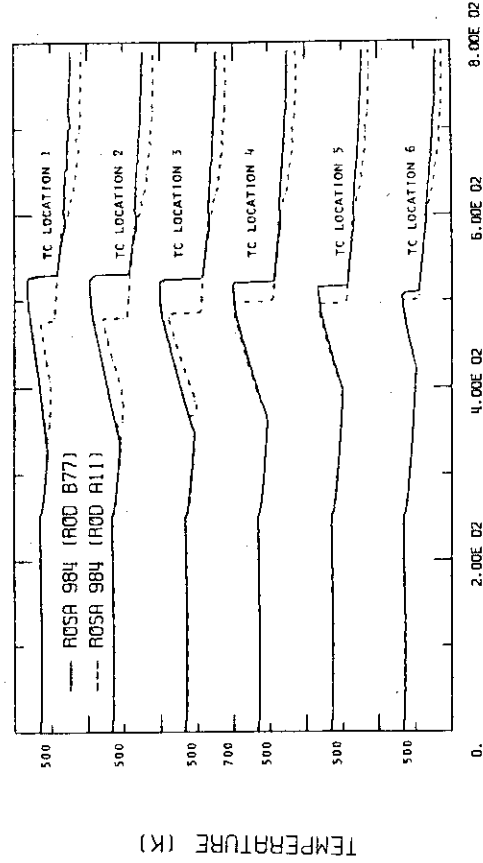


FIG. 4.2-12B ROD TEMPERATURES

SMALL BREAK LOCA

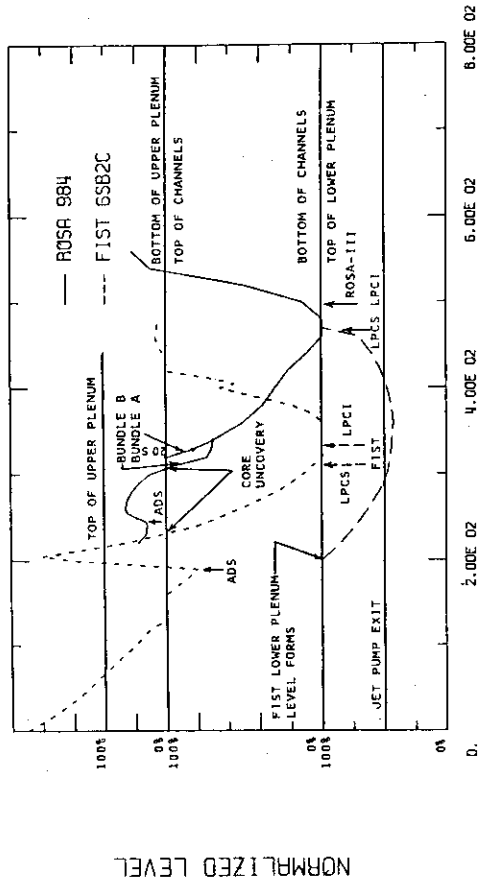


FIG. 4.2-10 MIXTURE LEVEL IN CORE SHROUD

SMALL BREAK LOCA

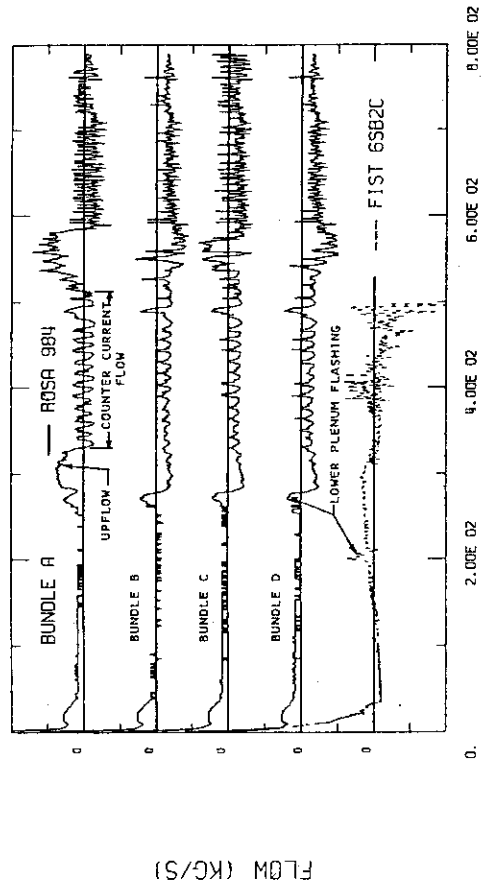


FIG. 4.2-11 BUNDLE INLET FLOWS

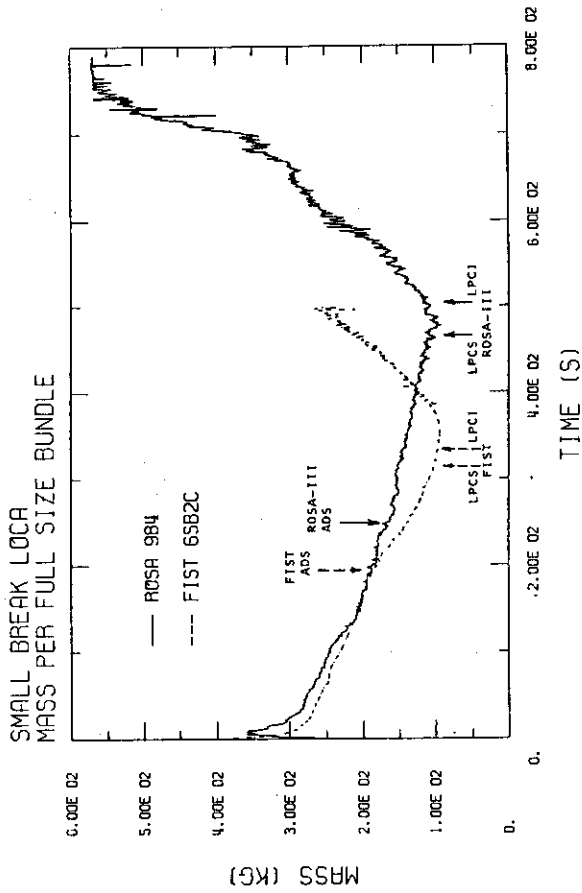


FIG. 4.2-14 TOTAL VESSEL LIQUID MASS

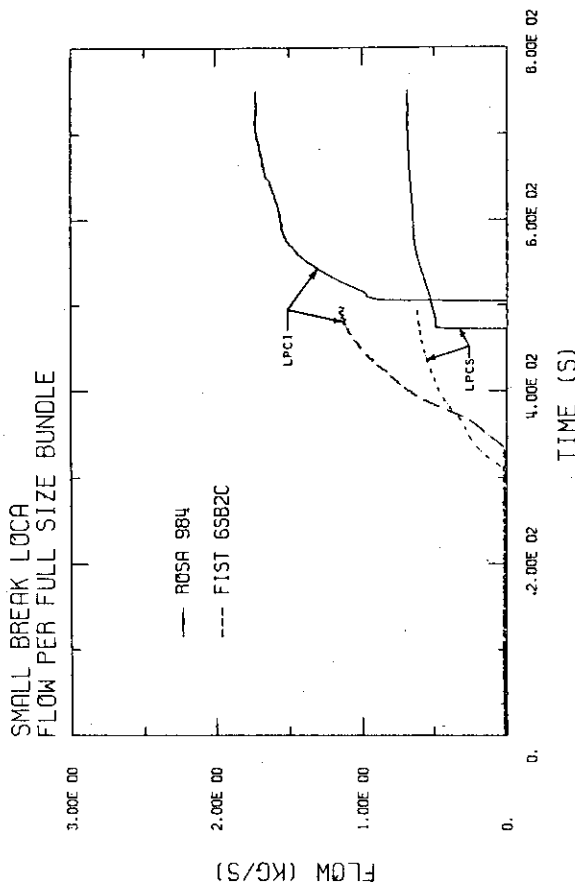


FIG. 4.2-13A LPCS AND LPCI FLOWS

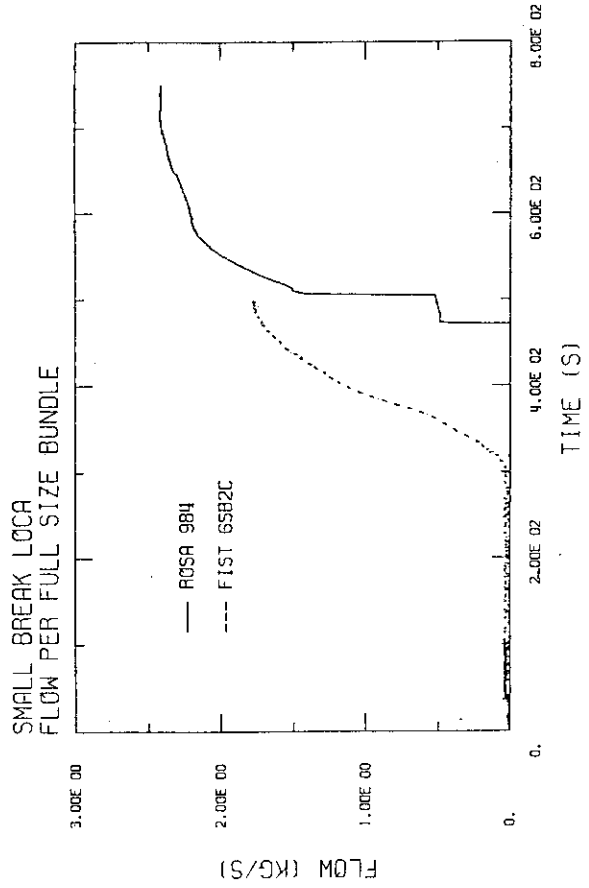


FIG. 4.2-13B TOTAL ECCS FLOW

4.3 MAIN STEAMLINE BREAK

The steamline break tests, although having similar initial and boundary conditions, were not performed to be counterpart tests in which the test specifications are exactly the same. For example, the FIST ECCS trips are activated by a timer, whereas the ROSA-III trips are activated by Level 1 and Level 2 signals, plus a specified time delay, (cf. Table 3.3-1). As a result, the number of ECC Systems activated, and the timing of their injections, is not the same in the two tests. However, these tests are sufficiently similar to make it worthwhile including them in this evaluation.

The timing of key events in the system responses are compared in Table 4.3-1. For the steamline break tests, these events fall into four major groups which describe these transients. First, are events associated with the test initiation, i.e., the break flow begins, the recirculation pumps start coastdown, the feedwater valve closes, and the power decay is initiated. The rapid system depressurization rate, that is characteristic of a large steamline break, leads quickly to the second group of events, which include downcomer flashing, level swell and, in ROSA-III, the Level 2 trip. Initiation of ECCS injection begins the third major group of events. The system refilling and, in ROSA-III, bundle reflood, begins the fourth. The following paragraphs discuss these events and responses.

The steamline break flow rates for the first 25 seconds are shown in Figure 4.3-1A. FIST, with a 25% larger break area, has a larger break flow for the first 5.5 seconds. At FIST MSIV closure, the FIST and ROSA-III breaks become the same for the remainder of the test. At six seconds, the FIST downcomer two-phase mixture level swells to cover the steamline, which explains why the FIST break flow initially remains slightly greater than ROSA-III. Figure 4.3-1B shows that over the long term the break flows become equal, and then FIST falls lower due to lower system pressure.

The system pressure responses are compared in Figure 4.3-2A for the first 25 seconds, and in Figure 4.3-2B for the entire test duration. FIST, with the initially larger break area, depressurizes more rapidly than ROSA-III for the first five seconds. At five seconds (6 MPa), the water in the FIST Lower plenum, downcomer, guide tubes, and bypass reaches its saturation temperature and steam generated by flashing reduces the depressurization rate. The initial water temperature is higher in ROSA-III than FIST, and flashing begins at 4.2 seconds (6.7 MPa). After five seconds, the pressure curves (Figure 4.3-2B) have the same slopes.

In spite of some differences in the test conditions (Table 3.3-1), the system pressures agree very well. This good agreement of the pressure response is attributed to the same volumetric scaling of the fluid mass in each region, equal break areas, and the same initial enthalpy distribution. The comparison of initial fluid volume and break area, per one full-size bundle, between ROSA-III and FIST, Table 3.3-1, shows good agreement. The small difference between the pressure responses is due to the larger steam flow rate during the first 5.5 seconds in FIST.

The core flows are compared in Figure 4.3-3. The measurements of core flow are reasonable accurate up to the time of lower plenum flashing because the fluid is a single phase liquid. After lower plenum flashing, the fluid is a two-phase steam-water mixture and, with a greater uncertainty in fluid density, the measurements of core flow are approximate. This comparison shows the ROSA-III core flow coasting down more rapidly than FIST, as was the case in the large and small break LOCA tests previously discussed. Because flashing and the subsequent level swell occur early in these tests, the core flow transients have a minor impact on the system responses.

The feedwater flow, Figure 4.3-4, is the last boundary condition to be considered. The feedwater valves close very near the beginning of the tests, so these flows have little effect on the test results.

As noted above, the water in the ROSA-III lower plenum, downcomer, guide tube, and bypass starts to flash at 4.2 seconds. The resulting expansion of the two-phase fluid mixture forces steam and water from the lower plenum into the downcomer, as well as into the bundles. This added mass, and the expansion of the downcomer fluid, causes a rapid swelling of the downcomer-mixture level. The location of the two differential pressure measurements in the ROSA-III downcomer are shown in Figure 2-3. These measurements for the steamline break (RUN 952) are shown in Figure 4.3-5A. The upper measurement (WL 4) represents the BWR wide range level instrument, and level trip signals are taken from this instrument in ROSA-III. This measurement includes the effects of friction due to flow in the downcomer. After flashing begins, this measurement is no longer the "true" mixture level, but is the "collapsed" level, or static head between the pressure taps. These taps are at elevation 3.90m and the top of the vessel, 6.04m. This spans Level 1 at 4.25m and Level 2 at 4.76m. Figure 4.3-5A shows the ROSA-III "collapsed" upper downcomer level (wide range instrument) initially rising as flashing swells fluid mixture into this region from below the pressure tap at 3.9m. After the initial level swell, as steam breaks through, the level falls back. The Level 2 indication, which trips the HPCS, is reached at 71 seconds and, with the specified time delay, injection begins at 94 seconds. Level 1, which trips the LPCS and LPCI is not reached due to level swell during blowdown and mass recovery during reflood. The differential pressure measurement from the lower downcomer instrument (D4) shows a rapid decrease in the first 22 seconds as steam voids are formed. That swells the fluid mixture into the region above 3.9m. However, no mixture level or steam pocket was observed by the conductivity probes in the lower downcomer of ROSA-III. HPCS injection adds additional liquid, which contributes to the prevention of the Level 1 trip.

Figure 4.3-5B shows that the FIST downcomer "collapsed" level response is very similar to ROSA-III for the first 150 seconds. This measurement is from the wide range level instrument, shown in

Figure 2-3. Level 2 is reached in 22 seconds, 49 seconds earlier than in ROSA-III. This is similar to the small break case in which the greater recirculation flow during the coastdown transient transfers more mass from the downcomer into the in-shroud region. As in ROSA-III, Level 1 is not reached, also due to CCFL holdup of liquid in the upper regions. Liquid is held above the FIST jet pumps, downcomer bend, and dryer bottom, which forms steam pockets, Figure 4.3-6. Therefore, if the LPCS and LPCI systems had been initiated on level trip, as in ROSA-III, they too would not have been activated*. In FIST, however, the ECCS is activated by a simulated containment over pressure trip. HPCS starts injecting after a 27-second delay, and the low pressure systems start injecting when system pressure is below the injection pumps shut off head. This is 88 seconds for the LPCS and 95 seconds for the LPCI, and leads to refill of the system.

The estimated downcomer two-phase mixture levels are compared in Figure 4.3-6. The levels are normalized with the recirculation line suction as 0% and Level 3 as 100%. The steamline at the top of the ROSA-III vessel is covered by the two-phase mixture from 15 seconds to 31 seconds, and gradually decreases thereafter. In FIST, the downcomer-mixture level swells above the top pressure tap (14.88m) of the wide-range level instrument, and covers the steamline (16.15m) from 6 seconds to 80 seconds, but does not swell to the top of the vessel. In both tests liquid is swept out of the break when the steamline is covered. Conductivity probes and differential pressure measurements in FIST led to the identification of the "steam pockets" shown, but it was not observed in ROSA-III.

Figure 4.3-7 compares the two-phase mixture levels inside the core shroud for both tests. As is the case for the downcomer region, the lower plenum, core, and upper-plenum regions are normalized for the

* The BWR downcomer does not have a flow geometry that would lead to CCFL affecting level trips. The downcomer is annular in shape, allowing a redistribution of upflowing steam.

comparison. The HPCS, LPCS, and LPCI performances are evaluated by comparing the mixture levels inside the core shroud and the heater rod surface temperatures of the two tests. As in the small break case, a two-phase mixture level is formed in the FIST lower plenum but not in ROSA-III. This is attributed to a smaller flow resistance through the jet pumps in FIST compared with ROSA-III. The smaller flow resistance results in relatively lower two phase flow in the core and larger fall back from the upper plenum. The down flow from the FIST bundle is limited by the SEO CCFL to form a level in the lower plenum and to keep the bundle full and refilling the system combined with the effect of the early actuation of HPCS.

Since the FIST bundle does not uncover, the rod temperatures remain close to saturation throughout. The level forming in the four ROSA-III bundles causes heatup (Figure 4.3-8B), and a PCT of 752K is reached at 108 seconds at position 4. The HPCS then refloods the core, quenching all rods by 221 seconds.

The HPCS flows, Figure 4.3-9A, reflects the earlier actuation time in FIST. Figure 4.3-9B shows the LPCS and LPCI flows, and the total ECCS injection flow is shown in Figure 4.3-9C. The total system mass, Figure 4.3-10, is the same for the two tests for the first 100 seconds. The HPCS maintains the system inventory thereafter, as seen in ROSA-III, and the addition of LPCS and LPCI refills the system, as seen in FIST.

A local redryout of fuel rods was observed in the ROSA-III steamline break test at the midplane of the peripheral highest power rods. Relatively higher heat flux and smaller HPCS injection flow resulted in the redryout, which was quenched completely by the manual actuation of LPCI at the end of the test.

Summary

The basic sequence of events and the system response in the two steamline break tests are very similar. After the initial 5.5 seconds, the FIST break is reduced to be the same as in ROSA-III and the system pressure responses, as well as the steamline break flows, are very similar. The liquid holdup in the FIST bundle by SEO CCFL, augmented by ECCS activation, keeps the bundle covered and there is no heat up. The delayed HPCS actuation in ROSA-III resulted in bundle heat up.

As this was not a counterpart test, there were significant differences in the ECCS trip settings. The ROSA-III ECC Systems trip on downcomer level, whereas FIST systems trip on simulated high containment pressure. By comparing the effects of each ECCS in ROSA-III with that in FIST, it is found that the early actuation of HPCS contributes to prevent core uncover and actuation of LPCS and LPCI contribute to complete core cooling.

Table 4.3-1

STEAMLINE BREAK COUNTERPART TESTS
TIMING OF KEY EVENTS

Key Events	Time (sec.)	
	ROSA 952	FIST 6MSB1
Break Valve Opens	0	0
Pump Coast-Down Begins	0	0
Feedwater Line Closes	1.3-3.2	0
Power Decay Initiated	9.0	0
Lower Plenum Flashing	4.2	5
MSIV Closed	NA	5.5
Break Size Changed ⁽¹⁾	NA	5.5
Level Covers Steamline	15	6
Recirc. Loops Isolated	NA	7
Level 2 Trip	71.0 ⁽²⁾	22
Level 1 Trip	No	No
Lower Plenum Level Forms	-	31
Jet Pump Exit Uncovered	NA	65
Level Uncovers Steamline	31	80
HPCS Flow Begins	94	27
LPCS Flow Begins	NA	88
LPCI Flow Begins	NA	95
Feedwater Flashing	95	NA
Jet Pump Exit Recovered	NA	120
Bundle Heat-Up Begins	27	None
PCT Occurs	108	None
PCT Temperature	752K	NA
PCT Location	Position 4 ⁽³⁾	NA
Bundle Quenched	221	NA
End of Test	450	335

(1) In FIST, the steamline break is changed from 501 mm² to 377 mm² at 5.5 seconds.

(2) Level 2 in ROSA-III Run 952 was detected by the upper downcomer level instrument (EL. 3.90-6.04 m), which corresponds to the wide range level instrument in the reference BWR.

(3) Bundle A

MAIN STEAMLINE BREAK LOCA

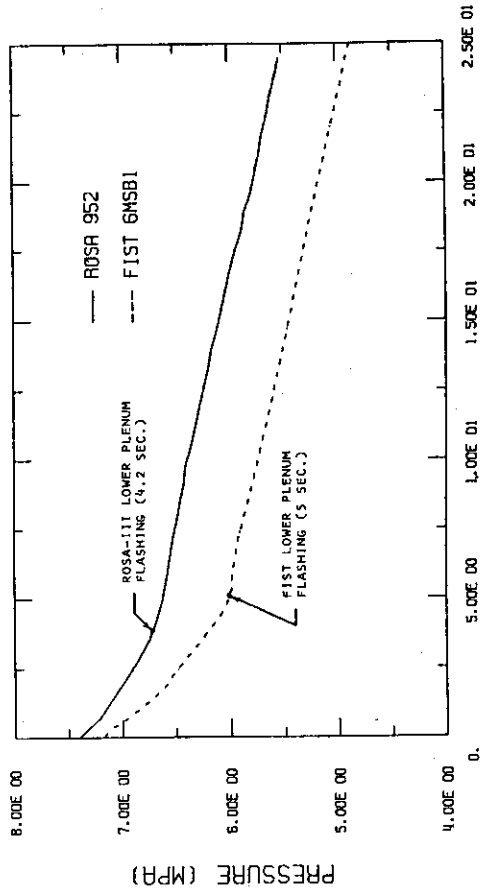


FIG. 4.3-2A SYSTEM PRESSURE

MAIN STEAMLINE BREAK LOCA

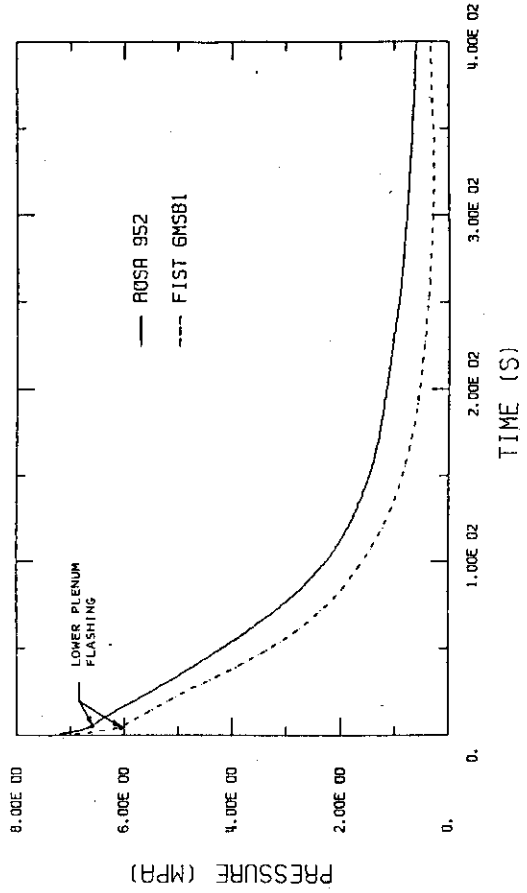


FIG. 4.3-2B SYSTEM PRESSURE

MAIN STEAMLINE BREAK LOCA
FLOW PER FULL SIZE BUNDLE

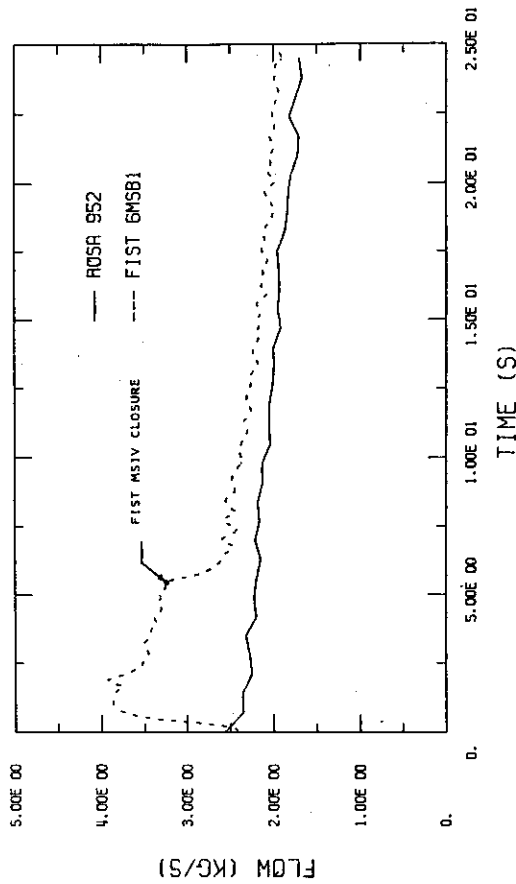


FIG. 4.3-1A BREAK FLOW

MAIN STEAMLINE BREAK LOCA
FLOW PER FULL SIZE BUNDLE

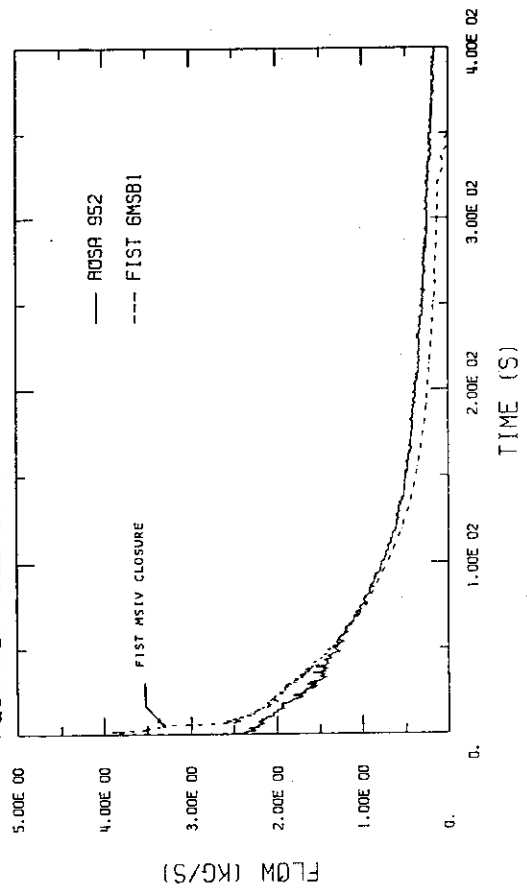


FIG. 4.3-1B BREAK FLOW

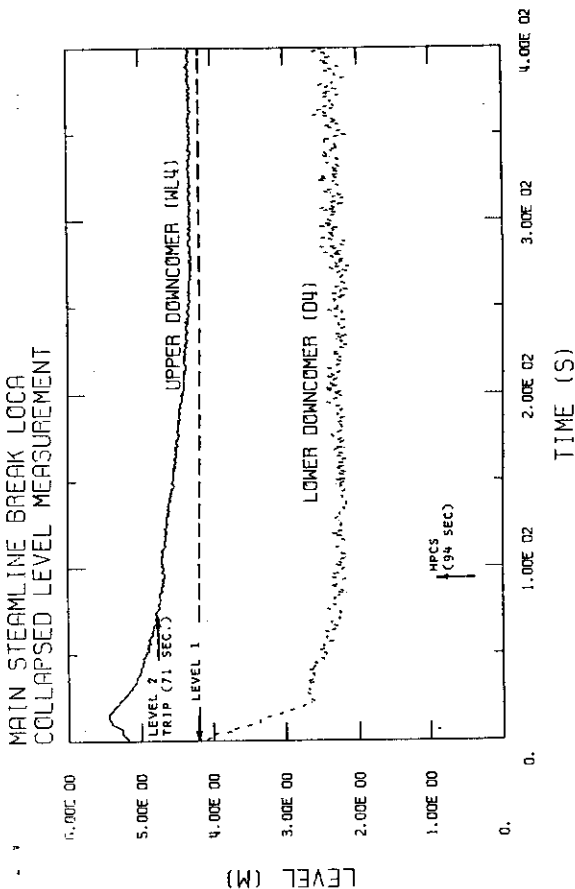


FIG. 4.3-5A ROSA 952 DOWNCOMER LEVEL

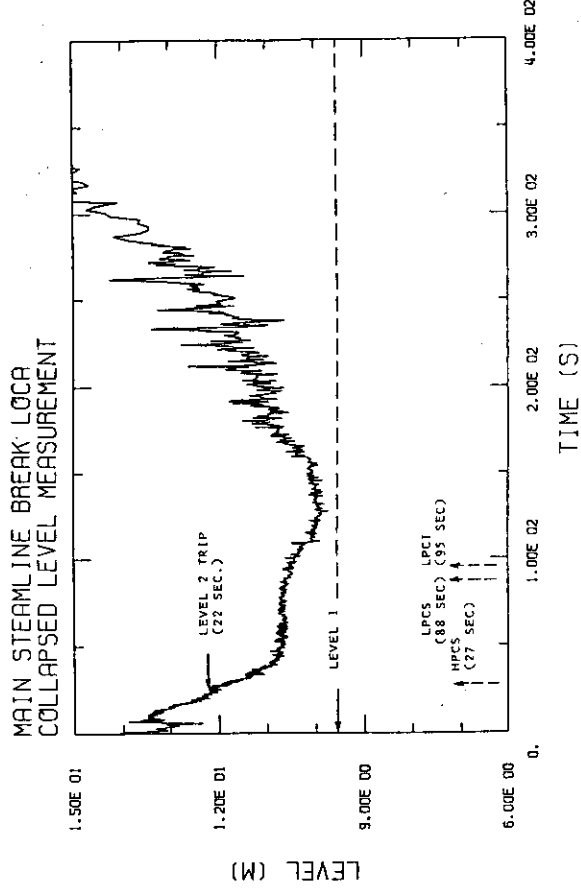


FIG. 4.3-5B FIRST 6MSB1 DOWNCOMER LEVEL

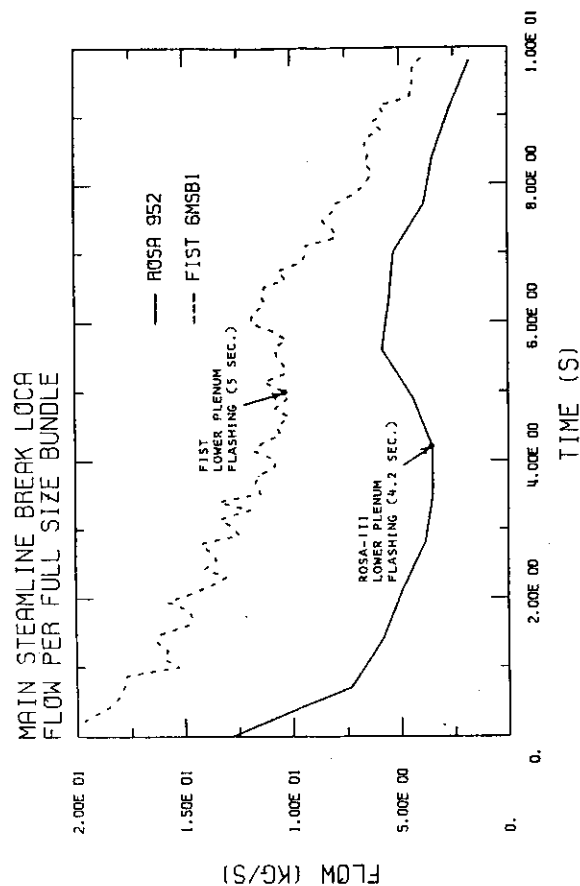


FIG. 4.3-3 CORE FLOW

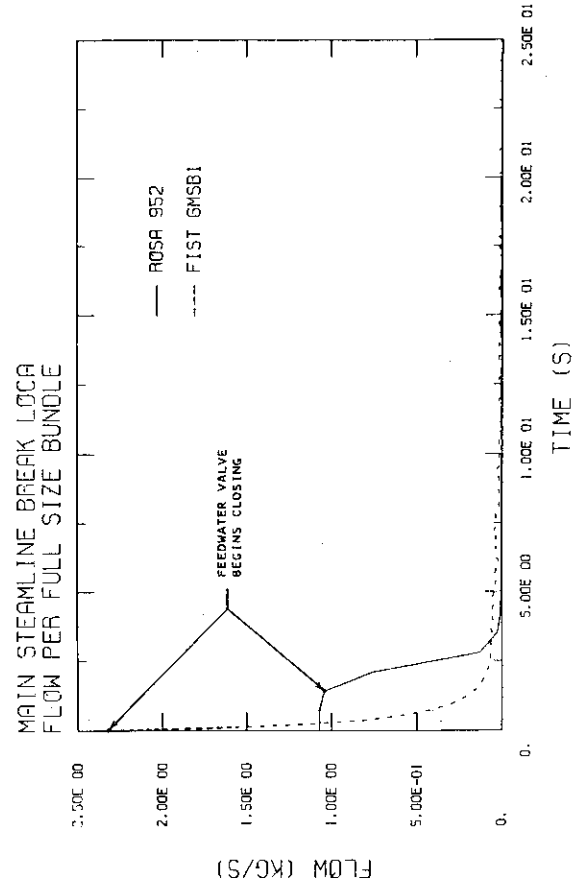


FIG. 4.3-4 FEEDWATER FLOW

MAIN STEAMLINE BREAK LOCA

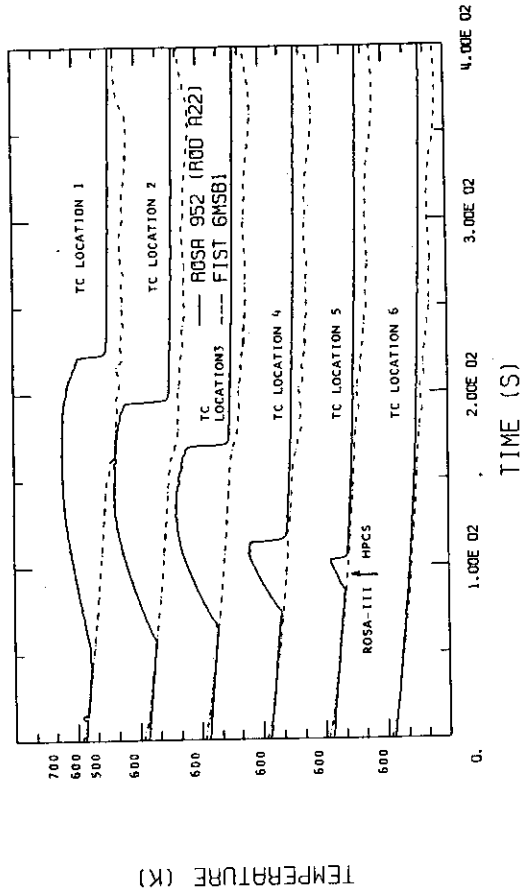


FIG. 4.3-8A ROD TEMPERATURES

MAIN STEAMLINE BREAK LOCA

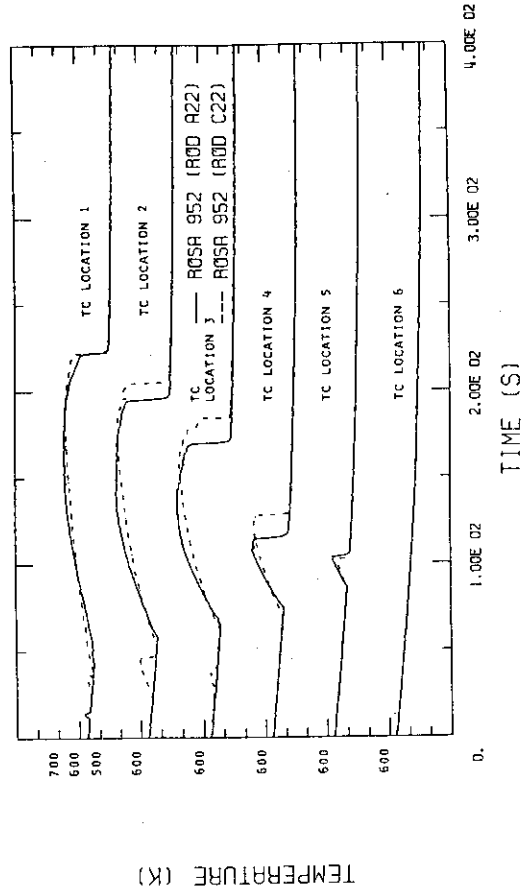


FIG. 4.3-8B ROD TEMPERATURES

MAIN STEAMLINE BREAK LOCA

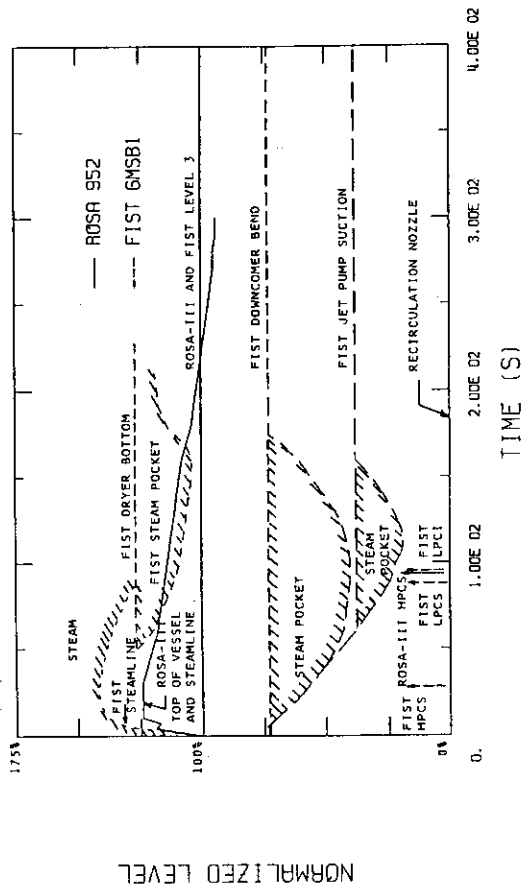


FIG. 4.3-6 MIXTURE LEVEL IN DOWNCOMER

MAIN STEAMLINE BREAK LOCA

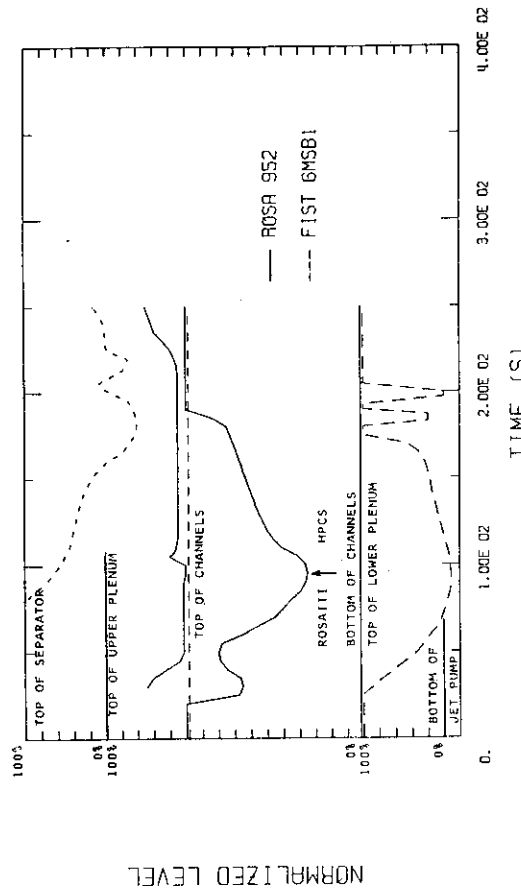


FIG. 4.3-7 MIXTURE LEVEL IN CORE SHROUD

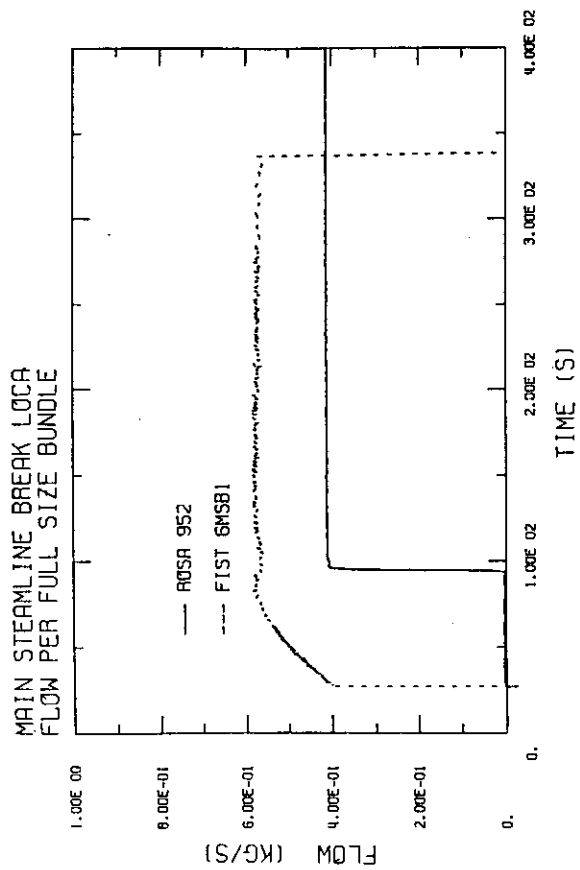


FIG. 4.3-9A HPCS FLOW

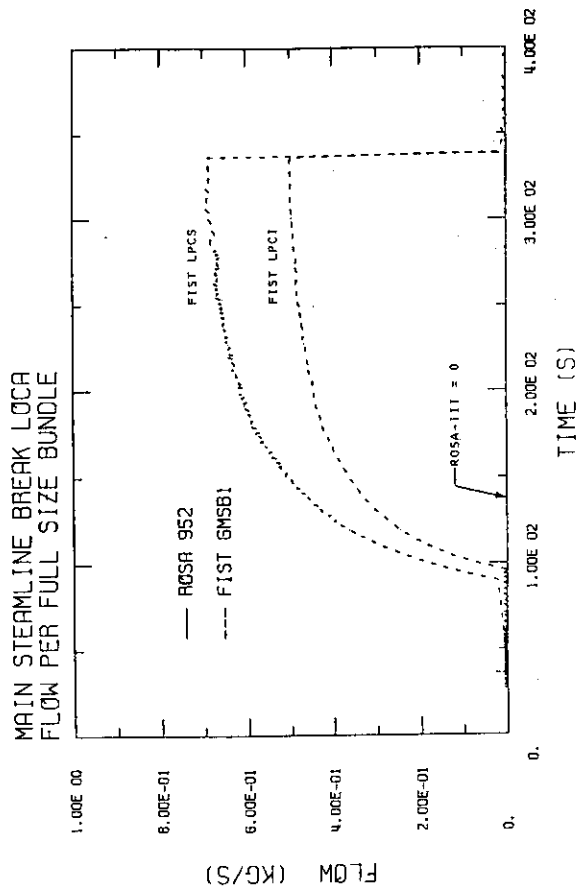


FIG. 4.3-9B LPCS AND LPCI FLOW

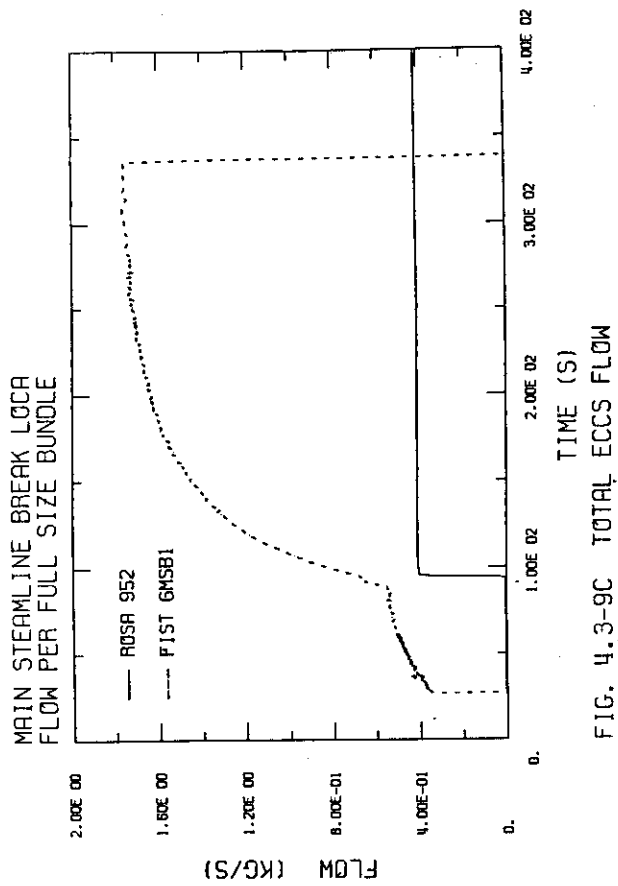


FIG. 4.3-9C TOTAL ECCS FLOW

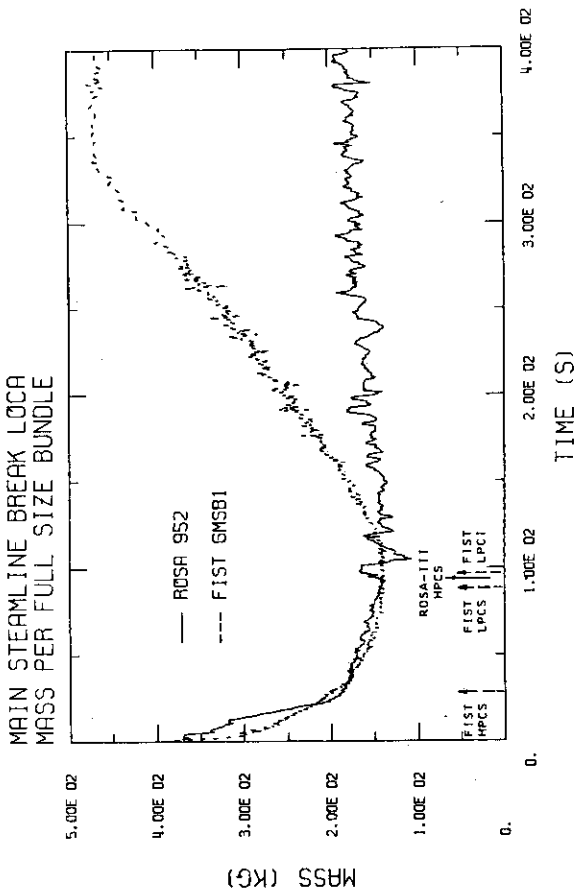


FIG. 4.3-10 TOTAL VESSEL LIQUID MASS

5. SUMMARY

A common understanding and interpretation is developed of the controlling phenomena observed in loss-of-coolant accident (LOCA) experiments performed in the ROSA-III and FIST BWR simulator facilities. Counterpart tests were performed in each facility to provide a common basis for this evaluation. The three sets of tests are large break, with HPCS, LPCS, and LPCI, small break, with LPCS and three LPCI's, and steamline break with HPCS, LPCS, and LPCI. Both facilities are scaled to simulate, in real time, BWR system responses to LOCA transients. In addition, ROSA-III has four half-length bundles in order to simulate parallel channel flow effects, and FIST has full height scaling to preserve static head effects.

Although scaled to different size BWR systems, and employing different solutions in the test facility design, the two facilities compare very well. The initial conditions and the system boundary conditions also compare very well. The transient response of these two systems to each of the three types of LOCA tests is found to be quite similar (i.e., pressure, system mass, etc.). The sequence of key events for each set of tests, and the controlling phenomena, are the same in both facilities. Some difference in timing of events is due to small differences in facility scaling compromises and/or tests conditions.

Parallel channel flow interaction is significant only in the large break test. FIST lower plenum steam vents through the jet pumps whereas ROSA-III redistributes steam such that more steam flows up one of its four bundles. The bundle heatup response and PCT's are similar.

The downcomer level response, and subsequent level trip timing, is different in the two small break tests. This is due to faster downcomer depletion by the recirculation flow in FIST during the flow coastdown period. The system responses, bundle cooling, and PCT's are essentially the same, offset by this timing difference.

The steamline break system responses are also very similar. However, due to different flow resistance through the jet pumps there is a difference in the mass distribution between regions in the system that leads to CCFL holdup of liquid in the FIST bundle and not in ROSA-III. Also ECCS timing is different because of trip modeling. As a result, the mixture level falls into the ROSA-III bundles, allowing some heatup, whereas the FIST bundle remains full of two-phase mixture and well cooled.

The overall comparison between ROSA-III and FIST system response in LOCA tests is very good. Small response differences are due to different scaling compromises in the facility design and/or in the specific test conditions.

6. CONCLUSIONS

A common understanding and interpretation of BWR system response and the controlling phenomena in LOCA transients has been achieved through the evaluation and comparison of these tests. The system responses in each facility to counterpart test conditions are quite similar. Differences that do occur are due to minor differences in modeling objectives, facility scaling, and test conditions. The sequence of events are the same in each facility, and the timing of these events are similar. Parallel channel flow interaction effects in ROSA-III, although noticeable in the large break tests, do not cause major differences. The same events occur in both small break tests, offset in time by the later ADS actuation in ROSA-III. The system responses of the two steamline tests are also similar, except for the ROSA-III bundle heatup that results from a different ECCS trip modeling.

The steamline break system responses are also very similar. However, due to different flow resistance through the jet pumps there is a difference in the mass distribution between regions in the system that leads to CCFL holdup of liquid in the FIST bundle and not in ROSA-III. Also ECCS timing is different because of trip modeling. As a result, the mixture level falls into the ROSA-III bundles, allowing some heatup, whereas the FIST bundle remains full of two-phase mixture and well cooled.

The overall comparison between ROSA-III and FIST system response in LOCA tests is very good. Small response differences are due to different scaling compromises in the facility design and/or in the specific test conditions.

6. CONCLUSIONS

A common understanding and interpretation of BWR system response and the controlling phenomena in LOCA transients has been achieved through the evaluation and comparison of these tests. The system responses in each facility to counterpart test conditions are quite similar. Differences that do occur are due to minor differences in modeling objectives, facility scaling, and test conditions. The sequence of events are the same in each facility, and the timing of these events are similar. Parallel channel flow interaction effects in ROSA-III, although noticeable in the large break tests, do not cause major differences. The same events occur in both small break tests, offset in time by the later ADS actuation in ROSA-III. The system responses of the two steamline tests are also similar, except for the ROSA-III bundle heatup that results from a different ECCS trip modeling.

7. REFERENCES

1. Anoda, Y., Tasaka, K., Kumamaru, H., and Shiba, M., "ROSA-III System Description for Fuel Assembly No. 4", JAERI-M 9363, Japan Atomic Energy Research Institute, 1981.
2. Thompson, JE, "BWR Full Integral Simulation Test (FIST) Program Test Plan", NUREG/CR-2575, EPRI NP-2313, GEAP 22053, General Electric Company, April 1982.
3. Suzuki, M., Anoda, K., Tasaka, K., Kumamaru, H., Nakamura, H., Yonomoto, T., Murata, H., and Shiba, M., "Recirculation Pump Suction Line 200% Break Integral Test at ROSA-III with Two LPCI Failures, Run 983", JAERI-M84-135, Japan Atomic Energy Research Institute, 1984.
4. Hwang, WS, Alamgir, Md., and Sutherland, WA, "BWR Full Integral Simulation Test (FIST) Phase 1 Test Results", NUREG/CR-3711, EPRI NP-3602, GEAP-30496, General Electric Company, November, 1983.
5. Suzuki, M., Anoda, Y., Tasaka, K., Kumamaru, H., Nakamura, H., Yonomoto, T., Murata, H., and Shiba, M., "Recirculation Pump Suction Line 2.8% Break Integral Test at ROSA-III with HPCS Failure, Run 984", JAERI-M 84-100, Japan Atomic Energy Research Institute, 1984.
6. Murata, H., Suzuki, M., and Tasaka, K., "An Analysis of 100% Steam Line Break Test in the ROSA-III Program by Using RELAP5/MOD1 Code (Analysis of Run 952, an HPCS Injection Test)", JAERI-M 83-210, Japan Atomic Energy Research Institute, 1983 (in Japanese).
7. Stephens, AG, "BWR Full Integral Simulation Test (FIST) Program Facility Description Report", NUREG/CR-2576, EPRI NP-2314, GEAP-22054, General Electric Company, December, 1982.
8. Findlay, JA, "BWR Refill-Reflood Program Task 4.4 - CCFL/Refill System Effects Test (30° Sector) - Evaluation of Parallel Channel Phenomena", NUREG/CR-2566, EPRI NP-2373, GEAP-22044, General Electric Company, March, (1982)

APPENDIX A.1

ROSA-III Test Facility and Test Procedure

Test Facility

The ROSA-III test facility is designed to simulate the major components the responses of the 3800 MW (thermal) BWR/6 251-848 system during a postulated loss-of-coolant accident (LOCA). The schematic diagram of the facility is shown in Figure 1-1. The maximum operating pressure and the fluid temperature cover the BWR fluid conditions both in steady state and in the transient, i.e., 9.0 MPa and 576°K. The basic scaling and design objectives are to provide a test apparatus for investigating, on a real-time basis, the expected thermal-hydraulic response of the BWR/6 core following a postulated LOCA.

The facility is a volumetrically scaled system of the BWR/6 with the scaling ratio of 1/424. The relative elevation of each component is reasonably simulated. Primary characteristics of the ROSA-III test facility are listed in Table A.1-1 in comparison with the corresponding values of a BWR/6-251.

The core region consists of four half-length bundles. Each bundle contains 62 heated rods and two unheated water rods arranged in an 8x8 square array with a 16.16 mm pitch, as shown in Figure A.1-1. The heated length of the core is 1.88 m and the outside diameter of the rods is 12.27 mm. Each rod is an indirect electrical heater with a nicrome heater element and an Inconel 600 sheath. Boron nitride (BN) is used as the insulator. The details of the heater rod are shown in Figure A.1-2. The rods have a chopped cosine axial power distribution and an axial peaking factor of 1.4 (Figure 2-2C). The power to the peak power bundle (Bundle A) can be up to 1.4 times greater than the power to the average power bundles (Bundles B, C, and D). The radial power distribution within a bundle has local peaking factors of 1.1, 1.0, and 0.875 (Figure A.1-1).

The ROSA-III test facility has two recirculation loops. One simulates the broken loop and the other the intact loop. Each loop is furnished with one recirculation pump and two jet pumps. Jet pumps are installed outside the main vessel to achieve satisfactory simulation of the recirculation system volume.

The facility has three different types of ECC Systems. They are the high pressure core spray (HPCS), the low pressure core spray (LPCS), and the low pressure coolant injection (LPCI) systems. The flow rate of each system is scaled to $1/424$ of the BWR/6 system flows.

The break device, Figure 1-1, consists of two blowdown valves, one quick shutoff valve and two break nozzles or orifices. The break area can be varied by changing the size of the nozzle or orifice.

Test Procedure

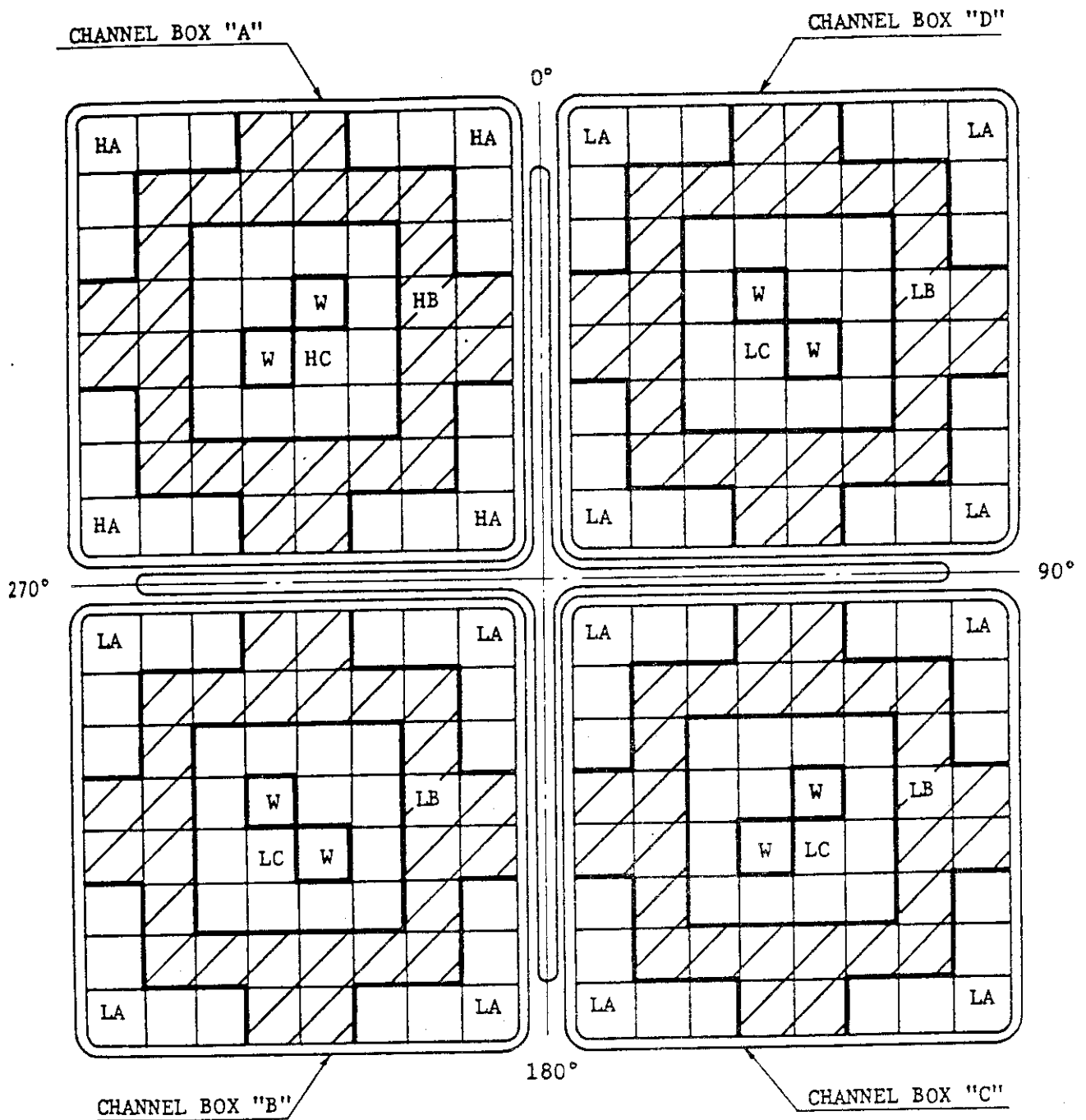
After the initial fluid conditions are established, the blowdown valves are opened and the core power is reduced in accordance with a predetermined curve. The core power before the initiation of the break should be 9 MW to produce the same transient expected in the BWR/6 system. Since the available core power is 4.4 MW, the power is maintained constant nine seconds after the break, and then reduced, simulating the heat transfer rate to the coolant in a BWR.

The ECCS is actuated automatically and injects water into the pressure vessel as soon as the actuation conditions, such as the low level in the downcomer and low system pressure, are reached. About 700 experimental data channels are recorded by a digital recording system with the sampling rate up to 30 Hz/channel. Measurements are made on the system pressure, the fluid temperature, the fuel rod surface temperature, the two-phase mixture level and other parameters.

Table A.1-1

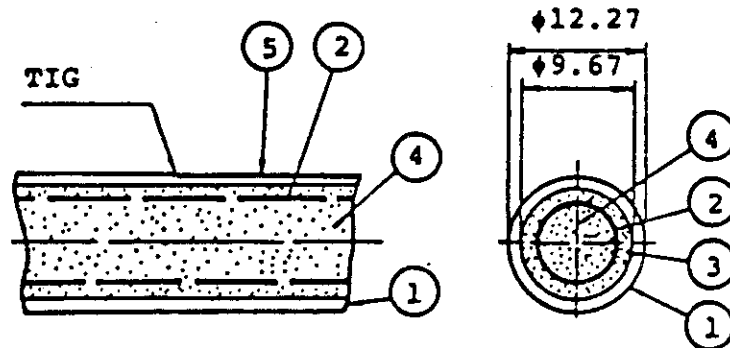
Primary Characteristics of ROSA-III and BWR/6-251

	BWR/6-251	ROSA-III	BWR/ROSA-III
Number of recirc. loops	2	2	1
Number of jet pumps	24	4	6
Number of separators	251	1	251
Number of fuel assemblies	848	4	212
Active fuel length (m)	3.76	1.88	2
Total volume (m ³)	621	1.42	437
Power (MW)	3,800	4.40	864
Pressure (MPa)	7.23	7.23	1
Core flow (kg/s)	1.54×10^4	36.4	424
Recirculation flow (l/s)	2,970	7.01	424
Feedwater flow (kg/s)	2,060	4.86	424
Feedwater temperature (K)	489	489	1



REGION	HA	HB	HC	LA	LB	LC	W
LOCAL PEAKING FACTOR	1.1	1.0	0.875	1.1	1.0	0.875	0
NUMBER OF RODS	20	28	14	60	84	42	8

FIGURE A.1-1 CORE CROSS-SECTION OF ROSA-III TEST FACILITY



NO	PARTS	MATERIAL
1	SHEATH	INCONEL 600
2	HEATER	NICHROME
3	INSULATOR	BN
4	INSULATOR	BN
5	THERMOCOUPLE	CA/INC 600

FIGURE A.1-2 DETAILS OF SIMULATED FUEL ROD

APPENDIX A.2

FIST Test Facility

The FIST facility is scaled from the BWR/6-218 standard plant. The facility is designed to model the thermal-hydraulic response from the initiation through the entire transient. The facility simulates these key features: full height, proportional regional volume distribution, full-size electrically heated bundle, functional hydraulic components, heated feedwater system which enables the facility to achieve steady-state operation, prototype level instrumentation, ECC Systems, and safety relief systems including ADS. A schematic of the FIST facility is shown in Figure 1-2.

A scaling criterion of $1/624$ is used in determining the regional volumes, mass, energy, and flow rates for the system, as well as in the geometrical scaling of the regions and components. The initial steady-state thermodynamic conditions in the test apparatus match those of the reference BWR during normal operation. This allows the real-time response to be characterized. Table A.2-1 summarizes the primary characteristics of the facility.

The FIST heater rods are of the direct (skin-heater) type, i.e., the heating element is the outer wall of the rod. The axial heat generation rate of the conducting tube is dependent on the local wall thickness. By varying wall thickness along the length, the axial power shape in Figure 2-2B is obtained. The same axial profile, but at a different total power in a rod is obtained by adding a constant amount to the wall thickness along the entire length. The rods, shown in Table A.2-2, generate total powers which are in the ratio of 1.04, 1.01, and 0.97 to the average rod power. There are 8 rods with a local peaking of 1.04, 30 rods with 1.01, 24 rods with 0.97, and two simulated water rods that are unheated. The FIST heater rods are 4.135m (162.8 in.) long, have a heated length of 3.81m (150 in.), and an outside diameter of 12.27mm (0.483 in.). The heated length is made of Inconel-600 tubing. The interior of the heated length portion of the heater rods is filled with a ceramic cement in which are embedded up to six Inconel-sheathed, chromel-alumel thermocouples.

The two recirculation loops are shown in Figure 1-2. Each loop independently provides the drive flow for its jet pump. Each loop consists of a standard, fixed-speed centrifugal pump with a flywheel to provide rotating inertia simulation, remotely controlled loop isolation and flow control valves, suction and drive line piping, a flow-metering orifice, and other instrumentation. The LOCA recirculation breaks are simulated in Loop No. 2. Blowdown piping, break orifices or nozzle, and quick-closing valves are connected to this loop. The jet pumps are full height, provide full scaled core flow, and simulate the reverse flow loss characteristics.

The emergency core cooling system (ECCS), as shown in Figure 1-2, consists of the high pressure core spray (HPCS), the low pressure core spray (LPCS), and the low pressure coolant injection (LPCI). Each of the three systems consists of a pump, piping containing remotely operable valves, and instrumentation to monitor and control the flow of the emergency coolant from a common heated supply tank to the test vessel.

The instrumentation system consists of the 426 experimental measurements: 8 pressure, 126 differential pressure, 45 conductivity probes, 21 material temperature, 82 fluid temperature, 112 heater rod temperature, and 32 miscellaneous. This system measures the bundle temperature, the global pressure response, the mass distribution, the local fluid conditions including the mixture levels, local conditions at particular components such as the upper tieplate, the primary flow rates crossing the system boundaries, the flow rates within the system internals, and the heat losses.

Table A.2-1

Primary Characteristics of FIST and BWR/6-218

	BWR/6-218	FIST	BWR/FIST
Number of recirc. loops	2	2	1
Number of jet pumps	24	2	12
Number of separators	251	1	251
Number of fuel assemblies	624	1	624
Active fuel length (m)	3.81	3.81	1
Total volume (m ³)	424.25	0.684	620.6
Power (MW)	2895	4.64	624
Pressure (MPa)	7.17	7.17	1
Bundle flow (kg/s)	9586.9	15.36	624
Bypass flow (kg/s)	1077.8	1.73	624
Feedwater flow (kg/s)	283.6	0.455	624
Feedwater temperature (K)	489	489	1

Table A.2-2

FIST Heater Pattern

1.01	1.01	1.01	0.97	0.97	1.01	1.01	1.01
1.01	0.97	1.04	1.01	1.01	1.04	0.97	1.01
1.01	1.04	0.97	0.97	0.97	0.97	1.04	1.01
0.97	1.01	0.97	water rod	1.01	0.97	1.01	0.97
0.97	1.01	0.97	1.01	water rod	0.97	1.01	0.97
1.01	1.04	0.97	0.97	0.97	0.97	1.04	1.01
1.01	0.97	1.04	1.01	1.01	1.04	0.97	1.01
1.01	1.01	1.01	0.97	0.97	1.01	1.01	1.01